The effect of apolipoprotein E isoforms and sortilin in brain lipid homeostasis and Alzheimer's disease

Inaugural-Dissertation

to obtain the academic degree

Doctor rerum naturalium (Dr. rer. nat.)

submitted to the Department of Biology, Chemistry and Pharmacy

of Freie Universität Berlin

by

ANTONINO ASARO

2019

The work was carried out from 06/2015 to 07/2019 under the supervision of Prof. Dr. Thomas E. Willnow at the Max Delbrück Center for Molecular Medicine in Berlin.

1st Reviewer: Prof. Dr. Thomas E. Willnow

Max Delbrück Center for Molecular Medicine

2nd Reviewer: Prof. Dr. Frank Heppner

Charité - Universitätsmedizin Berlin

Date of defense: 14.11.2019

TABLE OF CONTENTS

SUMMARY

Alzheimer's disease (AD) is an age-related neurodegenerative disorder that affects millions of patients worldwide. The gene encoding various isoforms of the brain lipid carrier apolipoprotein (APO) E is the most important genetic risk factor for the sporadic form of AD suggesting an important contribution of brain lipid metabolism to neurodegenerative processes. However, the mechanism whereby brain lipid homeostasis may affect brain health and disease, and the isoform-specific role of APOE in this process remains highly controversial.

In my thesis, I focused on the functional characterization of sortilin, a neuronal clearance receptor for APOE. Specifically, I hypothesized that sortilin may interact with apoE3 to safeguard a protective brain lipid metabolism, and that such neuroprotective lipid profile may be lost in the presence of apoE4, the AD risk bearing variant of the lipid carrier. To test my hypothesis, I performed comparative analyses of lipid profiles in the brain of mouse models with targeted replacement of murine *Apoe* with either human apoE3 or apoE4. In addition, these mice were either wildtype or genetically deficient for sortilin. In my studies, I identified perturbation in brain levels of docosahexaenoic acids (DHA), the most common polyunsaturated fatty acid (PUFA), as well as in endocannabinoids (eCBs), fatty acids-based neurotransmitters as a consequence of the *APOE* and sortilin genotypes. I identified the underlying molecular mechanism by showing that sortilin binds and stabilizes the fatty acid binding protein 7 (FABP7), an intracellular carrier for PUFA and eCBs. FABP7 facilitates the neuronal metabolism and activity of these lipids through their action on the PPAR family of nuclear hormone receptors. This functional interaction of sortilin and FABP7 in lipid metabolism requires the presence of apoE3. Loss of sortilin in apoE3 mice impairs sorting and stability of FABP7 and compromises its action in neuronal PUFA and eCB homeostasis, resulting in a pro-inflammatory state. Similar detrimental effects are seen in the presence of apoE4 that disrupts the ability of sortilin to direct intracellular sorting and proper activity of FABP7.

Taken together, my investigations have identified a unique pathway involving sortilin as well as carriers for extracellular and intracellular transport of lipids, namely apoE3 and FABP7 that control the anti-inflammatory metabolism of PUFA

and eCBs, and how this pathway may support the functional integrity of the brain through the action of PPARs. My findings emphasize the relevance of lipids for the functional integrity of the human brain, and why aberrant alterations in this biological system may contribute to the risk of AD in carriers of the apoE4 genotype.

ZUSAMMENFASSUNG

Die Alzheimer Krankheit ist eine altersbedingte neurodegenerative Erkrankung, die Millionen von Patienten betrifft. Der wichtigste genetische Risikofaktor für die sporadische Form der Alzheimer Krankheit ist das Lipidtransportprotein Apolipoprotein E (APOE), welches in verschiedenen Isoformen beim Menschen vorkommt. Obwohl APOE essentiell für den Lipidstoffwechsel und für neurodegenerative Prozesse im Gehirn scheint, ist seine Funktionsweise und seine isoform-spezifische Rolle bei der Alzheimer Krankheit immer noch höchst umstritten.

In meiner Doktorarbeit habe ich mich auf die funktionelle Charakterisierung von Sortilin, einem neuronalen Rezeptor für APOE fokussiert. Insbesondere habe ich die Frage untersucht, ob eine Interaktion von Sortilin mit APOE3 einen protektiven Lipidstoffwechsel im Gehirn gewährleistet und ob eine solche neuroprotektive Funktion des Rezeptors bei der Risikovariante APOE4 nicht gegeben ist. Um meine Hypothese zu testen, habe ich vergleichende Analysen der Lipidprofile im Gehirn von Mausmodellen durchgeführt, welche die menschlichen APOE Varianten APOE3 oder APOE4 ausbilden. Darüber hinaus waren diese Mäuse im Bezug auf Sortilin entweder wildtypisch oder gendefizient.

In meinen vergleichenden Studien der Lipide im Gehirn meiner vier Mausmodelle identifizierte ich Veränderungen im Stoffwechsel von Docosahexaensäure (DHA), der häufigsten mehrfach ungesättigten Fettsäure (PUFA) sowie in Endocannabinoiden (eCBs), fettsäurebasierten Neurotransmittern in Abhängigkeit von APOE- und Sortilin-Genotyp. Ich konnte den molekularen Mechanismus, der dieser Veränderung zu Grunde liegt, weiter aufklären und zeigen, dass Sortilin das Fettsäure-Bindeprotein 7 (FABP7) bindet und stabilisiert. FABP7 ist der intrazelluläre Transportfaktor für PUFA und eCBs und steuert den neuronalen Metabolismus und die Aktivität dieser Lipide. Insbesondere kontrolliert FABP7 die Interaktion der eCBs mit nukleären Hormonrezeptoren der PPAR Genfamilie. Die Liganden induzierte Aktivierung dieser Rezeptoren bedingt ein entzündungshemmendes Genexpressionsprofil im Gehirn. Diese funktionelle Interaktion von Sortilin und FABP7 im entzündungshemmenden Fettstoffwechsel von Neuronen verlangt die Anwesenheit von APOE3. Der Verlust von Sortilin bei

APOE3-Mäusen stört die korrekte intrazelluläre Sortierung und die Stabilität von FABP7 und unterbricht das neuronale PUFA- und eCB-Gleichgewicht. Letzendlich führen diese Störungen zu einem Verlust neuroprotektiver Aktivitäten der PPARs und bedingen einen pro-inflammatorischen Zustand des Gehirns. Ähnliche pathologische Auswirkungen zeigten sich auch in Anwesenheit von APOE4. Anders als bei der Interaktion mit APOE3, führt die Bindung von APOE4 an Sortilin zu einer fehlerhaften Akkumulation des Rezeptors im Endozytoseweg der Zellen und zum Verlust seiner FABP7 Interaktion.

Zusammenfassend haben meine Untersuchungen einen neuartigen zellulären Mechanismus im Lipidstoffwechel des Gehirns aufgedeckt, der die Wirkungsweise von APOE4 als Hochrisikofaktor der Alzheimer Krankheit miterklären könnte. Dieser Stoffwechselweg umfasst die Interaktion des neuronal Rezeptors Sortilin mit extrazellulären (APOE) und intrazellulären (FABP7) Transportproteinen für PUFAs. Dieser Stoffwechselweg ermöglicht die entzündungshemmende Wirkung von PUFA und eCBs über PPARs im Gehirn. Dieser neuroprotektive Stoffwechselweg wird durch die Anwesenheit von APOE4 gestört, da es die Funktionsweise von Sortilin blockiert.

Zusammengefasst unterstützen meine Ergebnisse die Bedeutung des neuronalen Lipidstoffwechsels für die funktionelle Integrität des menschlichen Gehirns und geben eine mögliche Erklärung für Störungen des Lipidstoffwechsels als Ursache für das Risiko von Morbus Alzheimer bei Trägern des APOE4-Genotyps.

LIST OF FIGURES

LIST OF TABLES

LIST OF ABBREVIATIONS

2-AG	2-arachidoylglycerol
ABCA7	ATP binding cassette (ABC) transporter A7
AD	Alzheimer's disease
AEA	Anandamide
AICD	APP intracellular domain
ANOVA	Analysis of variance
APOE	Apolipoprotein E
Apoer2	ApoE receptor-2
APP	Amyloid precursor protein
ARA	Arachidonic acid
Aβ	Amyloid β-peptide
B2M	β-2-microglobulin
BACE1	β-site APP cleaving enzyme-1
BCA	Bicinchoninic acid
BDNF	Brain-derived neurotrophic factor
BrdU	Bromodeoxyuridine
BSA	Bovine serum albumin
C	Celsius
c-Myc	Avian myelocytomatosis virus oncogene cellular homolog
cDNA	Complementary DNA
CHO cells	Chinese hamster ovary cells
CHO-S	CHO-Sortilin
CHO-S/F	CHO-Sortilin-FABP7
CHX	Cycloheximide
CLU	Clusterin

CNS	Central nervous system
co-IP	Co-immunoprecipitation
CSF	Cerebrospinal fluid
Ct	Cycle threshold
CTF	Carboxy-terminal fragment
CYP450	Cytochrome P450
DAB	Diaminobenzidine
DAGL	Diacylglycerol lipase
DAPI	4',6-Diamidino-2'-phenylindole
DG	Dentate Gyrus
DHA	Docosahexaenoic acid
DiHDHA	Dihydroxy-docosahexaenoic acid
DMEM	Dulbecco's Modified Eagle Medium
DNA	Desoxyribonucleic acid
dNTP	Deoxynucleotide
DPBS	Dulbecco´s Phosphate-buffered saline
dsDNA	Double-stranded DNA
eCB	Endocannabinoid
EDP	Epoxy-docosapentaenoic acid
EDTA	Ethylenediaminetetraacetic acid
EOAD	Early-onset Alzheimer's disease
FA	Fatty acid
FAAH	Fatty acid amide hydrolase
FABP5	Fatty acid binding protein
FABP7	Fatty acid binding protein 7
FACL4	Fatty acid-CoA ligase 4

FATP1	Fatty acid transport protein 1
FCS/FBS	Fetal calf serum
FTLD	Frontotemporal lobar degeneration
g	Gram
GAPDH	Glyceraldehyde-3-phosphate dehydrogenase
GFAP	Glial fibrillary acidic protein
GFP	Green fluorescent protein
GGA	Golgi-localizing γ-adaptin ear homology domain, ARF-interacting
GPR40	G-protein-coupled receptor 40
GWAS	Genome-wide association study
h	Hour(s)
HAB	Head activator binding protein
HCl	Hydrochloric acid
HDHA	Hydroxy-docosahexaenoic acid
HDL	High-density lipoprotein
HEK	Human embryonic kidney cells
HPLC	High-performance liquid chromatography
i.p.	Intraperitoneal
IF	Immunofluorescence
IH	Immunohistology
IP	Immunoprecipitation
KLF10	Krueppel-like factor 10
KO	Knock-out
l	Liter
LC-MS	Liquid chromatography-mass spectrometry
LDL	Low-density lipoprotein

LDLR	Low-density lipoprotein receptor
LEA	Linoleoyl-ethanolamide
LOAD	Late-onset Alzheimer's disease
LOX	Lipoxygenase
LRP	Low-density lipoprotein receptor-related protein
LRP1	Low-density lipoprotein receptor-related protein 1
M	Molar
m	Milli
MAGL	Monoacylglycerol lipase
MCI	Mild cognitive impairment
MMP9	Matrix metallopeptidase 9
MRI	Magnetic resonance imaging
mRNA	Messenger RNA
n	Number of experiments or samples analysed
NaCl	Sodium chloride
NaOH	Sodium hydroxide
NAPE-PLD	N-acyl phosphatidylethanolamine-specific phospholipase D
NCS	Neuronal stem cells
NP-40	Nonidet-P40
OEA	Oleyl-ethanolamide
p	Probability value
P/S	Penicillin/Streptomycin
PACS1	Phosphofurin acidic cluster sorting protein 1
PCR	Polymerase Chain Reaction
PDL	Poly-D-lysine
PEA	Palmitoyl-ethanolamide

PFA	Paraformaldehyde
PGRN	Progranulin
PICALM	Phosphatidylinositol Binding Clathrin Assembly Protein
PLA	Proximity ligation assay
PolyI:C	Polyriboinosinic-polyribocytidilic acid
PPAR	Peroxisome proliferator-activated Receptor
PPARg	Peroxisome Proliferator Activated Receptor Gamma
PSEN	Presenilin
PUFA	Polyunsaturated fatty acids
qRT-PCR	Quantitative real-time PCR
RAB	Ras-related in brain
RAP	Receptor-associated protein
RNA	Ribonucleic acid
RT	Room temperature
sAPP	Soluble APP
SDS	Sodium dodecyl sulfate
SEM	Standard error of the mean
SNP	Single nucleotide polymorphism
SORCS	Sortilin-related receptor CNS expressed
SORLA	Sortilin-related receptor with A-type repeats
ssDNA	Single-stranded DNA
SVZ	Subventricular zone
T/E	Trypsin/EDTA
TBS	Tris-buffered saline
TGN	Trans-Golgi-network
Tm	Melting temperature

tM	Mander's coefficient
TNFa	Tumor necrosis factor
TREM2	Triggering receptor expressed on myeloid cells 2
TRK	Tyrosine kinases receptor
VEGF	Vascular endothelial growth factor
VLDL	Very Low Density Lipoprotein
VPS10P	Vacuolar protein 10 sorting protein
WB	Western blotting
WT	Wild type
µ	Micro

1. INTRODUCTION

1.1. Alzheimer's disease (AD)

1.1.1. Clinical and neuropathology features of AD

At the beginning of the twentieth century, Alois Alzheimer reported the case of a woman who died a few years after developing a clinically unusual form of dementia at age 51. Later, similar cases were reported and led to the recognition of this condition as unique disease, termed Alzheimer's disease (AD) (Berchtold and Cotman 1998). After more than one hundred years, huge strides have been made to uncover its underlying mechanisms but still to date no cure has been developed. Today, AD is the most common form of age-related dementia. The disease begins with a gradual decline of memory after which other symptoms of behavioral and cognitive deficits take over. Initially, AD is characterized by short-term memory loss that is difficult to diagnose because it may also be attributed to ageing and stress. However, as the disease progresses, other forms of cognition become impaired resulting in difficulties in thinking, in disorientation and in mood swings. Additional serious symptoms such as difficulty in speaking as well as behavioral changes can interfere with the patient performing everyday tasks (Rao et al. 2014). The occurrence of these symptoms is the consequence of multiple lesions in different brain regions. In the brain of AD patients, progressive disruption of vital processes in neurons result in loss of synaptic activity and eventual neuronal cell death (Selkoe 1991). For this reason, AD belongs to the category of neurodegenerative disorders characterized by chronic loss of structure and function of neurons. At late stages of the disease, AD patients display significant cerebral atrophy with a decrease in brain volume (Blennow et al. 2001). The decrease in cortical thickness can be detected by magnetic resonance imaging (MRI) and correlated to the progression of cognitive dysfunction (Putcha et al. 2011). Several mechanisms have been implicated in this drastic loss of neuronal connections and ultimate cell death, including protein deposits forming extracellular amyloid plaques and intracellular neurofibrillary tangles, as well as brain inflammation, oxidative stress, and mitochondrial dysfunction (Blennow et al. 2001). A major culprit of AD is the amyloid-β (Aβ) peptide, a principal neurotoxic component of the amyloid (senile) plaques that deposit in the extracellular space

around neurons. Aβ is produced by proteolytic breakdown of the amyloid precursor protein (APP), a type-1 transmembrane protein expressed and proteolytically processed in many cell types. Functions have been assigned both to the full-length precursor but also to the proteolytic breakdown products of APP. The extracellular domain of full-length APP binds various extracellular matrix components essential for its activity in cell-matrix adhesion (Kibbey et al. 1993) (Beher et al. 1996). In addition, APP has a trophic function as hippocampal neurons deficient in APP show decreased viability and retarded neurite development (Perez et al. 1997). In support of the role for APP in neuronal viability and function, APP knock-out mice exhibit a decrease in locomotor activity (Zheng et al. 1995). In a physiological process occurring in many cell types, full-length APP can also be proteolytically processed, forming new protein fragments with additional functions. In detail, APP can follow two alternative processing fates, amyloidogenic or non-amyloidogenic, depending on whether neurotoxic Aβ is produced or not. In the amyloidognenic pathway, APP is cleaved by β-secretase leading to the secretion of sAPPβ. Then, the γ-secretase complex cleaves the remaining membrane-anchored carboxy-terminal fragment (CTFβ), releasing the Aβ peptide and the APP intracellular domain (AICD) (Figure 1.1). Cleavage by γ-secretase is imprecise and generates Aβ peptides with varying amino acid lengths. The predominant forms are Aβ40 and Aβ42 (Haass et al. 2012). The Aβ42 peptide is more prone to oligomerization and aggregation than Aβ40, suggesting that the imprecise γ-secretase cleavage influences neurotoxicity of the produced Aβ species (Haass and Selkoe 2007). Ultimately, Aβ peptides form insoluble amyloid fibrils, that accumulate as senile plaques (Hardy and Higgins 1992). Of note, the extent of plaque deposition does not correlate well with the cognitive decline in AD patients (Sloane et al. 1997) (Crystal et al. 1988). Rather, it is the concentration of toxic soluble Aβ oligomers that are better correlated with the AD symptoms. Thus, current hypotheses suggest that the toxic insult of these soluble oligomers cause synaptic dysfunction and neuronal death in AD (Selkoe 2008) (Kamenetz et al. 2003). Production of Aβ is prevented in the non-amyloidogenic pathway when APP is initially processed by α-secretase activity, which cuts within the Aβ peptide sequence. Cleavage by α-secretase disrupts the

Aβ peptide and produces the soluble extracellular fragment, sAPPα and the membrane-anchored carboxyterminal fragment α (CTFα) (Figure 1.1).

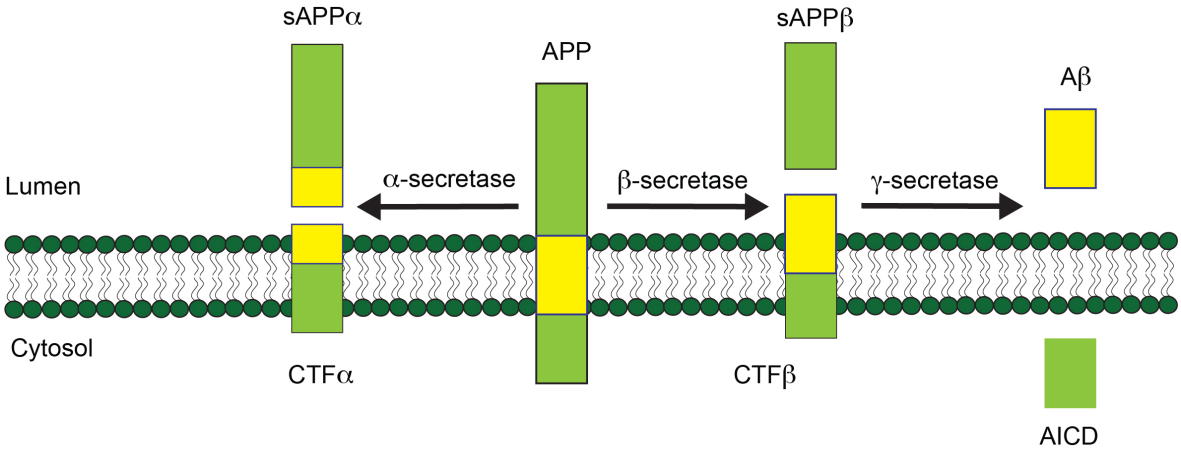

Figure 1.1: Amyloidogenic and non-amyloidogenic processing of the amyloid precursor protein (APP).

In the amyloidogenic pathway (to the right), APP is processed by β-secretase, releasing soluble APPβ (sAPPβ) and the membrane-anchored carboxy-terminal fragment β (CTFβ). Further processing of CTFβ by γ-secretase produces the neurotoxic Aβ peptide and the APP intracellular domain (AICD). In the non-amyloidogenic pathway (to the left), APP is cleaved by α-secretase activity, which destroys the Aβ peptide and produces sAPPα and the membrane-anchored fragment CTFα.

The underlying mechanisms whereby APP functions are coordinated between its full-length form and the proteolytic cleavage products remain unclear (Müller and Zheng 2012). However, it is well appreciated that mechanisms that increase APP processing to Aβ (amyloidogenic processing), or that impair catabolism of the peptide in the brain are responsible for its adverse aggregation in the brain parenchyma and consequently, its neurotoxic deposits in AD (Pearson and Peers 2006).

1.1.2. Epidemiology and risk factors of AD

Today, around 50 million people worldwide are affected by age-related dementia and this number is expected to increase even more as people live longer and no cure or treatment is available (World Health Organization, 2018). The combined economic and social burden of AD is enormous. This devasting disorder profoundly affect the lives of patients and their families (Winblad et al. 2016). AD accounts for 60-70% of all dementia cases in the world. Already today, major

attention and health care costs are allocated to this disease as it is becoming a major public health problem. AD is a complex and heterogeneous disorder affected by multiple risk genes and environmental factors. Based on heritability (familial vs sporadic) and age of onset (early vs late), AD can be classified into different disease types. Among these, the early-onset familial form of AD (EOAD) accounts for less than 1% of AD cases. In EOAD, affected people carry dominantly inherited mutations in 3 genes, encoding for amyloid precursor protein (*APP*), presenilin 1 (*PSEN1*) or presenilin 2 (*PSEN2*) (Campion et al. 2002). Presenilins are subunits of the γ-secretase complex. Recently, potentially pathogenic sequence variations in *SORL1* were found in EOAD patients as well (Pottier et al. 2012) (Nicolas et al. 2016) (Verheijen et al. 2016). Mutations in familial disease genes typically accelerate the cleavage of APP and lead to an increase in Aβ42 levels or in the Aβ42/Aβ40 ratio (Scheuner et al. 1996). However, the vast majority of patients over the age of 65 are afflicted by the late-onset sporadic form of the disease (LOAD), caused by a combination of genetic and environmental risk factors (Rao et al. 2014).

While it has been established that familial EOAD is primarily determined by genetics, the aetiology of sporadic LOAD remains to be fully elucidated. A large number of environmental factors have been associated with increased or decreased risk for the sporadic form of AD. Ageing is the obvious determinant of AD risk as there is an exponential increase in dementia in individuals 65 years and older (Evans et al. 1989). Several studies have shown that AD patients have fewer years of education and higher prevalence of heart disease than persons without AD (Luchsinger et al. 2001). Moreover, obesity and diabetes increase the risk of AD (Profenno et al. 2010). The Mediterranean diet rich in unsaturated lipids contained in olive oil, vegetables and fish is correlated with a reduction in the incidence of AD (Scarmeas et al. 2011), while smoking, lack of physical activity, and hypertension increase it. Still, these environmental factors do not usually provide sufficient sensitivity and/or specificity to be employed as predictive risk markers of the disease (Reitz, Brayne, et al. 2011).

Even as LOAD risk is associated with environmental factors, it still involves a strong genetic component. Genome-wide association studies (GWAS) have significantly advanced our knowledge regarding the genetic risks of LOAD by

identifying multiple genetic risk loci. Among those risk genes are, *CLU,* encoding an apolipoprotein involved in lipid transport, *PICALM* with a role in trafficking of synaptic vesicles (Harold et al. 2009), and *TREM2,* encoding a receptor that activates microglial response (Guerreiro et al. 2013) (Hampel et al. 2013). Furthermore, *SORL1,* encoding a neuronal sorting receptor for APP termed SORLA has been repeatedly associated with LOAD in GWAS studies (Lambert et al. 2013) (Miyashita et al. 2013). *SORL1* was initially implicated in LOAD due to the fact that SORLA levels were decreased in the brain of AD patients compared with healthy controls (Scherzer et al. 2004). Later, it had been shown that several allelic variants in the *SORL1* gene are causally linked to the pathogenesis of AD by altering APP trafficking and consequently increasing Aβ production (Rogaeva et al. 2007). Typically, LOAD-associated risk variants in *SORL1* impair its transcription, splicing or translation efficiency and likely confer LOAD risk by reducing SORLA levels in the brain of affected individuals.

1.1.2.1. The apolipoprotein E

In recent years, the one gene that has been consistently found to be associated with sporadic LOAD across multiple ethnicities is *APOE*, the gene encoding for apolipoprotein (APO) E (Corder et al. 1993) (Harold et al. 2009).

APOE is a glycoprotein highly expressed in the central nervous system (CNS), predominantly by astrocytes but also by microglia and neurons after injury (Xu et al. 2006) (Pitas et al. 1987) (Grehan et al. 2001). APOE is a lipid carrier. It is secreted into the brain interstitial fluid where it is lipidated, forming discoid-shaped lipid particles that structurally resemble high-density lipoprotein found in the circulation. Lipid-loaded APOE deliver essential lipids to both neurons and glia via binding to endocytic APOE receptors on the surface of target cells (Holtzman and Herz 2012) (Figure 1.2).

In contrast to many other species including rodents, humans have not one but three variants of the *APOE* gene. These human gene variants differ by two single nucleotide polymorphisms (SNPs), encoding three common isoforms, namely apoE2 (cys112, cys158), apoE3 (cys112, arg158), and apoE4 (arg112, arg158). The respective frequencies of these gene variants in the human population are 8.4%, 77.9%, and 13.7%. Of note, the frequency of the apoE4 allele is

dramatically increased to ~40% in patients with AD. Although all three *APOE* isoforms differ by only one or two amino acids, these changes alter the APOE structure and function significantly by changing its ability to bind lipids and/or APOE receptors (Corder et al. 1993) (Farrer et al. 1997).

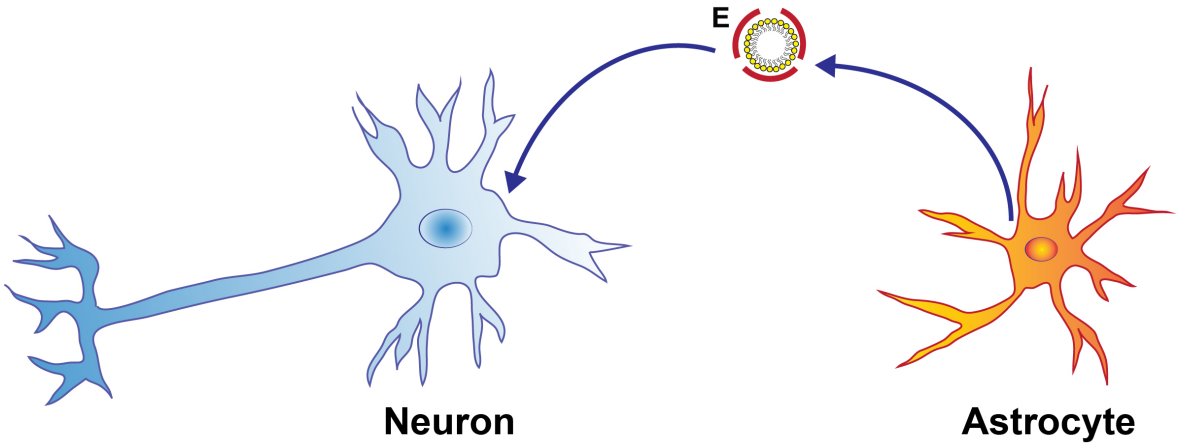

Figure 1.2: APOE metabolism in the brain.

APOE is primarily produced by astrocytes and lipidated in the extracellular space to form lipoprotein particles. APOE-containing lipoprotein particles deliver lipids to neurons that mediate cellular uptake via a structurally diverse class of endocytic APOE receptors.

The most significant LOAD risk gene is the apoE4 isoform. This allele dramatically increases the risk of AD at an earlier age of onset in a gene dose-dependent manner. Individuals carrying the homozygous apoE4 allele face an eight times higher risk of developing LOAD as compared to non-carriers. In contrast, the rare apoE2 allele seems to have a protective effect over the common apoE3 allele (Corder et al. 1993). So far, the molecular mechanisms whereby apoE4 constitutes a major risk factor for LOAD remains controversial. Conceptually, causative mechanisms may entail a gain of neurotoxic functions for apoE4, such as increasing the propensity of Aβ aggregation or disturbing brain activities. Alternatively, apoE4 may exhibit a loss of neuroprotective activities seen with apoE3, such as supporting mitochondrial function, neurogenesis, or brain lipid metabolism (Liu et al. 2013). One popular hypothesis states that APOE may controls Aβ production and deposition in an isoform specific manner. For example, APOE binds Aβ and mediates its cellular clearance in a isoform-specific manner, as apoE4 has a reduced Aβ binding affinity and is less efficient in mediating Aβ

clearance as compared with apoE3 (LaDu et al. 1994) (Castellano et al. 2011). However, there is also growing evidence to support additional roles for APOE in the onset and progression of AD. With relevance to my thesis project, several lines of evidence suggest Aβ-independent roles for APOE in AD pathogenesis through its isoform-specific effects on brain lipid metabolism.

1.1.3. Aberrant brain lipid homeostasis as cause of AD

Alois Alzheimer originally described three pathological hallmarks in the brain of Auguste Deter. The first two features are the well-studied neurofibrillary tangles and senile plaques. The third feature seen were intracellular lipid deposits that have not received much attention, perhaps due to the lack of appropriate analytical tools (Foley 2010). It is only in recent years that advancements in the field of lipidomics has provided strong evidence that multiple factors are involved in the pathology of AD where lipid homeostasis appears to be an essential contributor.

The *APOE* genotype has repeatedly been linked to Aβ metabolism, one of the neuropathological hallmarks of AD. These investigations led to important discoveries about the pathophysiological relevance of soluble oligomeric and/or insoluble plaque-associated forms of Aβ in AD. However, clinical trials that focused on targeting Aβ production and/or accumulation have consistently failed (Cummings et al. 2014) and major pharmaceutical companies are abandoning their efforts to find new drugs for the treatment of AD. Lack of success may be attributed to many factors but the strategy to target Aβ towards a cure for AD is currently under question and new disease mechanisms are being considered. Alzheimer's disease is a complex and multifactorial disease and experimental evidence supporting Aβ-independent causes of AD pathology is growing steadily. This statement particularly concerns hypotheses that suggest isoform-specific effects of APOE on brain lipid metabolism that may have protective versus adverse effects on brain health and the risk of AD.

Lipids have major roles in numerous biological systems, including cell membrane composition, energy storage, and cell signaling. The brain is the most lipid-rich organ in the human body and lipids are particularly relevant for brain health and function (Wood 2012). Thus, lipid alterations in the brain or in peripheral tissues have been consistently linked to neurodegenerative diseases including AD

(Adibhatla and Hatcher 2007). Cholesterol is the most studied lipid in the brain because of its abundance and *de novo* synthesis in the brain, likely reflecting the importance of cholesterol for CNS structure and function (Pfrieger and Ungerer 2011). Cholesterol in the brain is mostly present in the myelin sheaths, as well as in the lipid bilayer of the plasma membrane and endocytic vesicles of glial cells and neurons (Pfrieger 2003). Cholesterol derived from APOE-containing lipoproteins, produced by glia cells is essential for synaptogenesis (Mauch et al. 2001). Along these lines, studies have linked cholesterol metabolism to AD pathogenesis, for example by documenting altered plasma concentrations of brain-specific but also peripherally produced oxysterols in AD patients compared to non-demented subjects (Kölsch et al. 2004). Epidemiological studies have shown a protective effect of statins (cholesterol synthesis inhibitor) on the development of dementia (Jick et al. 2000) (Wolozin et al. 2007). Moreover, higher or lower cholesterol, the main component in the lipid raft, increases or decreases amyloidogenic processing, respectively, possibly by regulating the accessibility of β-secretase to its substrate APP in the lipid raft (Ehehalt et al. 2003) (Tarabal et al. 2007) (Marquer et al. 2011). Sphingolipids are another class of lipids also altered in the AD brain. The simplest form of sphingolipids are ceramides. They are composed of sphingosine, an aliphatic amino-alcohol, and a fatty acid. Sphingolipids with a more complex structure include cerebrosides, sulfatides, and gangliosides. Compared to control cases, AD patients show a decrease in gangliosides in the frontal and temporal cortices. Since gangliosides are markers of axodendritic arborization, these data suggest that the neuronal loss in AD brains may be responsible for the lipid alteration seen (Kracun et al. 1992) (Svennerholm and Gottfries 1994). In contrast, ceramides are increased in AD brain, probably because they act as second messenger molecules that regulate cell apoptosis and Aβ production (He et al. 2013).

APOE, the most important AD risk gene encodes a lipid transporter, underscoring the relevance of lipids for brain pathophysiology. In addition to *APOE*, GWAS have identified several other genes associated with AD risk that function in lipid or lipoprotein metabolism, including those encoding for the apolipoprotein clusterin (*CLU*) and the cholesterol transporter ATP binding cassette transporter A7 (*ABCA7*) (Tosto and Reitz 2013).

1.2. The sorting receptor sortilin

1.2.1. Structure and function of VPS10P-domain receptors

Lipids are supplied to brain cells via uptake of APOE-containing lipoprotein through APOE receptors. These receptors can influence APOE functions and, thus, are important for normal brain lipid metabolism but likely also for lipid alterations seen in AD. Several APOE receptors have been identified in the brain including the low-density lipoprotein (LDL) receptor (LDLR), the LDLR-related protein 1 (LRP1), the apolipoprotein E receptor 2 (ApoER2), and the very-low-density lipoprotein receptor (VLDLR). LDLR is mainly expressed in glia cells whereas LRP1 expression is neuronal (William Rebeck et al. 1993) (Rapp et al. 2006). Still, both LDLR and LPR1 are important for Aβ clearance as decreased expression of either receptor is associated with increased amyloid deposition in mouse models (Cao et al. 2006) (Van Uden et al. 2002). LRP1 KO mice also show a decrease in cholesterol levels in forebrain tissues when compared to WT animals (Liu et al. 2007). Interestingly, ApoER2 and VLDLR bind the signaling protein reelin resulting in protection from neurotoxicity by preventing the detrimental effects of Aβ on long-term potentiation (Durakoglugil et al. 2009). The same impaired synaptic activity is seen when apoE4 binds ApoER2, antagonizing reelin signaling at the neuronal cell surface (Chen et al. 2010).

Although several receptors had been implicated in APOE uptake in neurons, no alterations in brain APOE levels were seen in mouse models lacking any of APOE. The situation is different for sortilin, a recently identified neuronal receptor for APOE-containing lipoproteins (Carlo et al. 2013). Sortilin is a member of a class of intracellular sorting receptors, named vacuolar protein sorting 10 protein (VPS10P) domain receptor. VPS10P domain receptors are type-1 transmembrane proteins conserved throughout evolution that share a common protein module in their extracellular domain, the VPS10P domain. This 700 amino acids domain was initially identified in the vacuolar protein sorting 10 protein (VPS10P) in *Saccharomyces cerevisiae*. The yeast sorting receptor VPS10P delivers newly synthesized lysosomal enzymes from the Golgi to the vacuole, the yeast lysosome (Marcusson et al. 1994). In mammals, the VPS10P domain protein family consists of five members, designated sortilin, sorting-related receptor with A type repeats

(SORLA) as well as sortilin-related receptors CNS expressed (SORCS) 1, -2, and -3 (Figure 1.3). All the members of this family contain a large amino terminal luminal/extracellular domain, encompassing the VPS10P domain, followed by a single transmembrane domain and a short cytoplasmic tail at the carboxyl terminus. Sortilin is the only protein where extracellular domain only consists of a VPS10P domain. Other family members have additional structural motifs, such as leucine-rich domains, complement-type repeats, epidermal growth factor (EGF)-type repeats and fibronectin type III domains, all of which are involved in protein-protein interaction. The APP binding site in SORLA is located in the complement-type repeats in the extracellular domain, which is essential for shuttling APP to the TGN and to protect it from processing (Andersen et al. 2006). A further module is the β-propeller, which is involved in the regulation of ligand binding (Figure 1.3). Based on crystal structures, the VPS10P domain of sortilin and SORLA consist of a ten-bladed β-propeller that forms a large conical tunnel in which ligands bind (Quistgaard et al. 2009) (Kitago et al. 2015). Of note, the familial *SORL1* mutation G511R is located in the VPS10P domain of SORLA and disrupts the binding of Aβ to SORLA, resulting in impaired lysosomal targeting of Aβ by the mutant receptor (Caglayan et al. 2014). The short cytoplasmic tails of the VPS10P-domain receptors contain internalization signals and prototypical recognition motifs for a number of cytosolic adaptor proteins that traffic these receptors and their cargo between the cell surface and various intracellular compartments (Willnow et al. 2008).

The intracellular fate of sortilin and SORLA was intensively studied. Sortilin and SORLA predominantly localize to the late Golgi compartment, with only a minor fraction of the receptor pool being present at the cell surface. From the cell surface, SORLA and sortilin may deliver internalized ligands via early and late endosomes to lysosomes for catabolism or retrogradely from early endosomes back to the TGN for resecretion. Information on the trafficking paths of SORCS receptors is limited. SORCS1's subcellular localization varies between its splice forms. But the receptor is mostly implicated in the delivery of cargo to lysosomes. SORCS2 was shown to be equally distributed between intracellular organelles and the plasma membrane. Instead, localization of SORCS3 depends on the cell line used for the tracking of this receptor. For example, overexpression of SORCS3 in

Chinese hamster ovary (CHO) cells resulted in a predominant cell surface exposure of the receptor and a low internalization rate (reviewed in (Hermey 2009) (Willnow et al. 2008)) (Westergaard et al. 2005) (Nielsen et al. 2008).

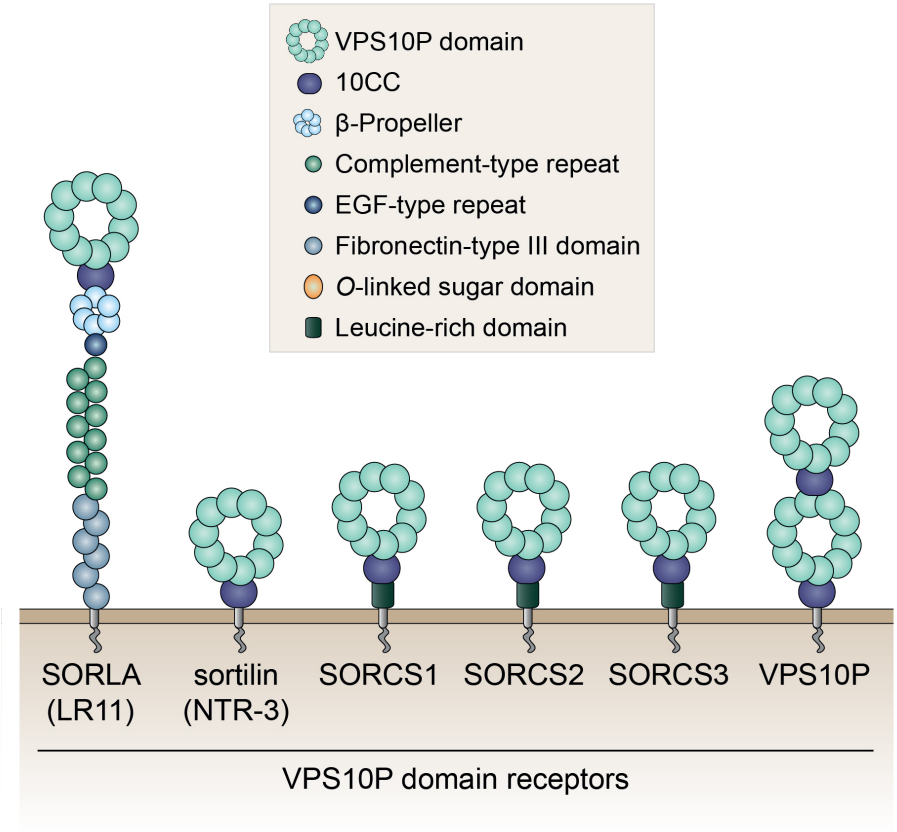

Figure 1.3: Structural organization of the vacuolar protein sorting 10 protein (VPS10P) domain receptor family.

Sorting protein-related receptor with A-type repeats (SORLA), sortilin, sortilin-related receptors CNS expressed (SORCS) 1, -2, and -3 and VPS10P (Saccharomyces cerevisiae) are type-1 transmembrane receptors that share a common extracellular domain, the VPS10P domain. Some receptors of the family carry additional functional domains depicted here.

Sortilin and SORLA are trafficked between biosynthetic and endocytic compartments through binding to a number of cytosolic adaptor proteins, including AP-1 and 2 (adaptor proteins 1 and 2), GGA-1,-2,-3 (Golgi-localizing, γ-adaptin ear homology domain, ARF-interacting proteins), PACS1 (phosphofurin acidic cluster sorting protein 1), and the retromer complex. SORLA binds AP-2 protein for its internalization (Nielsen et al. 2007). Its intracellular transport between Golgi and endosomes is regulated by AP-1 and GGA for anterograde transport from the TGN to endosomes (Nielsen et al. 2007) (Jacobsen et al. 2002) or PACS1 and retromer

for retrograde transport from endosomes to TGN (Schmidt et al. 2007) (Burgert et al. 2013). Retromer binding results in a retrograde sorting of SORLA, reducing APP processing in endosomes. In contrast, GGA interaction defines anterograde sorting of the receptor and its cargo Aβ to lysosomes for catabolism of the peptide (Dumanis et al. 2015).

1.2.2. Mammalian VPS10P domain receptors in health and disease

VPS10P domain receptors bind a wide variety of ligands, including neurotrophins, various tyrosine kinase receptors, synaptic adhesion and transmission molecules, and they mediate sorting of these ligands between different subcellular compartments. VPS10P domain receptors are genetically or functionally implicated in a broad spectrum of human diseases including metabolic disturbances. Thus, SORLA is associated with obesity (Smith et al. 2010) (Parks et al. 2013), sortilin with hypercholesterolemia (Kathiresan et al. 2008) (Muendlein et al. 2009), whereas SORCS1 and 3 are associated with type-2 diabetes (Granhall et al. 2006) (Clee et al. 2006). In addition, these receptors are associated with neurodegenerative and psychiatric diseases, in line with their predominant expression in the developing and adult mammalian nervous system. Several members of this gene family have been associated with AD, foremost SORLA. Numerous studies have revealed two distinct molecular mechanisms by which SORLA acts as a risk factor in AD. Firstly, SORLA was shown to interact with APP affecting its intracellular transport from endosomal compartments back to the TGN, essentially blocking proteolytic processing into Aβ. Thus, overexpression of SORLA reduces the number of APP molecules subjected to amyloidogenic processing and reduces Aβ production (Andersen et al. 2005) (Schmidt et al. 2007) (Offe et al. 2006) (Rogaeva et al. 2007). Secondly, SORLA interacts with newly generated Aβ peptides in endosomal compartments and sorts Aβ to the lysosome for degradation (Caglayan et al. 2014). The role of SORLA as a negative regulator of APP processing was supported by correlating low levels of SORLA in mouse models and AD patients with enhanced Aβ deposition (Andersen et al. 2005) (Dodson et al. 2008) (Rohe et al. 2008).

Although the mechanisms explaining the association of SORCS receptors with AD are poorly understood, epidemiological studies suggest that genetic variations in

SORCS1, *SORCS2,* and *SORCS3* are also associated with the risk of LOAD (Reitz, Tokuhiro, et al. 2011) (Liang et al. 2009) (Reitz et al. 2013). In addition, SORCS2 is implicated in a number of psychiatric diseases, including bipolar disorder and schizophrenia (Christoforou et al. 2010), and in the protection of neurons from oxidative stress following epilepsy (Malik et al. 2019).

The VP10P domain receptor with relevance to AD studied in my PhD thesis is sortilin. Sortilin was originally identified as a potential lipoprotein receptor in human brain extract (Petersen et al. 1997). Subsequent studies showed that this receptor not only binds lipoproteins (Nilsson et al. 2008) but several other ligands relevant for brain health and disease, particularly neurotrophins and their receptors. Neurotrophins are soluble growth factors that mediate neuronal survival through signaling via tropomyosin receptor kinases (Trk). Sortilin affects neurotrophic and apoptotic processes in the brain by both controlling the release of pro-forms of neurotrophins (pro-NT) (Chen 2005) and by sorting of TrK receptors A, B ,and C (Vaegter et al. 2011). In addition to Trk receptors, the effect of all neurotrophins is regulated by the receptor p75NTR. Sortilin was shown to form a co-receptor with p75NTR that specifically recognizes pro-NTs to induce apoptosis in cultured neurons (Nykjaer et al. 2004) and *in vivo* (Jansen et al. 2007). This process is pathophysiologically relevant, since release of pro-NTs is increased in AD, implicating sortilin-mediated neurotrophin regulation in age-related neurodegeneration (Fahnestock et al. 2001).

Other studies suggest a more direct role for sortilin in amyloidogenic processing by regulating the levels of Aβ and senile plaque burden in the brain of AD mouse models. In detail, sortilin was shown to bind APOE and to mediate neuronal catabolism of APOE- bound Aβ complex. A role for sortilin in brain APOE metabolism was supported by the aberrant accumulation of APOE in the brain of mice lacking this clearance receptor (Carlo et al. 2013). Besides regulating Aβ clearance in the brain, sortilin has also been proposed to increase Aβ production by trafficking APP (Gustafsen et al. 2013) or the β-secretase BACE1 (Finan et al. 2011).

In addition to a potential function of sortilin in AD, the receptor may also play a crucial role in another neurodegenerative disorder called frontotemporal lobar

degeneration (FTLD). FTLD is characterized clinically by dementia with prominent behavioral alterations (Cairns et al. 2007). A major cause of FTLD is mutations in the progranulin (*GRN*) gene. Most *GRN* mutations results in haploinsufficiency of PGRN, suggesting that PGRN has a protective role in the brain (Baker et al. 2006) (Gass et al. 2006). PGRN is an actively secreted glycoprotein precursor of granulin with anti-inflammatory properties (Chitramuthu et al. 2017). Sortilin regulates PGRN levels by mediating PGRN endocytosis, delivering it to lysosomes for degradation (Hu et al. 2010).

1.2.3. Role of sortilin in lipid homeostasis

While the role of sortilin in the brain received major attention, new studies have emerged that suggested potentially important functions for this receptor in peripheral metabolic tissues as well. Thus, *SORT1*, encoding sortilin, showed a genome-wide association with hypercholesterolemia and the risk of myocardial infarction in multiple GWAS (Kathiresan et al. 2008) (Willer et al. 2008). The underlying molecular mechanism whereby sortilin may control plasma cholesterol levels remains highly controversal. Receptor-mediated reduction of plasma cholesterol levels may be achieved by sortilin acting as a lipoprotein receptor in the liver that mediates hepatic clearance (Strong et al. 2012) of circulating cholesterol-rich lipoproteins. An alternative hypothesis argues that sortilin reduces plasma cholesterol levels by facilitating intracellular degradation of newly produced lipoprotein particles (Musunuru et al. 2010). On the other hand, other studies suggested that sortilin may increase (rather than decrease) cholesterol levels by reducing release of cholesterol-rich lipoprotein particles from the liver (Kjolby et al. 2010) or by acting as a sorting receptor for PCSK9, facilitating its secretion from hepatocytes. PCSK9 binds LDLR and causes its lysosomal degradation, resulting decreased uptake of circulating cholesterol-rich lipoproteins (Gustafsen et al. 2014).

New studies from the Willnow lab now suggest that sortilin may not only act as a lipoprotein receptor in the liver. Rather, it may have a similar function in neurons in the brain, an activity that may play a central role in normal brain lipid metabolism but also in APOE-dependent risk of AD. In detail, studies documented the ability of sortilin to bind APOE and to mediate its uptake in primary neurons. Importantly,

mice lacking sortilin accumulate murine APOE, possibly due to the impaired clearance of the apolipoprotein by neurons lacking this APOE receptor (Carlo et al. 2013). An important role for sortilin as a neuronal APOE receptor was also supported by alterations in sulfatide levels seen in the brain of receptor-deficient mice. Sulfatides, are a major class of lipids found in the myelin sheath of axons, They are believed to be extracted by APOE-containing lipoproteins and delivered to neurons for clearance. In support of the role of sortilin in APOE metabolism, sortilin knock-out mice show an increase in sulfatides in the their brain compared to the wild-type mice (Carlo et al. 2013). The same result of increased sulfatides levels is also seen in the brain of mice lacking murine APOE (Han et al. 2003).

Taken together, these studies suggested sortilin as the main receptor for uptake of APOE in neurons in the brain, and its potential contribution to brain lipid metabolism and the associated risk of AD. However, the mouse studies on APOE and brain lipid metabolism described above were all performed in wild-type and receptor mutant mice expressing murine *Apoe*. Thus, the relevance of sortilin for metabolism and action of human *APOE* variants, specifically for the risk of AD seen with apoE4 as compared with apoE3 were not answered by these studies. Clarifying this important question was the major aim of my thesis project.

2. AIM OF THE STUDY

AD is the most common form of age-related dementia with the brain lipid transporter APOE being the most well-known risk factor for the sporadic form of the disease. Lipids play crucial roles in brain physiology and possibly in the occurrence of AD. However, the exact role for APOE in these processes remains poorly understood. Sortilin is the main APOE receptor in neurons, mediating the uptake of APOE-containing lipoprotein particles in these cells *in vitro* and *in vivo* and may provide explanatory models for the role of neuronal lipid metabolism in brain health and disease. Still, the relevance of sortilin for human APOE isoforms specific effects on brain (patho)physiology remain unexplored. Accordingly, it was the aim of my PhD project to elucidate the cellular and molecular mechanisms whereby sortilin may impact APOE-isoform specific mechanisms in brain lipid profiles and promote protective or adverse effects of the lipid metabolism in AD. To do so, I made use of targeted replacement mice expressing human apoE3 or apoE4 instead of the murine protein and crossed them with mouse models either wild-type or genetically deficient for sortilin. Applying targeted lipidomics and functional investigations of the lipid metabolism in these mouse models *in vivo* and in neurons derived thereof *in vitro,* and corroborating my findings in specimens from AD patients, I aimed at a better understanding of why apoE4 is the main risk for sporadic AD and what the functional relevance of sortilin and lipids in this process may be.

3. MATERIALS AND METHODS

3.1. Reagents

3.1.1. Oligonucleotides

Table 3.1: List of DNA primers used for genotyping PCR.

Gene	Primer orientation	Primer sequence
Sortilin	Sort f2	GGG ACC AAA GGG CTA GAT TGC
	Sort r2	TCC GAA GGA GAC ACT CAC AAT TC
	bGH poly A for	ATG CGG TGG GCT CTA TGG CTT CTG

Table 3.2: List of TaqMan probes used for genotyping.

Target SNP (minor/major variant)	Assay ID
rs429358 (C/T)	C___3084793_20
rs7412 (T/C)	C____904973_10

Quantitative real-time PCR (qRT-PCR) was performed using either TaqMan probes ordered from Thermo Fisher or SYBR green dye and DNA primer ordered from Qiagen.

Table 3.3: List of TaqMan probes used for qRT-PCR.

Gene	Assay ID
Actb	Mm02619580_g1
Gapdh	Mm99999915_g1
B2m	Mm00437762_m1
Gfap	Mm01253033_m1
Tnfa	Mm00443260_g1

Vegf	Mm00437306_m1
Fabp7	Mm00445225_m1
Sort1	Mm00490905_m1
Human APOE	Hs00171168_m1
Mgll	Mm00449274_m1
Dagla	Mm00813830_m1
Faah	Mm00515684_m1
Napepld	Mm00724596_m1

Table 3.4: List of DNA primer used with SYBR green dye for qRT-PCR.

Gene	**Catalog number**
Klf10	PPM05167F-200
Mmp9	PPM03661C-200
Pparg	PPM05108C-200

3.1.2. Antibodies

All peroxidase labeled secondary antibodies for Western blotting were purchased from Sigma-Aldrich and used at the dilution 1:5000. Fluorophore-conjugated secondary antibodies for immunofluorescence were purchased from Thermo Fischer Scientific (Alexa Fluor 647 Dye) and used at the dilution 1:1000.

Table 3.5: List of primary antibodies used in this study.

Target protein	**Commercial provider**	**Catalogue number**	**Dilution**	**Application**
Rab5	Cell Signaling	#2143	1:500	IF
Rab11	Cell Signaling	#5589	1:500	IF

Tubulin	abcam	ab6046	1:1000	WB
FABP7	Millipore	ABN14	1:1000	WB
GAPDH	Genetex	GTX627408-01	1:1000	WB
APOE	Millipore	AB947	1:1000	WB
Sortilin	BD Transduction Lab.	612101	1:1000	WB
FABP5	Biovendor	RD181060100	1:1000	WB
TUJ1	Sigma-Aldrich	T8578	1:1000	WB
Sortilin	R&D Systems	AF2934	1:500	IF
Myc tag	Origene	TA150121	1:500	IF
BrdU	Linaris	LOB0030G	1:500	IH

*IF, immunofluorescence; WB, Western blotting; IH, immunohistology

3.1.3. Plasmids

Expression construct for murine FABP7 with Myc-DDK tag was bought from Origene (MR200772). Instead, the expression constructs for human apoE3 and apoE4 were kindly provided by Prof. Joachim Herz (University of Texas Southwestern Medical Center, USA).

3.1.4. Buffer solutions and cell culture media

Table 3.6: List of buffer solutions and cell culture media.

Buffer Solution	**Composition**
Enzyme solution	2 mg Cystein
	1 mM $CaCl_2$
	0.5 mM EDTA, pH = 8
	in DMEM

Stop solution	5 % FBS (Gibco, 10270106),
	1% penicillin/streptomycin (Gibco, 15150122)
	2.5 mg/ml albumin (Sigma-Aldrich, A9418)
	2.5 mg/ml trypsin inhibitor (Sigma-Aldrich, T9253)
	in DMEM
Neuronal Plating Media	2% B-27 (Gibco, 17504044)
	1% GlutaMAX (Gibco, 35050061)
	1% penicillin/streptomycin (Gibco, 15150122)
	in Neurobasal (Gibco, 21103049)
DMEM complete medium	10% FBS
	1% penicillin/streptomycin (P/S)
	in DMEM
IP lysis buffer	10 mM Tris/Cl pH 7.5;
	150 mM NaCl;
	0.5 mM EDTA;
	0.5% NP-40
	in water
IP dilution/wash buffer	10 mM Tris/Cl pH 7.5
	150 mM NaCl
	0.5 mM EDTA
	0.1% triton-100
	in water

RIPA buffer	50 mM Tris-HCl pH 7.4
	150 mM NaCl
	0.1% SDS
	0.5% sodium deoxycholate
	1% NP-40
	in water
lysis buffer	50 mMTris HCL, pH 7.4
	140 mM NaCl
	1% Triton X-100
	in water
Base solution	25 mM NaOH
	0.2 mM EDTA
	in water
Neutralization solution	40 mM Tris-HCl
	in water
Wash Buffer/dialysis buffer	5 mM tris-HCl pH 7.4
	50 mM NaCl
	5mM $MnCl_2$
	in water
Elution buffer	5 mM tris-HCl pH 7.4
	1 M NaCl
	in water

Cryoprotectant solution IH	30% glycerol
	30% ethylene glycol
	0.02 M phosphate buffer pH 7.4
	in water
Blocking solution IH	0.3% Triton
	10% donkey serum
	1% BSA
	in TBS

3.2. *in vivo* and *ex vivo* experiments

The generation of mice lacking sortilin (Jansen et al. 2007) and *Apoe* targeted replacement (Knouff et al. 1999) strains of mice has been described. All lines were backcrossed to C57Bl6/J mice for at least seven generations. Animals were routinely genotyped by PCR and qRT-PCR using the primers listed in the Chapter 3.1.1. and the genotyping procedures are described in Chapter 3.5.1. All animal experiments were approved by local ethics committees (LAGESO, Berlin, Germany). Animals were housed in the facility with the controlled environmental parameters under a 12 h light/12 h dark cycle. Mice were fed with standard chow (4.5% crude fat, 39% carbohydrates). Only male mice were used in all experiments at 10-13 weeks old, unless stated otherwise. Mice were sacrificed by cervical dislocation. Cortical brain area was rapidly dissected and frozen using dry ice. The tissues were stored at -80°C till further processing.

3.2.1. Neurogenesis

Bromodeoxyuridine (BrdU) is a thymidine analog that incorporates into dividing cells during DNA synthesis. BrdU labelling is the most used technique for studying adult neurogenesis in situ because of its ability to monitoring cell proliferation. Adult neurogenesis resides in two main locations in the adult brain, the

subventricular zone (SVZ) lining the lateral ventricles, and the hippocampal dentate gyrus (DG).

BrdU (Sigma-Aldrich, B5002) was injected intra-peritoneally (i.p.) at a concentration of 50 mg/kg body weight. A 10 mg/ml stock solution of BrdU was prepared in sterile normal saline (0.9% NaCl) by sonication for 10 minutes followed by shaking at 300 rpm for 45 minutes at room temperature in the dark. Mice were anesthetized via i. p. administration of Ketamine/Xylazine. The dose of the drugs used: Ketamine (Ketavet®, Zoetis) 150 mg/kg body weight, Xylazine (Rompun®, Bayer) 20 mg/kg body weight. Mice in the surgical plane of anesthesia were transcardially perfused with PBS and then with 4% paraformaldehyde (w/v) in PBS. Brains were dissected and postfixed with the same fixative overnight at 4°C. Brains were further rinsed in PBS and transferred in 30% sucrose (w/v) in PBS. After being equilibrated in the sucrose solution, brains were frozen and sectioned (40 µm coronally) on a sliding microtome SM2000R (Leica Biosystems). Brain free-floating sections were stored at -20°C in a cryoprotectant solution (composition in Table 3.6).

After an extensive washing in TBS-T (Tris-buffered saline with 0.1% Triton X-100), the sections were treated with 6% H_2O_2 in TBS for 30 min at RT to quench the endogenous peroxidase. To allow the anti-BrdU antibody access to the BrdU within the DNA, the sections needed a DNA hydrolysis step where they were treated with 2 N HCl for 45 min at 40°C followed by 0,1 M borate buffer, pH 8.5 for 10 min at room temperature. Then, the sections were blocked for one hour at room temperature (RT) in blocking solution. Thereafter, the sections were incubated with rat anti-BrdU overnight at 4°C in blocking solution. After being washed in TBS-T (3x), the sections were incubated with donkey anti-rat biotin SP (Jackson ImmunoResearch, 712-065-153) for two hours at RT. The VECTASTAIN® ABC Kit (Vector Laboratories) is widely accepted as one of the most sensitive, economical and reliable immunoperoxidase detection systems available to detect any molecule that is biotinylated. The kit is composed by two paired reagents: Reagent A (Avidin DH, an avidin that is modified using a proprietary process to eliminate non-specific binding) and Reagent B (biotinylated peroxidase H with enhanced enzyme activity). Thus, the sections were incubated one hour at RT with

VECTASTAIN® ABC Reagents and then for 5 minutes at RT with the peroxidase substrate solution. In this case DAB (3,3′-Diaminobenzidine) (Sigma-Aldrich, D5905) was used. DAB is a derivative of benzene oxidized by hydrogen peroxide in a reaction catalyzed by peroxidase. DAB substrate solution was prepared in TBS with fresh 30% hydrogen peroxide and 8% of NiCl (metal enhancer). The reaction was stopped with tap water (3x) and then the sections were washed in TBS (3x), and finally mounted onto glass slides using Roti®-Histokitt II mounting medium.

Bright field microscopy (Leica DMI6000B inverted microscope) was used for image acquisition of subventricular zone (SVZ) and hippocampal dentate gyrus (DG) of the mouse brain models. Finally, BrdU-positive cells were counted using the ImageJ plugin ITCN.

3.2.2. Golgi staining

Morphological alterations in neuronal dendrites and dendritic spines can be studied using the Golgi technique. FD Rapid Golgistain Kit (FD NeuroTechnologies) has not only dramatically improved and simplified the Golgi technique but has also proven to be extremely reliable and sensitive for demonstrating morphological details of neurons.

Mice were anesthetized via i. p. administration of Ketamine/Xylazine. Then, they were transcardially perfused with PBS. For the tissue preparation, brains were removed from the skull as quickly possible, rinsed with distilled water and then incubated with indicated solutions according to the manufacturer's recommendations (FD Rapid Golgistain Kit, FD NeuroTechnologies). Sections (200 µm thickness) were cut on a vibratome with the chamber temperature set at -22°C. Each section was mounted on gelatin-coated slides with a specific kit solution. After absorption of excess solution left on slide with a strip of filter paper, sections were naturally dried at room temperature for three days in the dark. For the staining procedure, sections were treated according to the manufacturer's recommendations (FD Rapid Golgistain Kit, FD NeuroTechnologies) and finally mounted using Permount™ Mounting Medium.

Bright field microscopy (Leica DMI6000B inverted microscope) was used for image acquisition of pyramidal neurons in cortical layers II/III. Subsequently, the Fiji plugin “simple neurite tracer” was used to trace the dendrites of Golgi-stained pyramidal neurons and quantified the number and length of apical and basal dendrites, as well a quantitative assessment of neuronal complexity using an additional Fiji plugin called “Sholl analysis”.

3.2.3. PPARs target genes assay

The Mouse PPAR Targets RT² Profiler PCR Array (Qiagen) enables quick and reliable gene expression analysis of 84 key genes involved in peroxisome proliferator-activated receptor (PPAR) activation and response.

Total RNA was extracted from mouse cortical tissues using the TRIzol reagent (Thermo Scientific, 15596026). Chloroform was added to the homogenates at the ratio 1:5 (v/v). The mixture was subjected to centrifugation at 12000 x g, 4°C for 10 min. The upper, aqueous phase containing RNA was taken and gently mixed with 70% ethanol at the ratio 1:1 (v/v). The resulting solution was applied to silica-membrane column of RNeasy Mini Kit (Qiagen). RNA concentrations were determined using the NanoDrop ND-1000 spectrophotometer. Equal amounts of purified RNA, 1 µg, were used for complementary DNA (cDNA) synthesis using RT^2 First Strand Kit (Qiagen).

RT-PCR measurement of PPAR target genes was performed in combination with RT2 SYBR Green ROX qPCR Mastermix (Qiagen) using the 7900 HT Fast Real time PCR System (ThermoFisher) according to the manufacturer’s recommendations (PPAR Targets RT2 Profiler PCR Array, Qiagen). The target genes analysis was performed using Data Analysis Webportal (Qiagen) which ensures that each sample has passed the PCR Array Reproducibility, RT (reverse transcription) Efficiency, and Genomic DNA Contamination quality controls.

Finally, the Ct values were extracted and the comparison in transcript levels of different genes was calculated using the cycle threshold (Ct) comparative method (2^{-ddCT}) normalizing to Ct values of internal control gene *Actb*.

3.2.2. Primary culture

Primary cortical neurons were isolated from newborn mice (postnatal day 0). Animals were sacrificed by decapitation. Cortices were rapidly dissected in cold HBSS containing Ca2+ and Mg2+ (Lonza, BE10-527F) and subjected to the digestion with papain (Sigma-Aldrich P3125) in enzyme solution for 1h at 37°C by vigorous shaking. 20-25 units of papain in 1 ml of the enzyme solution (composition in Table 3.6) were used for the digestion of one half of cortex. The digestion was stopped by replacing the enzyme solution with stop solution (composition in Table 3.6) for 5 min at 37°C under vigorous shaking. Afterwards, the tissue was washed (2x) in Neurobasal plating medium. Finally, the tissue was gently resuspended in the same medium using a pipette, and plated in 6-well plates coated with poly-D-lysine (Corning 356413) at a density of 40-60,000 cells/cm. Neurons were cultured for 10-12 days in vitro before being used for western blotting or qRT-PCR. The medium was not changed during the culture period.

Primary astrocyte cultures were prepared from newborn mice (postnatal day 0-1). Brains were rapidly dissected in cold HBSS and subjected to the digestion using mechanical dissociation (plastic Pasteur pipette and pipette tips) after enzymatic digestion with trypsin (Biochrom, # L2103-20) and DNAse (Worthington, #LS 002139). Afterwards, the tissues were washed (2x) DMEM complete medium and plated on poly-L-lysine (Sigma-Aldrich, #P1274) coated T75 flasks and maintained in DMEM complete medium. After two days, the cultures were vigorous washed with PBS prior to medium change. Cells were cultured for 4 more days before samples were collected for Western blot and qRT-PCR analyses.

3.3. *in vitro* experiments

Chinese hamster ovary (CHO-K1) cells and HEK293 were grown on 10 cm culture dishes at 37°C, 5% CO_2 in a 95% humidified environment in DMEM complete medium. Cells were subcultured at 1:6-1:12 ratio upon reaching confluency. For splitting, cells were detached from the culture dish surface using 0.05% trypsin/EDTA (Gibco 25300054). Transient transfections were performed using Lipofectamin® 2000 (Invitrogen) according to manufacturer's recommendations.

CHO stably cell line were generated by transfecting either mouse sortilin and myc-tagged mouse FABP7 (Origene, MR200772) (CHO-S/F or CHO-S) expression plasmids and by selecting transfected cells with puromyicin (10 μg/ml, Gibco, A11138-03) for sortilin and G418 (500 μg/ml, Gibco, 10131-027) for FABP7 until all non-transfected cells had died. Single cell colonies were picked, expanded, and tested for sortilin or sortilin/FABP7 expression by immunofluorescence staining and Western Blot. Stable cell lines were cultured in the presence of the respective antibiotic.

3.3.1. Co-immunoprecipitation (Co-IP)

For co-IP experiment, myc-tagged proteins were isolated by immunoprecipitation using the Myc-Trap® that utilizes small recombinant antibody fragments covalently coupled to the surface of magnetic agarose beads. In detail, CHO cells stable expressing FABP7 and sortilin were growth until confluence and then lysed in the IP lysis buffer containing protease Inhibitor cOmplete cocktail (Roche, 04693116001). The lysates were cleared by centrifugation at 12000 x rpm, 4°C for 10 minutes. Protein concentration was determined using BCA protein Assay Kit (Thermo Fisher, 23225). 300 μg of the lysates were diluted in IP dilution buffer and pre-cleared with control beads (Chromotek, bmab-20) for 15 minutes at 4°C under continuous rotation. Then the lysate were incubated with Myc-Trap Magnetic Agarose (Chromotek, ytma-20) for one hour at 4°C under continuous rotation. Antibody/protein complexes were isolated from the lysates using a magnetic rack and washed (3x) with IP wash buffer. Proteins were eluted by incubating the magnetic beads in 2x Laemmli buffer (Sigma-Aldrich, S3401-10VL) for 10 min at 95°C. Proteins were resolved on polyacrylamide gels and analyzed by Western blotting.

3.3.2. Proximity ligation assay (PLA) and co-localization studies

Proximity ligation assay (PLA) is a powerful tool to test protein interactions with high specificity and sensitivity in cells. Protein targets can be readily detected and localized with single molecule resolution and objectively quantified in unmodified cells. Typically, It employs two primary antibodies raised in different species that detect two proteins of interest. Then, if both oligonucleotide-conjugated secondary

antibodies (PLA probes) are in close proximity, this allows for their hybridization by connector oligonucleotides, forming a circular DNA strand that can be amplified by PCR (amplification step). The DNA synthesis reaction results in several-hundredfold amplification of the DNA circle. Incorporation of fluorescence-labelled oligonucleotides in the PCR product enables localized detection of protein interaction.

Here, Chinese hamster ovary (CHO-K1) cells stably overexpressing mouse sortilin and myc-tagged mouse FABP7 were grown on glass coverslips coated with 0.1 % gelatin (from porcine skin) in DPBS for 1 hour at room temperature prior to use. Gelatin was aspirated and dish quickly washed with 1X DPBS before plating. Upon 70% confluency, the cells were treated for 24 hours with conditioned medium containing 5 µg/ml of human apoE3 and apoE4. Cells were then fixed in 4% PFA for 10 minutes at room temperature, washed with DPBS (3X, 10 minutes) and stored at 4°C in DPBS for no longer than 2 weeks. Cells were permeabilized with 0.3% triton/PBS for 15min RT. Then, the cells were blocked, incubated with primary antibodies and subjected to proximity ligation assay (PLA) using Far-Red PLA probes, followed by ligation and amplification performed according to the manufacturer's recommendation (Sigma-Aldrich).

To determine the degree of co-localization between FABP7-Sortilin (PLA signals) with endosomal markers, after the PLA amplification step, the cells were incubated with primary and secondary antibodies to co-stain the cells for the indicated marker proteins. Antibodies used were anti-Rab5 (Cell Signaling, #2143, 1:500), anti-Rab11 (Cell Signaling, #5589, 1:500), as well as Alexa Fluor 647-conjugated secondary antibody. Finally, the cells were counterstained with DAPI and mounted in DAKO fluorescence mounting medium.

For Confocal images of immunofluorescent stained cells, a Leica SPE laser-scanning microscope was used at the MDC imaging core facility. Images were acquired using the Leica LAS AF Lite software. Microscopy images were quantified using Fiji software. Colocalization analysis was performed with the Colocalization Threshold plugin with manual selection of the region of interest (ROI). Single z-plane images were used for calculating Mander's coefficient (tM) that is proportional to the fluorescence intensity of the colocalizing pixels in each

channel with tM=0 representing no colocalization and tM=1 representing perfect colocalization (MANDERS et al. 1993).

3.3.3. Protein stability by the cycloheximide chase assay

Protein stability of FABP7 in CHO cells has been achieved by cycloheximide (CHX) (Sigma-Aldrich, C7698), an antibiotic produced by the bacterium *Streptomyces griseus*. CHX is an inhibitor of protein biosynthesis due to its prevention in translational elongation. It is broadly used in cell biology in terms of determining the half-life of a given protein without confounding contributions from transcription or translation.

In details, cells expressing (CHO-S) or lacking sortilin (CHO) were seeded in 6-well plates and transiently transfected with a FABP7 expression construct. 48 hours post transfection, replicate cultures of transfected cells were treated with 10 µg/ml of cycloheximide in DMEM complete medium and collected at time points 0, 4, 8, and 12 hours later. Confluent 6-wells were lysed in lysis buffer containing proteinase inhibitors for 30 minutes at 4 °C. Cell debris was removed by centrifugation for 10 min at 12,000 x rpm at 4 °C and the supernatant was transferred to a new tube. Protein lysates were analyzed by Western Blot and levels of FABP7 were quantified using the Image Studio Lite software and normalized to the loading control protein GAPDH.

3.3.4. APOE production

HEK 293 cells were plated in 10 cm dishes and transiently transfected using Lipofectamine 2000 (ThermoFisher) according to manufacturer's instructions with pcDNA3.1 zeo(+) human apoE3, or pcDNA3.1 zeo(+) human apoE4. APOE lipoproteins were naturally secreted from cells. Cell supernatants were conditioned for 48 hours in DMEM without FCS (Chen et al. 2010). Then, cells debris were removed by centrifugate the supernatant at 300g per 3 minutes. Finally, the concentration of APOE isoforms in the cell media was determined by western blot analysis comparing APOE signal intensities to those from serial dilutions of recombinant human APOE (MBL, JM-4699-500) included in the same blots.

3.4. Human studies

3.4.1. Brain tissue

Brain autopsy specimens from the frontal cortex of AD patients and control subjects were obtained from the Netherlands Brain Bank (Netherlands Institute for Neuroscience, Amsterdam) and the MRC London Brain Bank for Neurodegenerative Diseases (Institute of Psychiatry, King's College London). The ethnicity of samples was white. All material was collected from donors for or from whom a written informed consent for a brain autopsy and the use of the material and clinical information for research purposes had been obtained by the Netherlands Brain Bank or the MRC London Brain Bank. Detailed personal information, including age, gender, neuropathological stage, *APOE* genotypes, of the individuals were provided by the brain banks. Pieces of brain tissue were either lysates for western blotting or used for lipidomics analysis.

3.4.2. CSF samples and APOE-containing particles isolation

Cerebrospinal fluid (CSF) samples from AD patients and controls were obtained from a local biomaterial bank. The study was approved by an institutional review board (Ethikausschuss 2 Charité; BIH CRG 2a, EA2/118/15). Written informed consent was obtained from all individuals prior to participating in this study.

Thus, human liquor and murine HDL samples were subjected to APOE affinity chromatography using HiTrap Heparin columns (GE Healthcare, 17-0406-01). First the samples were dialyzed using Slide-A-Lyzer Dialysis Cassette (ThermoFisher, 66382) in wash/dialysis buffer (see Table 3.6) overnight at 4°C in agitation. Then according to the manufacturer's protocol HiTrap™Heparin HP Column was equilibrate with wash/dialysis buffer and the CSF samples were conveyed over the column. The flow-through (APOE-free particles) was collected, while APOE-containing particles stick to the column. Heparin-bound lipoproteins were eluted with elution buffer containing high concentration of salt and then concentrated using Amicon centrifugal filter units (Millipore, UFC801024) previous washed with 1 % albumin Fatty acids-Free in PBS. All CSF samples were stored at -80°C until further processing for lipidomics analyses. The enrichment of APOE

in the eluate fractions but not in the heparin column flow-through is documented by western blotting.

3.5. Common and shared techniques

Plasmid cDNA preparation and isolation form bacteria, SDS polyacrylamide gel electrophoresis and Western Blot were performed using standard procedures. Of note, mouse tissues lysates for immunoblotting were obtained by homogenization of tissues in RIPA buffer, instead mouse primary culture and in vitro cells with lysis buffer (see Table 3.6 for buffer solutions). The intensities of immunoreactive bands signals were quantified by densitometric scanning of blots using the Image Studio Lite software.

3.5.1. Genotyping

Genomic DNA for PCR or SNP genotyping was obtained from mouse ear or tail. Biopsied tissue was incubated for 30 min at 95°C in base solution, followed by addition of the equal volume of neutralization solution.

Extracted DNA was used in PCR with the following cycling conditions: (1) initial denaturation (2 min, 94°C), (2) denaturation (15 sec, 94°C), (3) annealing (15 sec, 57°C for sortilin) (4) elongation (30 sec, 72°C). Steps (2) to (4) were repeated 40 times in total. Primers used for PCR are listed in Table 3.1. The composition of the reaction mixture was as follows: Taq DNA polymerase (NEB M0267; 0.03 U/µl), 1x ThermoPol Buffer, 0.2 mM of each deoxynucleotide triphosphates, 0.2 µl primers. PCR products were resolved on 2% agarose gels. Expected sizes of PCR products used for determination of mouse genotypes were for sortilin allele – 293 bp (WT) and 206 bp (KO).

APOE isoforms genotyping was performed using pre-designed TaqMan-based SNP genotyping assays (Thermo Fisher). These assays contain two allele-specific probes labelled either with FAM or VIC dye that specifically recognize the major or minor allele, respectively. Genomic DNA was diluted to a concentration of 1 ng/µl and 5 µl of the diluted DNA solution were pipetted into a 384-well-plate. A water sample was included as negative control. Covered with a dry paper tissue, wells were dried over night before adding the SNP genotyping probe-mastermix. PCR

amplification and fluorescent measurement of the wells was performed using QuantStudio 6 Flex Real-Time PCR-System (Thermo Fisher) SNP genotypes of all samples were assigned by the software based on FAM/VIC fluorescence ratios.

3.5.2. Quantitative RT-PCR

To extract total RNA from mouse tissues, they were first homogenized in TRIzol reagent (Thermo Scientific, 15596026). Chloroform was added to the homogenates at the ratio 1:5 (v/v). The mixture was subjected to centrifugation at 12000 x g, 4°C for 10 min. The upper, aqueous phase containing RNA was taken and gently mixed with 70% ethanol at the ratio 1:1 (v/v). The resulting solution was applied to silica-membrane column of RNeasy Mini Kit (Qiagen).

DNase treatment of the sample was performed directly on the purification column by addition of RNase-free DNase I (Qiagen) prepared according to manufacturer's instructions and incubated for 15 min at room temperature after the first washing step. RNA concentrations were determined using the NanoDrop ND-1000 spectrophotometer. Equal amounts of purified RNA, 50 ng to 1 µg, were used for complementary DNA (cDNA) synthesis using High Capacity RNA to cDNA Kit (Applied Biosystems).

Samples were measured in triplicates using the 7900 HT Fast Real time PCR System (Thermo Fisher) using commercially available Taqman Gene Expression Assays or DNA oligonucleotides flanking the target region and SYBR green dye. TaqMan probes and DNA oligonucleotides are specified in Table 3.3 and Table 3.4. The data were analysed using the cycle threshold (CT) comparative method (2^{-ddCT}) normalizing to CT values of internal control gene. The Ct value of each sample represents the number of cycles needed for the emitted fluorescence signal to cross a defined threshold. The abundance of the target mRNA is therefore inversely correlated to the Ct value. The Ct value for a house keeping mRNA was subtracted from the Ct value for the mRNA of interest to ensure equal amount of cDNA in each well (dCt). For comparison of multiple samples, the dCt value of the internal control was subtracted from the dCt values of the other samples (ddCt) and data were presented as $\log_2$ change in expression.

In the case of SYBR green, the PCR specificity was verified performing the dissociation (melting) curve analysis. Post-amplification melting-curve analysis is a simple, straightforward way to check real-time PCR reactions for primer-dimer artefacts and to ensure reaction specificity. As the temperature steadily increases, the fluorescence will drop suddenly each time the temperature reaches the characteristic melting point (Tm) of a DNA fragment. Tm refers to the temperature at which 50% of DNA in a sample has denatured from double-stranded DNA (dsDNA) to single-stranded DNA (ssDNA). Pure, homogeneous PCR products produce a single, sharply defined melting curve with a narrow peak. In contrast, primer dimers melt at relatively low temperatures and have broader peaks.

3.5.3. Lipid analysis

Targeted lipidomics was performed on brain cortex specimens from human subjects or mice or on APOE-containing lipoproteins isolated from human cerebrospinal fluid by the company Lipidomix GmbH (Berlin, Germany) (as followed.

For FA profiling, 30 mg of human or mouse brain cortex were hydrolyzed with 100 µl 10 mol/l NaOH within 60 min at 80°C. The samples were neutralized with 100 µl acetic acid. An 50 µl aliquot was diluted 1:10 with methanol containing internal standards (50 µg of C15:0 and C21:0; 5 µg of C20:4-d8 and C18:2-d4, and 1 µg of C20:5-d5 and C22:6-d5; Cayman Chemical, Ann Arbor MI). HPLC measurements were performed using an Agilent 1290 HPLC system with binary pump, autosampler and column thermostat equipped with a Phenomenex Kinetex-C18 column 2.6 µm, 2.1 x 150 mm column (Phenomenex, Aschaffenburg) using a solvent system of acetic formic acid (0.1%) and acetonitrile. The solvent gradient started at 70 % acetonitrile and was increased to 98 % within 10 min and kept until 14 min with a flow rate of 0.4 ml/min and 5 µl injection volume. The HPLC was coupled with an Agilent 6470 triplequad mass spectrometer with electrospray ionisation source and operated in negative selected ion mode.

For eCB profiling, 10 mg cortex tissue was homogenized in 300 µl distilled water. Then, 25 µl citric acid (0.4 mol/l), 10 µl of internal standards (10 µg/ml DHA-Ethanolamid-D4, Anandamid-D4, EPA-Ethanolamid-D4; Cayman Chemical, Ann Arbor MI) and 1 ml ethyl acetate were added. The samples were shaken for

10 min, centrifuged for 3 min at 3500 rpm and the upper phase recovered. Next, 1 ml ethyl acetate was added to the lower (sample) phase, followed by shaking for further 10 min and centrifugation for 3 min at 3500 rpm. Again, the upper phase was recovered and both supernatants combined. The solvent was removed to dryness at 40°C under a stream of N_2, before the pellets were resuspended in 100 µl acetonitrile and eCB measured. HPLC-measurement was performed using an Agilent 1290 HPLC system with binary pump, autosampler, and column thermostat equipped with a Phenomenex Kinetex-C18 column 2.6 µm, 2.1 x 150 mm column (Phenomenex, Aschaffenburg, DE) using a solvent system of formic acid (0.1 %) and methanol. The solvent gradient started at 5 % methanol and was increased to 95 % within 10.6 min under gradient conditions and kept until 15 min with a flow rate of 0.7 ml/min and a 10 µl injection volume. The HPLC was coupled with an Agilent 6490 triplequad mass spectrometer with atmospheric pressure chemical ionization source operated in positive selected ion mode.

3.5.4. Statistical analysis

Statistical analysis was performed using the GraphPad Prism 7.0 software. Two experimental groups were compared using an unpaired Student's t-test. For experiments, when testing for the influence of two independent variables, two-way ANOVA with Bonferroni multiple comparison post-test was used. P-values of less than 0.05 were considered statistically significant with * representing $p<0.05$, ** representing $p<0.01$, *** representing $p<0.001$, and **** representing $p<0.0001$. All quantitative data are shown as the mean ± standard error of the mean (SEM), if not otherwise stated.

4. RESULTS

4.1. The fatty acid profile is altered in the brain of mice lacking sortilin and with apoE4 genotype

Lipids are fundamental for the structural and functional integrity of the brain and APOE, the most abundant apolipoprotein in the central nervous system, represents the major carrier of cholesterol and phospholipids to neurons (Holtzman and Herz 2012). Thus, alteration of brain lipid homeostasis may explain the Alzheimer's disease (AD) risk associated with the apoE4 variant in humans. However, this area of research has been understudied as the amyloid and tau hypotheses have dominated the field of AD research for many years. Previously, Dr. Anne-Sophie Carlo in the Willnow laboratory found that sortilin controls murine lipoprotein metabolism by acting as a neuronal receptor for APOE. Moreover, loss of sortilin results in an increase in brain lipid sulfatides (Carlo et al. 2013). Consequently, in order to elucidate the relevance of sortilin for APOE-dependent brain lipid homeostasis and to explain the risk of AD associated with the human apoE4 but not the apoE3 variant, lipidomics analyses were performed in mice either wild-type (WT) or homozygous for the *Sort1* null allele (KO) and expressing the human variants apoE3 (E3) or apoE4 (E4). More precisely, the murine *Apoe* gene locus in these mice was replaced with genes encoding the human isoforms E3 or E4 (Knouff et al. 1999). These two lines were crossed with mice either wild-type or genetically deficient for sortilin (Jansen et al. 2007).

In the brain, fatty acids (FA) are enriched, predominantly esterified to other lipids (total FA) such as cholesterol and phospholipids. Due their multitude of functions as signaling molecules, brain FA receive more and more attention in neuroscience. In collaboration with the company Lipidomix (Campus Berlin-Buch), cortices of my four mouse strains were isolated and subjected to liquid chromatography-mass spectrometry (LC-MS) to establish total cholesterol and fatty acid profiles. While the total cholesterol profile was unaltered (Figure 4.1A) comparing genotypes, the pool of total fatty acids was decreased in (E4;WT), (E4;KO) and (E3;KO) mice compared to (E3;WT) animals. Of note, no alteration in total FA content was observed in (E4;WT) compared to (E4;KO) mice (Figure 4.1B).

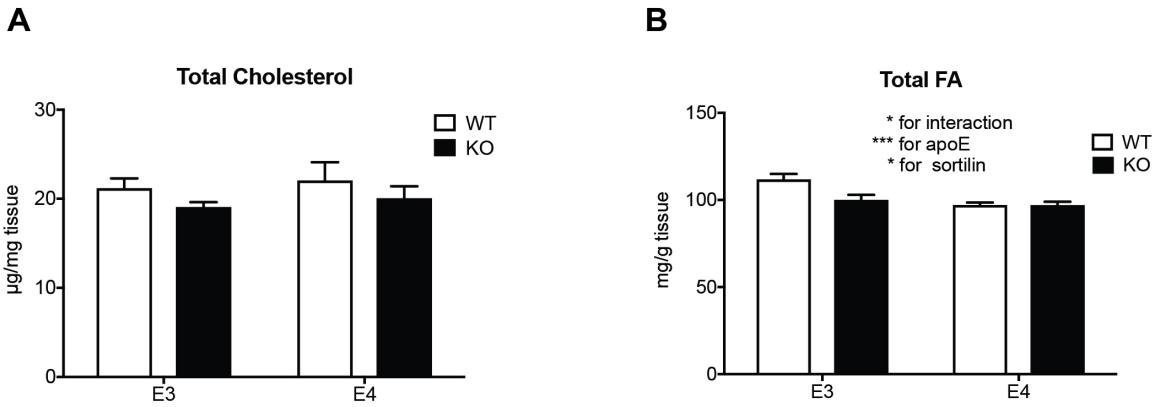

Figure 4.1: Total FA in murine brain cortex are altered by sortilin and E4 genotype.

(A) Levels of total cholesterol and (B) total fatty acids (FA) were quantified by liquid chromatography-mass spectrometry (LC-MS) in brain cortices of apoE3 and apoE4-targeted replacement mice at 3 months of age. The mice were either WT or KO for sortilin (E3;WT, E3;KO, E4;WT or E4;KO). Data are shown as mean ± SEM. n=6-12 animals per genotype. The significance of data was determined by Two-way ANOVA followed by Bonferroni post-hoc analysis (*, $p<0.05$; ***, $p<0.001$).

Fatty acids can be classified as saturated or unsaturated depending on the absence or presence of double bonds in their carbon chain. FA that have more than one carbon-carbon double bond are called polyunsaturated fatty acids (PUFA), while FA with only one carbon-carbon double bond are referred as monounsaturated FA. Moreover, unsaturated FA can be further classified depending on the position of carbon-carbon double bonds along the carboxylic acid chain (omega, ω; n-) (Fahy et al. 2005). To better understand which lipids were altered in the pool of FA measured above, in-depth analysis of mouse brain cortices according to FA lipid classes was performed. From this analysis, no obvious alterations in saturated and monounsaturated lipids were observed (Figure 4.2).

Further analysis of omega-6 and omega-3 unsaturated FA, the two most prominent and important PUFA present in the brain, revealed neither a change in arachidonic acid (ARA) (Figure 4.3A) nor in other members of the omega-6 PUFA class. Of note, an effect of the APOE allele was seen for linoleic acid, osbond acid and ecosadienoic acid (Figure 4.3B).

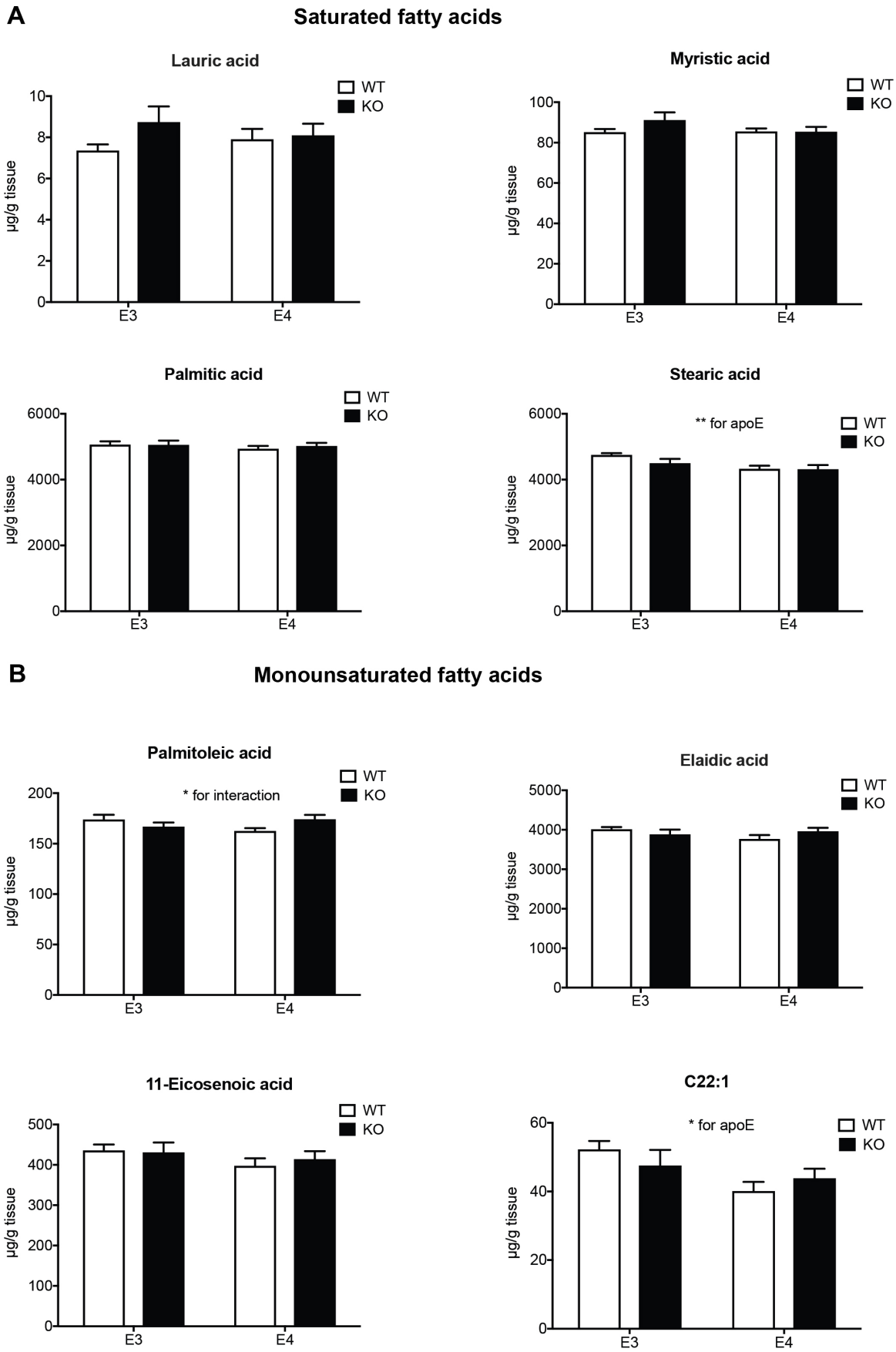

Figure 4.2: Saturated and monounsaturated lipids are unchanged in the mouse brain lacking sortilin.

(A) Saturated and (B) monounsaturated fatty acids were quantified by liquid chromatography-mass spectrometry (LC-MS) in brain cortices of E3 and E4-targeted replacement mice at 3 months of age. Mice were either WT or KO for sortilin (E3;WT, E3;KO, E4;WT or E4;KO). Data are shown as mean ± SEM. n=12 animals per genotype. The significance of data was determined by Two-way ANOVA followed by Bonferroni post-hoc analysis (*, p<0.05; **, p<0.01).

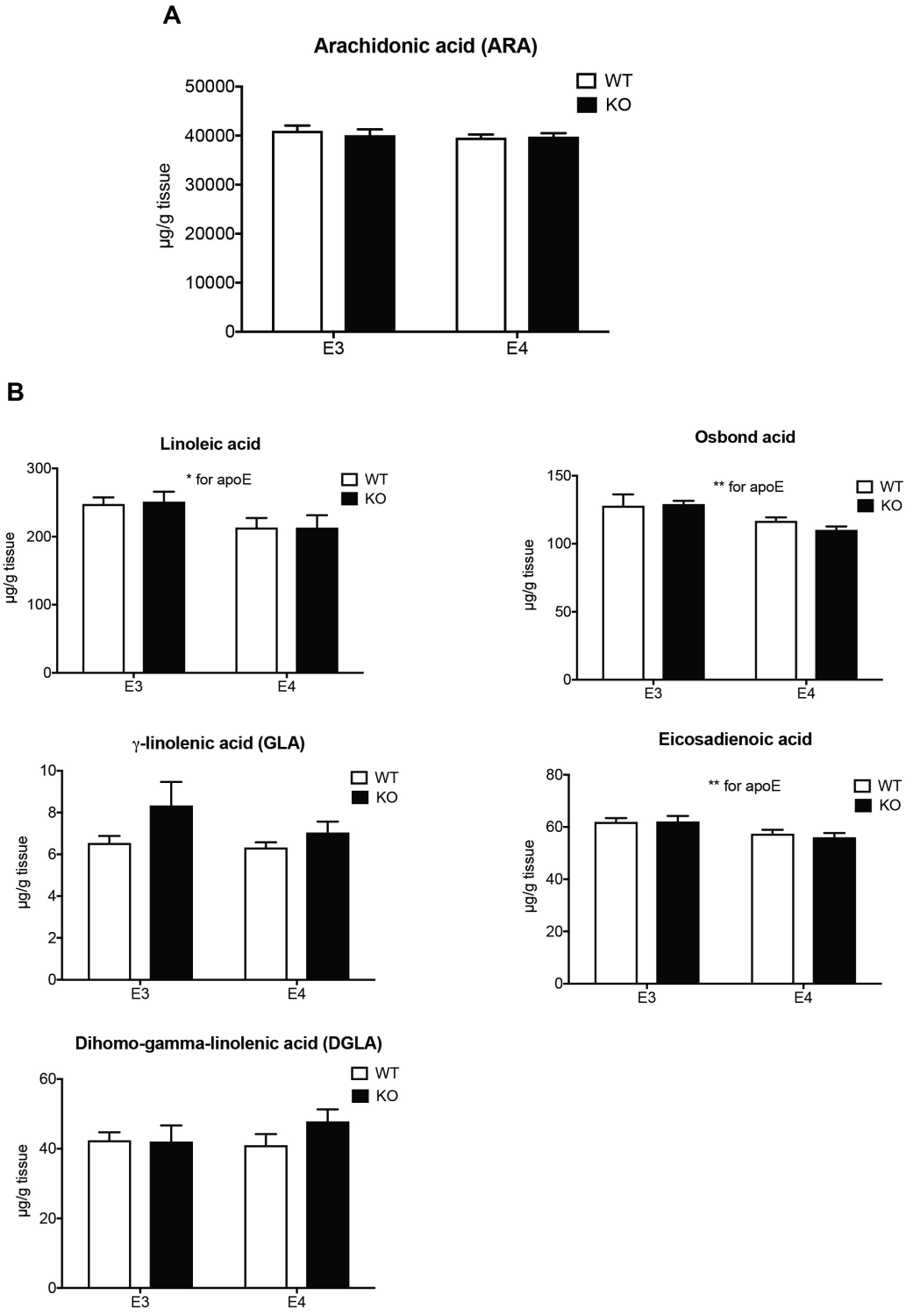

Figure 4.3: Arachidonic acid levels are unchanged between the mouse brain models.

(A) Levels of arachidonic acid (ARA) and (B) other unsaturated omega-6 lipids were quantified by liquid chromatography-mass spectrometry (LC-MS) in brain cortices of E3 and E4-targeted replacement mice at 3 months of age, either WT or KO for sortilin (E3;WT, E3;KO, E4;WT or E4;KO). Data are shown as mean ± SEM. n=12 per genotype. The significance of data was determined by Two-way ANOVA followed by Bonferroni post-hoc analysis (*, p<0.05).

However, a change was observed in the omega-3 PUFA docosahexaenoic acid (DHA) with levels being decreased in (E4;WT), (E4;KO), and (E3;KO) animals compared to (E3;WT) mice.

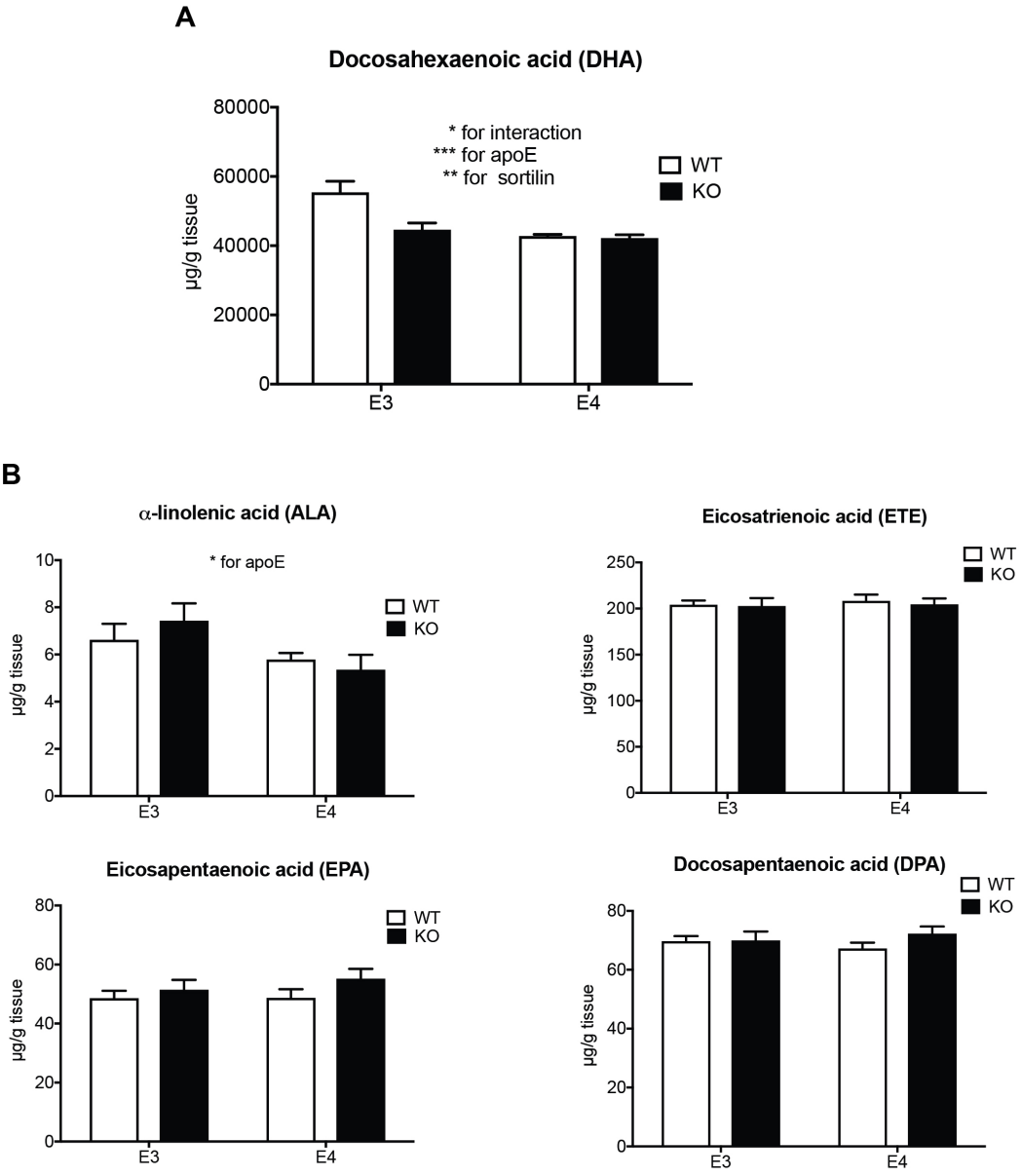

Figure 4.4: Docosahexaenoic acid levels in the murine brain are altered by sortilin and apoE4 genotype.

(A) Levels of docosahexaenoic acid (DHA) and (B) other omega-3 PUFA were quantified by liquid chromatography-mass spectrometry (LC-MS) in the brain cortices of E3 and E4-targeted

replacement mice at 3 months of age, either WT or KO for sortilin (E3;WT, E3;KO, E4;WT or E4;KO). Data are shown as mean ± SEM. n=12 animals per genotype. The significance of data was determined by Two-way ANOVA followed by Bonferroni post-hoc analysis (*, $p<0.05$; **, $p<0.01$; ***, $p<0.001$).

As seen for total FA before, the presence or absence of sortilin did not affect DHA levels in E4 mice (Figure 4.4A). While most members of the omega-3 lipid class were not altered, an effect of the APOE allele was however seen for linolenic acid (Figure 4.4B).

4.2. The DHA-based metabolite synaptamide is altered by sortilin and apoE4 genotype

DHA is one of the most extensively studied lipids in the brain. The continued interest in this lipid may be explained by its significant neuroprotective impact. Indeed, several studies have demonstrated that DHA has a positive impact during aging and in neurodegenerative diseases, such as AD (Echeverría et al. 2017). However, DHA is not acting alone as several of its beneficial effects are mediated by metabolites derived from enzymatic modification of DHA. In detail, DHA can be processed by a number of different enzymes such as lipoxygenase (LOX), cytochrome P450 (CYP), or N-acyl phosphatidylethanolamine-specific phospholipase D (NAPE-PLD) into hydroxy-docosahexaenoic acid (HDHA), epoxy-docosapentaenoic acid (EDP), or dihydroxy-docosahexaenoic acid (DiHDHA) and N-docosahexaenoylethanolamine (synaptamide), respectively (Figure 4.5A). These DHA-derived bioactive lipids have pleiotropic roles in the brain that include the regulation of inflammation, synaptic plasticity, and aging (Kuda 2018). No alterations in HDHA and DiHDHA levels were observed in the brains of mice expressing E3 or E4. However, an increase of EDP lipids were detected in the brain cortex of (E4;WT) and (E4;KO) compared to the respective (E3;WT) and (E3;KO) mice (Table 4.1). By contrast, synaptamide was decreased in (E4;WT), (E4;KO), and (E3;KO) mice compared with (E3;WT) animals. As seen for the total FA and DHA before, the presence or absence of sortilin did not affect synaptamide levels in E4 mice (Figure 4.5B). Although yet poorly studied, early work showed that synaptamide is structurally similar to the endocannabinoid (eCB) anandamide (Kim et al. 2011). For this reason, synaptamide is often called an

eCB-like lipid. eCBs are well-known PUFA-derived metabolites that control neuroprotective and pro-neurogenic processes. With relevance to my studies, eCBs have shown therapeutic potential in brain ageing and neurodegenerative conditions (Benito et al. 2007). Hence, further lipidomics analyses was performed to study if eCBs other than synaptamide were also altered in the mouse brain in response to sortilin and *APOE* genotypes.

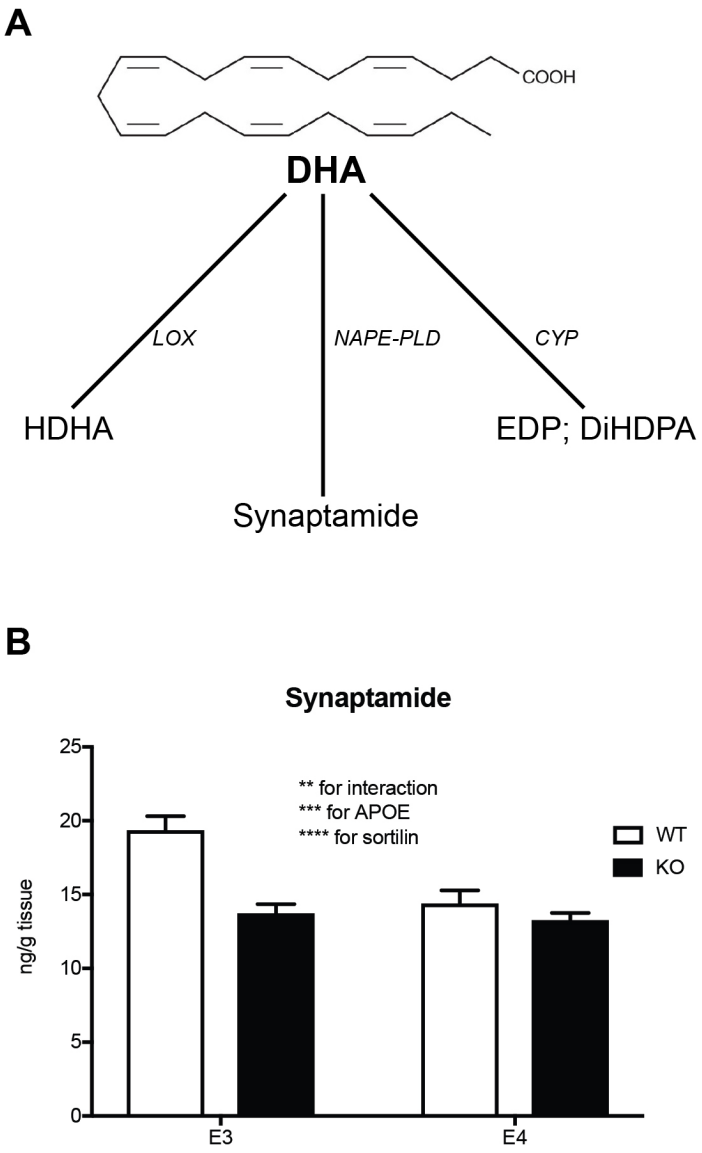

Figure 4.5: Synaptamide levels are affected by sortilin and E4 genotype.

(A) Pathways to produce DHA-based metabolites. (B) Synaptamide levels were quantified by liquid chromatography-mass spectrometry (LC-MS) in brain cortices of E3 and E4-targeted replacement mice at 3 months of age, either WT or KO for sortilin (E3;WT, E3;KO, E4;WT or E4;KO). Data are shown as mean ± SEM. n=12 animals per genotype. The significance of data was determined by

Two-way ANOVA followed by Bonferroni post-hoc analysis (*, p<0.05; ***, p<0.001; ****, p<0.0001).

Lipid Name	Enzyme	2way ANOVA
7,8-EDP	CYP	* For APOE
10,11-EDP	CYP	* For APOE
13,14-EDP	CYP	* For APOE
16,17-EDP	CYP	* For APOE
19,20-EDP	CYP	* For APOE
7,8-DiHDPA	CYP	ns
10,11-DiHDPA	CYP	ns
13,14-DiHDPA	CYP	ns
16,17-DiHDPA	CYP	ns
19,20-DiHDPA	CYP	ns
4-HDHA	LOX	ns
7-HDHA	LOX	ns
8-HDHA	LOX	ns
10-HDHA	LOX	ns
11-HDHA	LOX	ns
13-HDHA	LOX	ns
14-HDHA	LOX	ns
16-HDHA	LOX	ns
17-HDHA	LOX	ns
20-HDHA	LOX	ns
21-HDHA	LOX	ns
22-HDHA	LOX	* For sortilin

Table 4.1: DHA-derived metabolites are unchanged comparing the mouse brain models.

Epoxy-docosapentaenoic acid (EDP), dihydroxy-docosahexaenoic acid (DiHDHA), and hydroxy-docosahexaenoic acid (HDHA) were quantified by liquid chromatography-mass spectrometry (LC-MS) in brain cortices of E3 and E4-targeted replacement mice at 3 months of age, either WT or KO for sortilin (E3;WT, E3;KO, E4;WT or E4;KO). n=9-12 animals per genotype. The significance of data was determined by Two-way ANOVA followed by Bonferroni post-hoc analysis (*, $p<0.05$).

No alterations in the levels of the synaptamide analogue anadamide (AEA) or of linoleoyl-ethanolamide (LEA) were found (Figure 4.6A). By contrast, levels of 2-arachidoylglycerol (2-AG) were increased in (E4;WT), (E4;KO), and (E3;KO) mice compared to (E3;WT) animals (Figure 4.6B). Conversely, levels of palmitoyl-ethanolamide (PEA) and oleyl-ethanolamide (OEA) were decreased in (E3;KO) and (E4;KO) mice compared to the corresponding sortilin WT mice (Figure 4.6C).

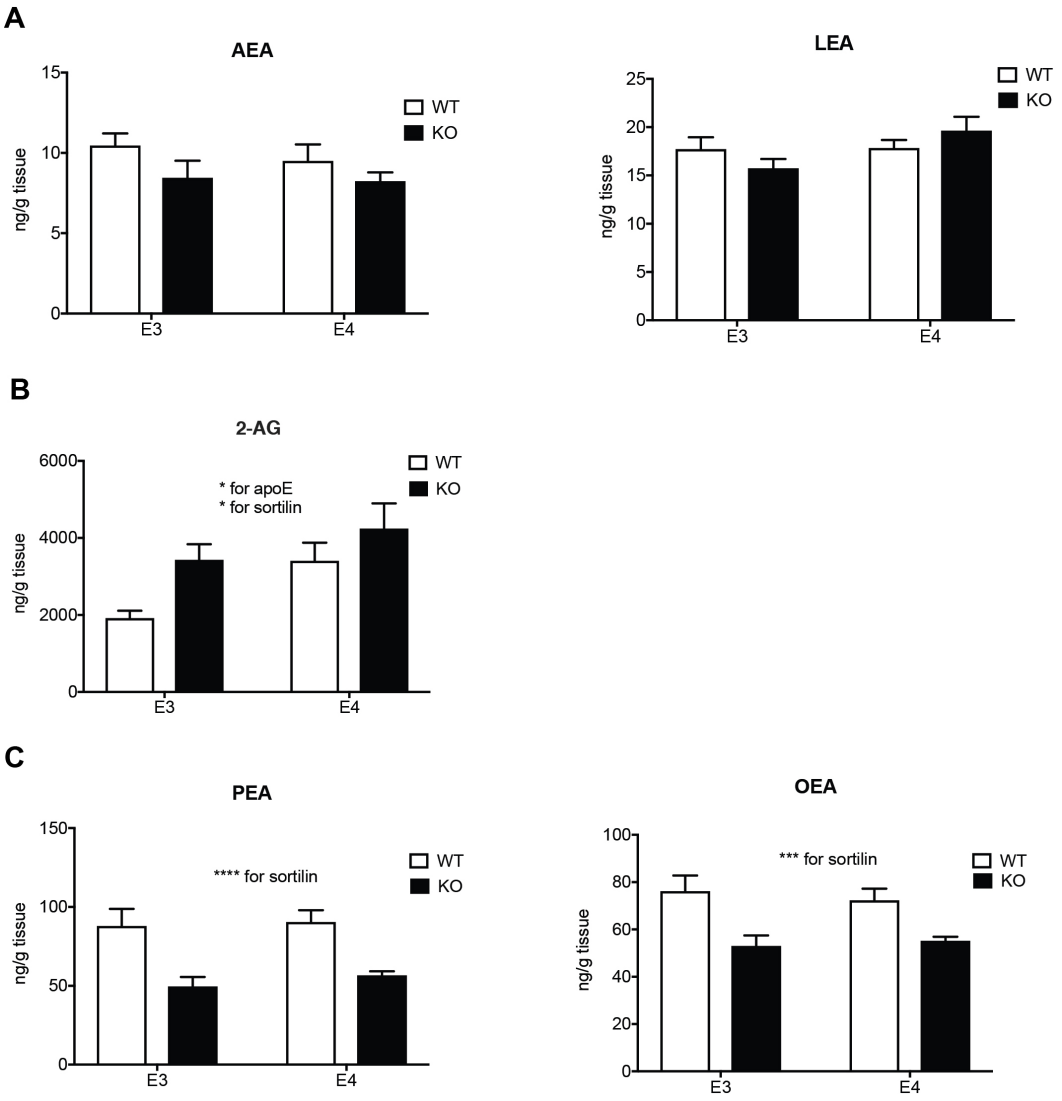

Figure 4.6: 2-AG levels are altered by sortilin and E4 allele.

(A) Levels of anadamide (AEA) and linoleoyl-ethanolamide (LEA), as well as (B) 2-arachidoylglycerol (2-AG), and (C) palmitoyl-ethanolamide (PEA) and oleyl-ethanolamide (OEA) lipids were quantified by liquid chromatography-mass spectrometry (LC-MS) in brain cortices of E3 and E4-targeted replacement mice at 3 months of age, either WT or KO for sortilin (E3;WT, E3;KO, E4;WT or E4;KO). Data are shown as mean ± SEM. n=12 animals per genotype. The significance of data was determined by Two-way ANOVA followed by Bonferroni post-hoc analysis (*, $p<0.05$; ***, $p<0.001$; ****, $p<0.0001$).

As in the murine brain, I also observed alterations in PUFA and eCB homeostasis in the brains of patients suffering from AD. Lipidomics analyses of frontal cortex specimens of AD patients showed changes reflecting the observed alterations in mice. Thus, the levels of synaptamide were significantly decreased in *APOE4/4* compared with *APOE3/3* carriers.

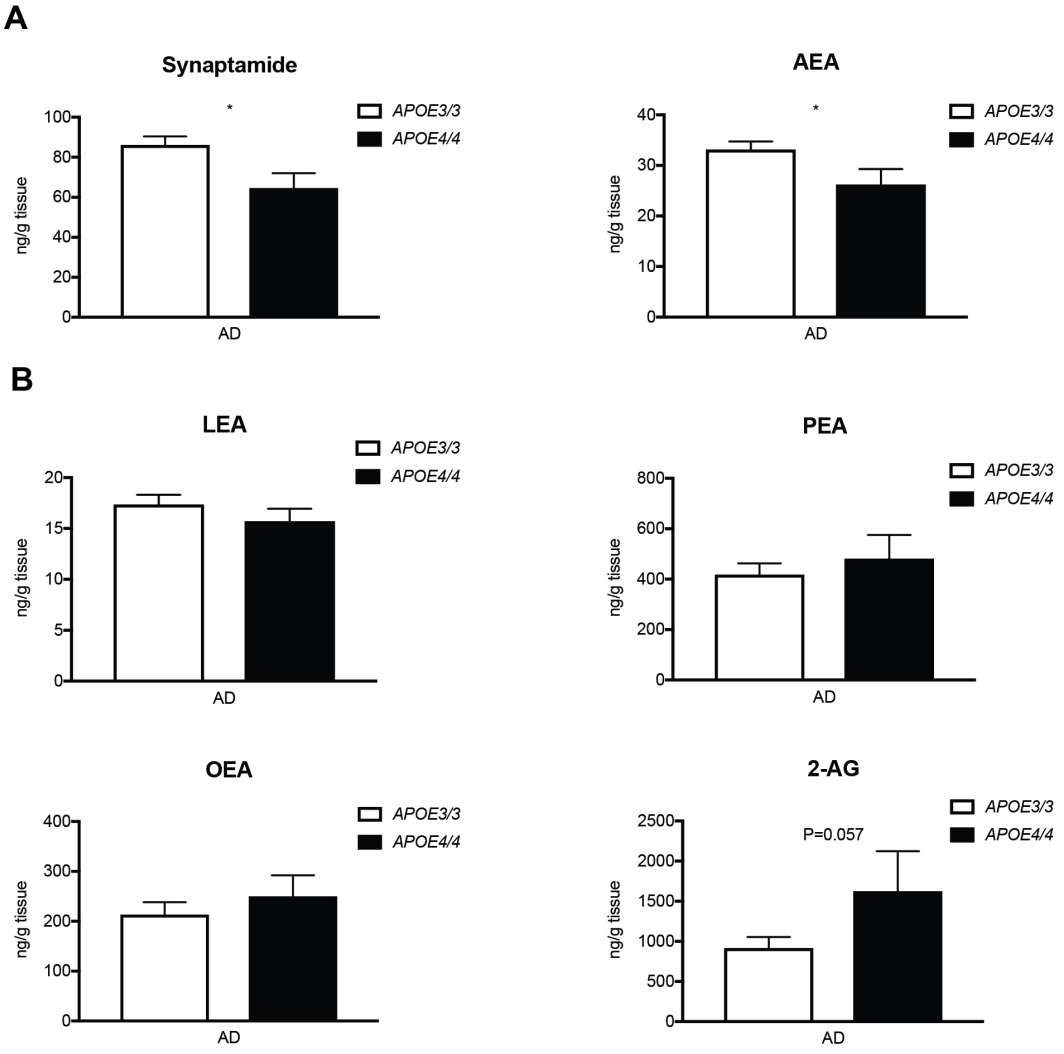

Figure 4.7: Synaptamide and AEA levels are altered in the human brain of AD patients.

Levels of synaptamide and AEA (A), and of LEA, PEA, OEA, and 2-AG (B) were quantified by liquid chromatography-mass spectrometry (LC-MS) in prefrontal cortex specimens of AD patients either *APOE3/3* or *APOE4/4* (n=10 for *APOE4/4*, n=34 for *APOE3/3*). Values are mean ± SEM. The significance of data was determined by Student's *t*-test (*, p<0.05).

Moreover, the levels of AEA were also decreased in *APOE4/4* vs. *APOE3/3* patients (Figure 4-7A), whereas the levels of 2-AG, OEA, LEA, and PEA were unaltered (Figure 4.7B). In accordance with findings in mice, levels of 2-AG were increased in *APOE4/4* compared to *APOE3/3* carriers with a *p* value that almost reached significance (p=0.057).

4.3. Neurogenesis and neuroplasticity are not affected by sortilin and *APOE* genotypes

It is now well-established that after birth new neurons are generated from neuronal stem cells (NCS) in the mammalian brain. Adult neurogenesis proceeds in two regions of the mammalian brain, namely the subgranular layer of the hippocampal dentate gyrus (DG) and the subventricular zone (SVZ) of the lateral ventricles. Adult neurogenesis plays an important role in learning and memory through the regulation of synaptic plasticity and ageing (Bartsch and Wulff 2015). Several lipids, including PUFA and eCBs, have been reported to affect adult neurogenesis. For example, adult rats fed DHA show an increase in neurogenesis in the hippocampi, due to enhancement of neuronal proliferation and suppression of cell death (Kawakita et al. 2006). Synaptamide was found to induce neuronal differentiation of NCS at concentrations even lower than those required from DHA (Rashid et al. 2013). Finally, inhibition of diacylglycerol lipases (DAGL), the enzyme important for 2-AG synthesis, suppresses neuronal proliferation in adult mice (Goncalves et al. 2008). Given the changes of PUFA and eCBs in mice deficient for sortilin, I next analyzed adult neurogenesis in the brains of the respective mouse models. The commonly used methods to query adult neurogenesis *in vivo* is the application of 5'-bromo-2'-deoxyuridine (BrdU). BrdU is a thymidine analogue incorporated into replicating DNA of proliferating cells. It's retained in the genome in subsequent cell divisions and can be detected using specific antibodies. To study adult neurogenesis in my mouse models, I injected BrdU intraperitoneally into mice. After 24 hours, the mice were sacrificed and their

brains were subjected to immunohistological detection of BrdU-positive cells in the hippocampal DG (Figure 4.8A). In the DG of 3 month old mice, the presence or absence of sortilin did not impact the extent of adult neurogenesis as no change in the number of BrdU-positive cells was seen in (E3;KO) compared to (E3;WT) mice (Figure 4.8B).

In rodents, adult neurogenesis is essential for olfaction as neural progenitor cells generated in the SVZ migrate along the rostral migratory stream to form distinct subtypes of neurons in the olfactory bulbs (Carleton et al. 2003).

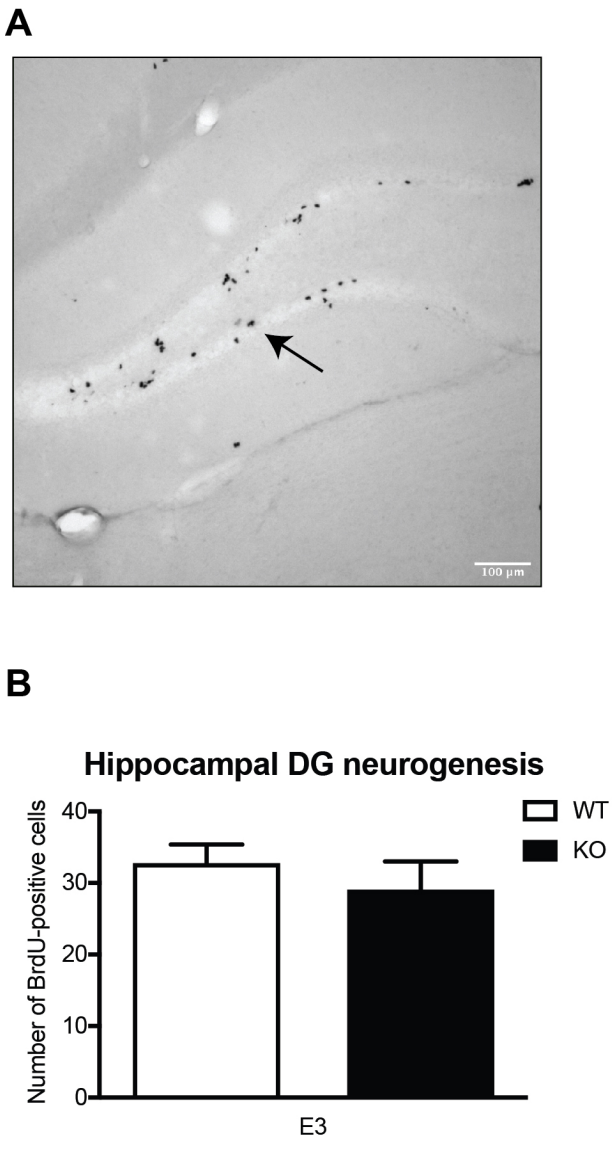

Figure 4.8: Adult neurogenesis in the dentate gyrus (DG) of E3 mice is not impacted by sortilin deficiency.

(**A**) Immunohistochemical detection of BrdU-positive cells in the hippocampal DG of (E3;WT) and (E3;KO) mice at 3 months old after 24h of BrdU application. Scale bar: 100 µm. (**B**) Quantification

of the total number of BrdU-positive cells in the hippocampal DG. Three to five coronal sections (40 μm) from each animal were used for analysis. (n=3 animals per genotype). Values are mean ± SEM.

Like in the stem cell niche of the DG, SVZ neurogenesis was also not affected by sortilin deficiency in E3 mice as the numbers of BrdU-positive cells were unchanged comparing (E3;WT) and (E3;KO) mice (Figure 4.9).

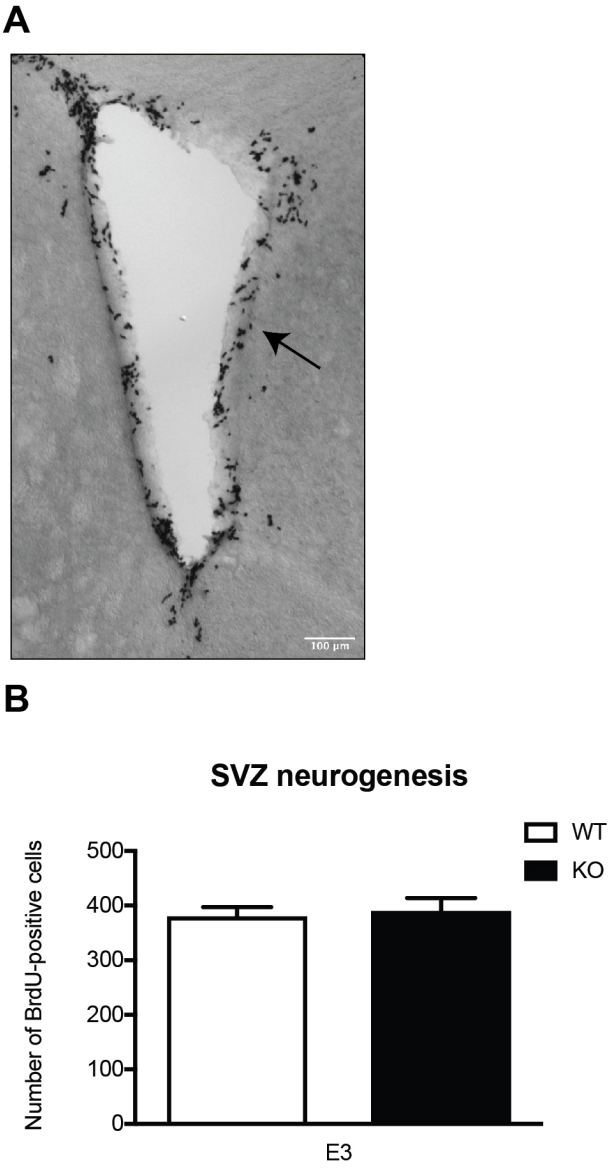

Figure 4.9: SVZ neurogenesis is not affected by sortilin in E3 mice.

(**A**) Immunodetection of BrdU-positive cells in the SVZ of (E3;WT) and (E3;KO) mice at 3 months old injected with BrdU for 24 hours. Scale bar: 100 μm. (**B**) Quantification of the total number of BrdU-positive cells in (E3;WT) and (E3;KO) mice. Two to four coronal sections (40 μm) per animal were used for counting. (n=5 animals per genotype). Values are mean ± SEM.

It has also been shown that PUFA promote dendritic arborization in primary neuronal cultures (Latifi et al. 2016). During adult life, the dynamic morphological changes of neuronal dendrites, called neuroplasticity, are tightly correlated with the functional integrity of the brain. Along these lines, the major risk factor of Alzheimer's disease, apoE4, decreases the dendritic complexity in mouse cortical neurons (Dumanis et al. 2009). Alteration of lipid homeostasis may impact the neuronal morphology, for this purpose, a commercial kit based on Golgi staining method was employed. The technique is named after his developer Camillo Golgi and uses silver nitrate impregnation that allows the visualization of neuronal cell soma, axons, dendrites and spines. Golgi's method stains randomly a limited number of cells, however the mechanism by which this happens is still largely unknown (Kang et al. 2017).

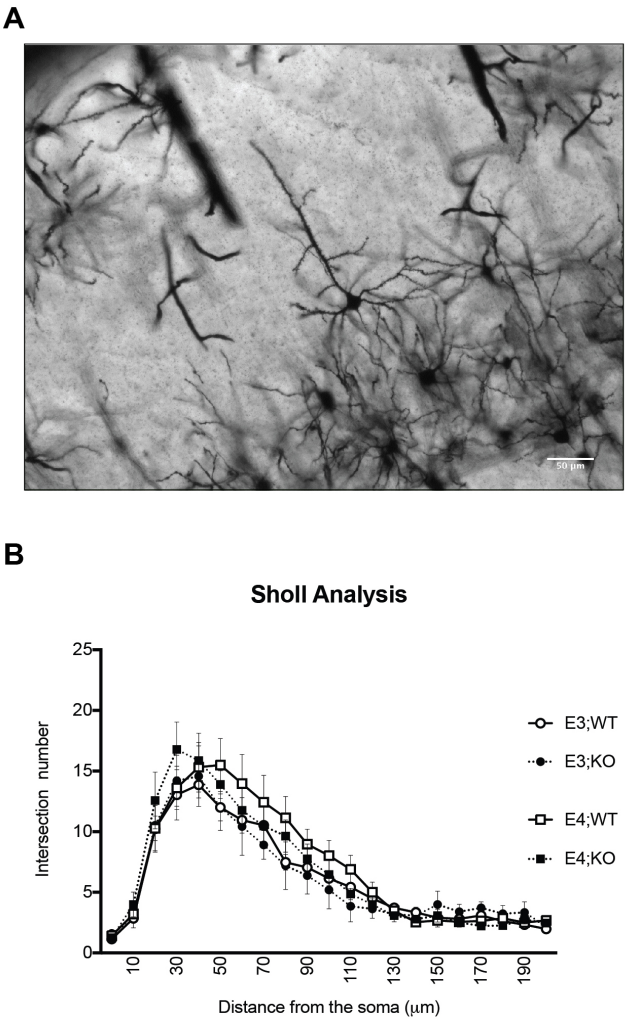

Figure 4.10: Sortilin and *APOE* genotypes do not alter dendritic complexity in neurons of the mouse cortex.

(**A**) Representative image of Golgi-impregnated pyramidal neurons in cortical layers II/III of (E3;WT), (E3;KO), (E4;WT) and (E4;KO) mice at 3 months of age. Scale bar: 50 µm. (**B**) Sholl analysis of neurons in cortical brain sections of (E3;WT), (E3;KO), (E4;WT) and (E4;KO) mice at 3 months of age. (n=3-4 animals per genotype, 7 neurons per mouse analysed). Values are mean ± SEM.

To test the effect of sortilin and APOE isoforms on the dendritic complexity and arborization of pyramidal neurons in cortical layers II/III, mouse brains were dissected, sectioned and stained using the Golgi staining method for neurons (Figure 4.10A). Subsequently, the Fiji plugin “simple neurite tracer” was used to trace the dendrites of Golgi-stained pyramidal neurons. This tool allows for the quantitative assessment of neuronal complexity using an additional Fiji plujin called “Sholl analysis” that creates a series of concentric shells around the neuron’s soma and quantifies the number of dendritic intersections per shell that occur at fixed distances from the soma. As shown in Fig. 4.10B, the Sholl profile of neurons was similar in all genotype groups. Also, using the Fiji plugin “simple neurite tracer” tool, no impact of sortilin and APOE isoforms on the numbers (Figure 4.11A) or the length (Figure 4.11B) of apical and basal dendrites in the various mouse strains was noted.

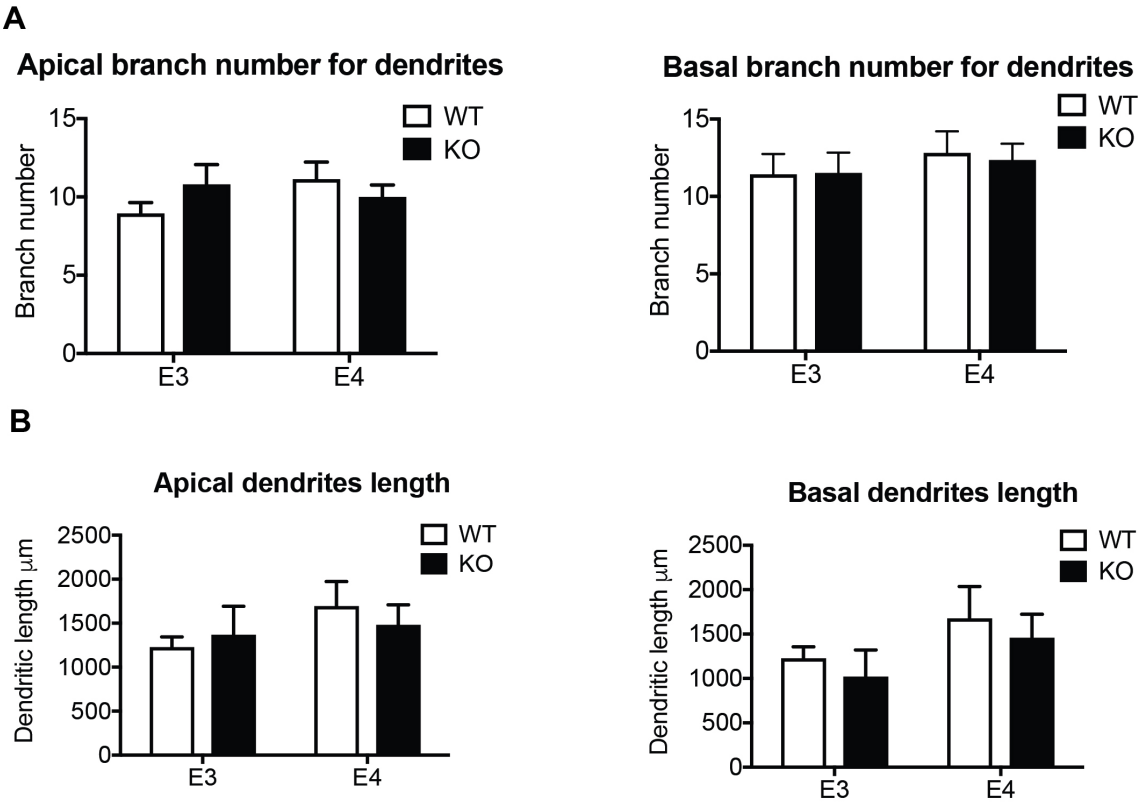

Figure 4.11: Sortilin and APOE isoforms do not affect dendritic arborization.

(**A**) Branch number for apical and basal dendrites and (**B**) length of apical and basal dendrites (in μm) in (E3;WT), (E3;KO), (E4;WT) and (E4;KO) at 3 month old mice. (n=3-4 animals per genotype, 7 neurons per mouse). Values are mean ± SEM.

4.4. PPARs pathway is altered in the brain of mice lacking sortilin and with apoE4 genotype

Alteration of PUFA and eCBs levels seen in E4 mice or in E3 animals lacking sortilin did not coincide with defects in adult neurogenesis or neuroplasticity in brain of the respective mouse strains. To investigate other possible consequences of altered levels of PUFA and eCBs for functional integrity of the mouse brain, I next focused on the activity of peroxisome proliferator-activated receptors (PPARs). PPARs are a class of ligand-induced nuclear receptors that are activated by PUFA to control target gene transcription. For this reason, I investigated the effect of the alteration in DHA and eCB levels on PPAR activities in my mouse models. Specifically, I used an unbiased systemic approach of a PCR profiler assay from Qiagen to quantify the transcript levels of 84 PPAR target genes in the brain cortex of these animals. In these studies, I identified 12 genes that were differentially expressed in the mouse models with a similar pattern seen for levels of 2-AG, synaptamide, and DHA before (Figure 4.12A). Among these targeted genes, I confirmed genotype-dependent alterations in the transcript levels of *Pparg*, *Mmp9* and *Klf10* by quantitative RT-PCR, specifically, a decrease in (E4;WT), (E4;KO) and (E3;KO) as compared with (E3;WT) mice. No alterations in mRNA levels were observed in (E4;WT) as compared with (E4;KO) animals (Figure 4.12B).

Since loss of sortilin and the presence of E4 affected the expression of PPAR targeted genes, I next investigated the consequences of altered PPAR activity for neuroinflammatory processes in the brain of aged mice. In the brain, activated PPARs have been studied with respect to their anti-inflammatory and anti-amyloidogenic actions (Bright et al. 2008). For example, treatment of AD mouse models with PPAR-γ agonists reduced the expression of pro-inflammatory cytokines and caused a concomitant decrease in the numbers of activated microglia and reactive astrocytes (Heneka et al. 2005). For this reason, I applied

quantitative RT-PCR to score the transcript levels of genes implicated in brain inflammatory processes.

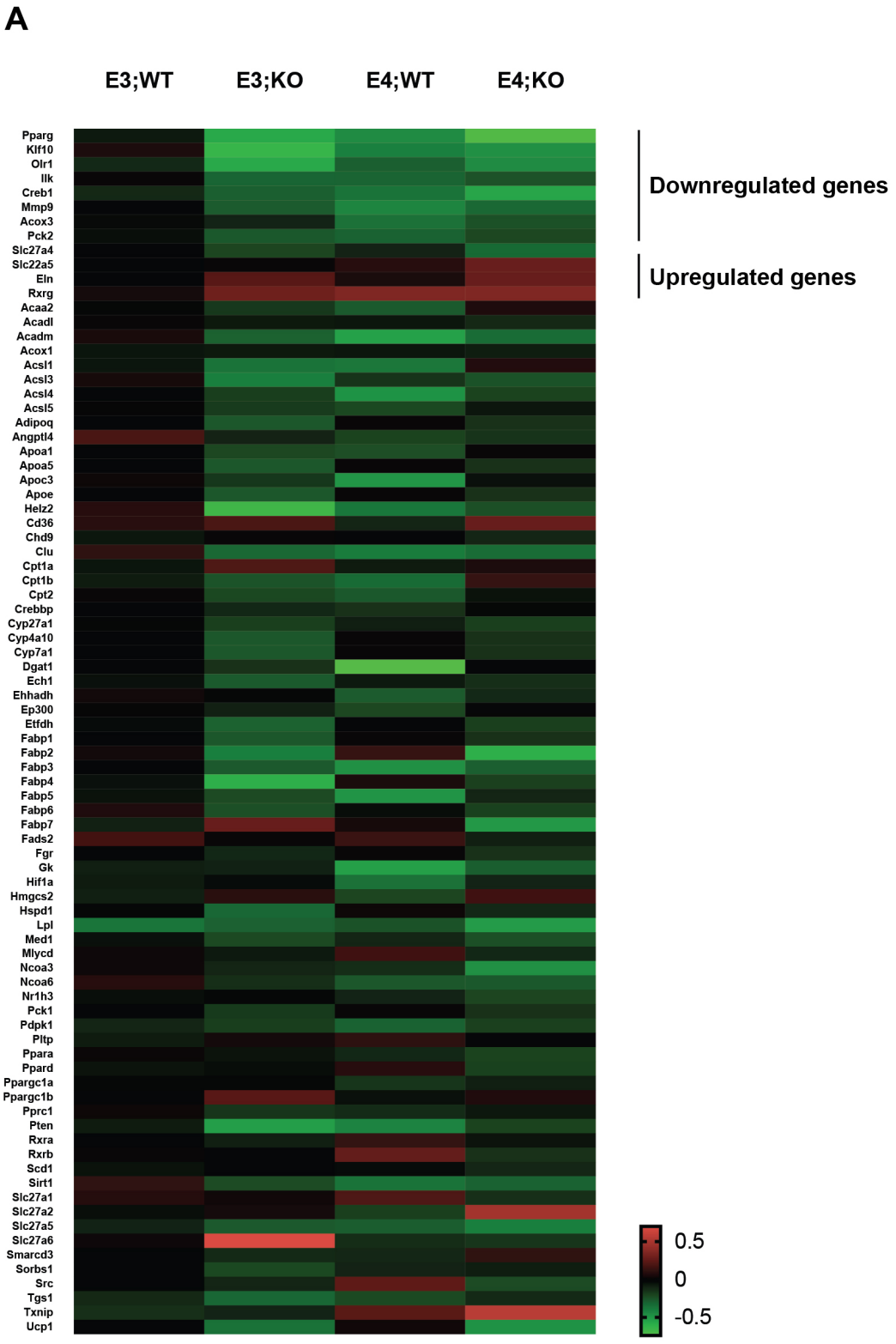

B

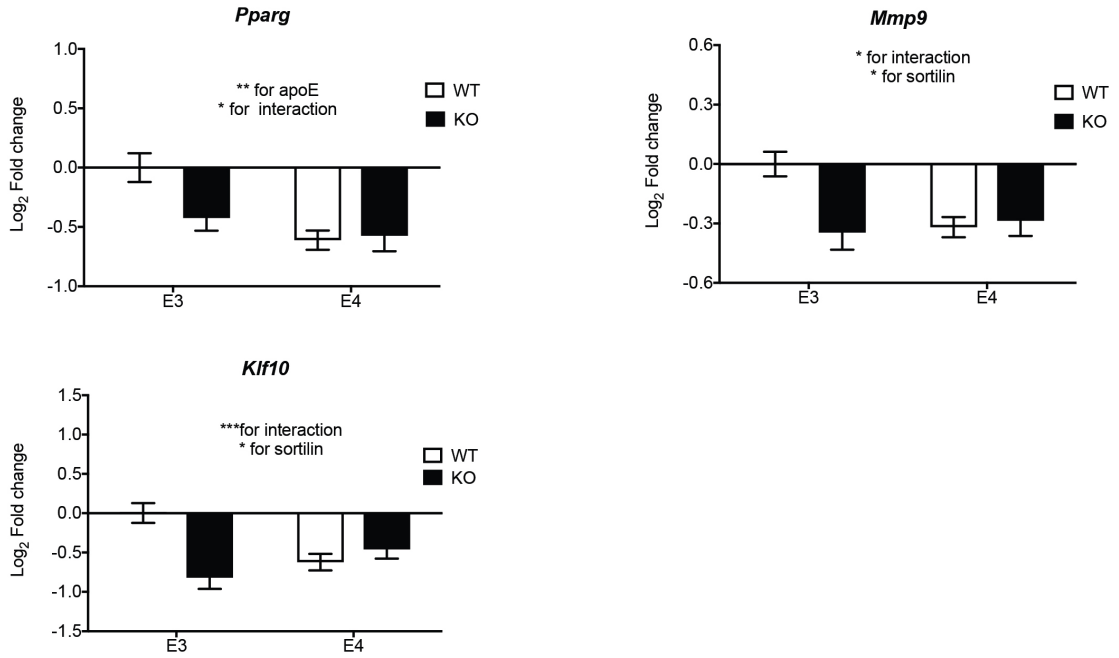

Figure 4.12: The expression of PPAR target genes is altered by sortilin and apoE4 allele in the mouse brain.

(A) Heat map of PPAR target genes using the PPAR Targets RT² Profiler PCR Array (Qiagen). Genes are either down- or up-regulated in (E3;WT) mice as compared with the three other genotypes (n=3-4 mice per genotype). (B) Quantitative RT-PCR analysis of transcript levels of the indicated PPARs target genes in (E3;WT), (E3;KO), (E4;WT), and (E4;KO) mice at 3 months of age. The values are given as mean ± SEM of log2 fold changes as compared with (E3;WT) mice set to 0 (n=7-8 mice per genotype). The significance of data was determined by Two-way ANOVA, followed by Bonferroni post-hoc analysis (*, $p<0.05$; **, $p<0.01$; ***, $p<0.001$).

In these studies, I detected a significant decrease in mRNA levels of the anti-inflammatory genes *Pparg* and vascular endothelial growth factor (*Vegf)* in (E4;WT), (E4;KO) and (E3;KO) compared with (E3;WT) mice (Figure 4.13A).

In addition, transcript levels of the pro-inflammatory genes tumor necrosis factor (*Tnfa)* and glial fibrillary acidic protein (*Gfap)* were increased in the three genotypes as compared with (E3;WT) animals (Figure 4.13B). A suspected pro-inflammatory state was confirmed by immunohistological detection of GFAP which showed a significant increase in the cortex of (E3;KO) as compared with (E3;WT) mice (Dr. Anna Malik, personal communication).

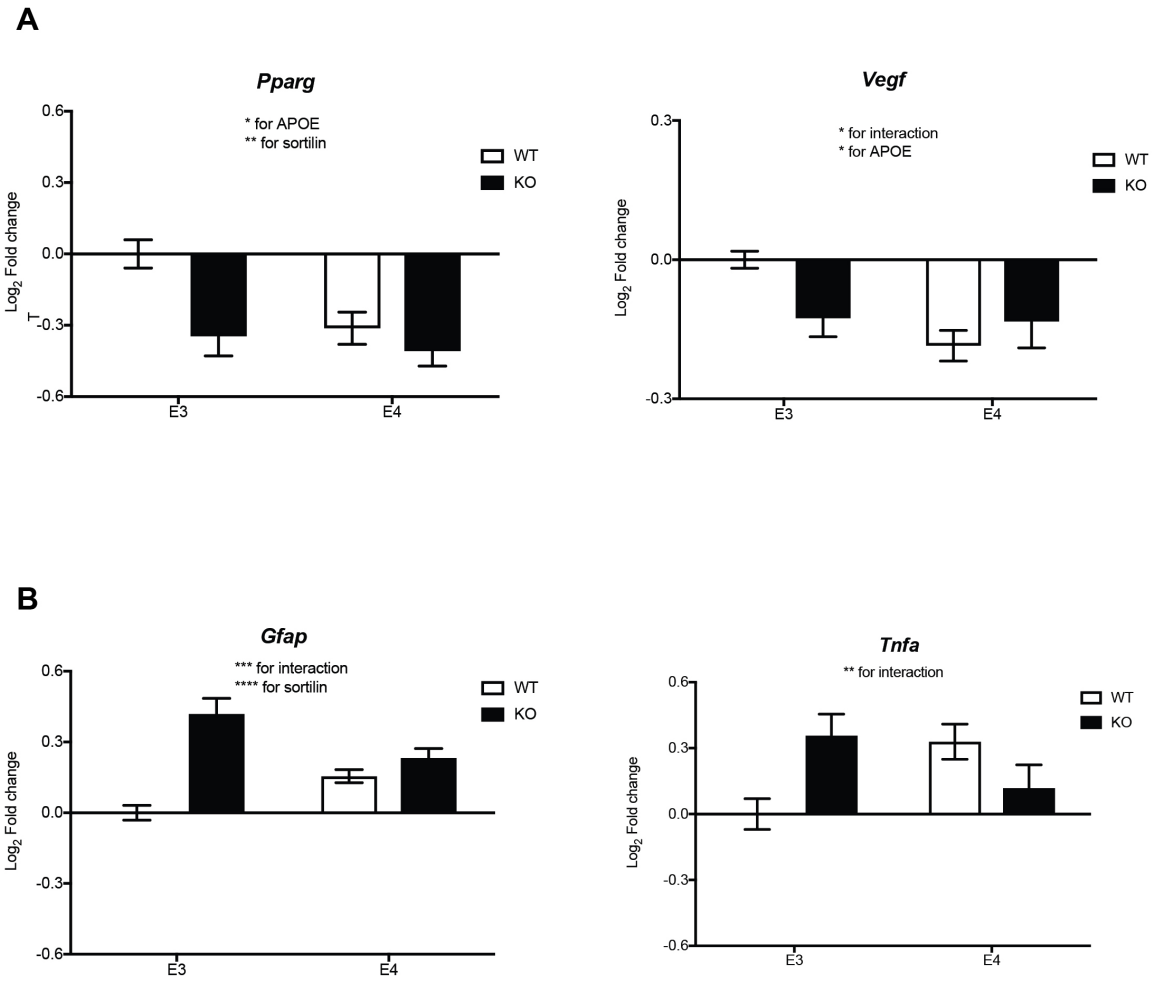

Figure 4.13: Inflammatory genes are affected by sortilin and *APOE* genotypes.

(**A, B**) Quantitative RT-PCR analysis of transcript levels of the indicated genes in (E3;WT), (E3;KO), (E4;WT), and (E4;KO) mice at 18 months of age. The values are given as mean ± SEM of log2 fold changes as compared to (E3;WT) mice set to 0 (n=8-10 mice per genotype). The significance of data was determined by Two-way ANOVA, followed by Bonferroni post-hoc analysis (*, $p<0.05$; **, $p<0.01$; ***, $p<0.001$; ****, $p<0.0001$).

4.5. Expression of enzymes in eCBs metabolism are not altered in the brain of mice lacking sortilin and with apoE4 genotype

Metabolic enzymes involved in the synthesis and degradation of eCBs are central to the regulation of the biological and pathological roles of these lipids. Little is known about the biosynthetic pathway that produces synaptamide. However, due to its chemical structure, it is believed to be synthesized from DHA by the enzyme N-acyl phosphatidylethanolamine phospholipase D (NAPE-PLD). Its

degradation to DHA is executed by fatty acid amide hydrolase (FAAH) (Kim et al. 2011) (Figure 4.14A).

2-AG is synthesized by diacylglycerol lipase (DAGL) and degraded by monoacylglycerol lipase (MAGL) (Basavarajappa 2007) (Figure 4.14A).

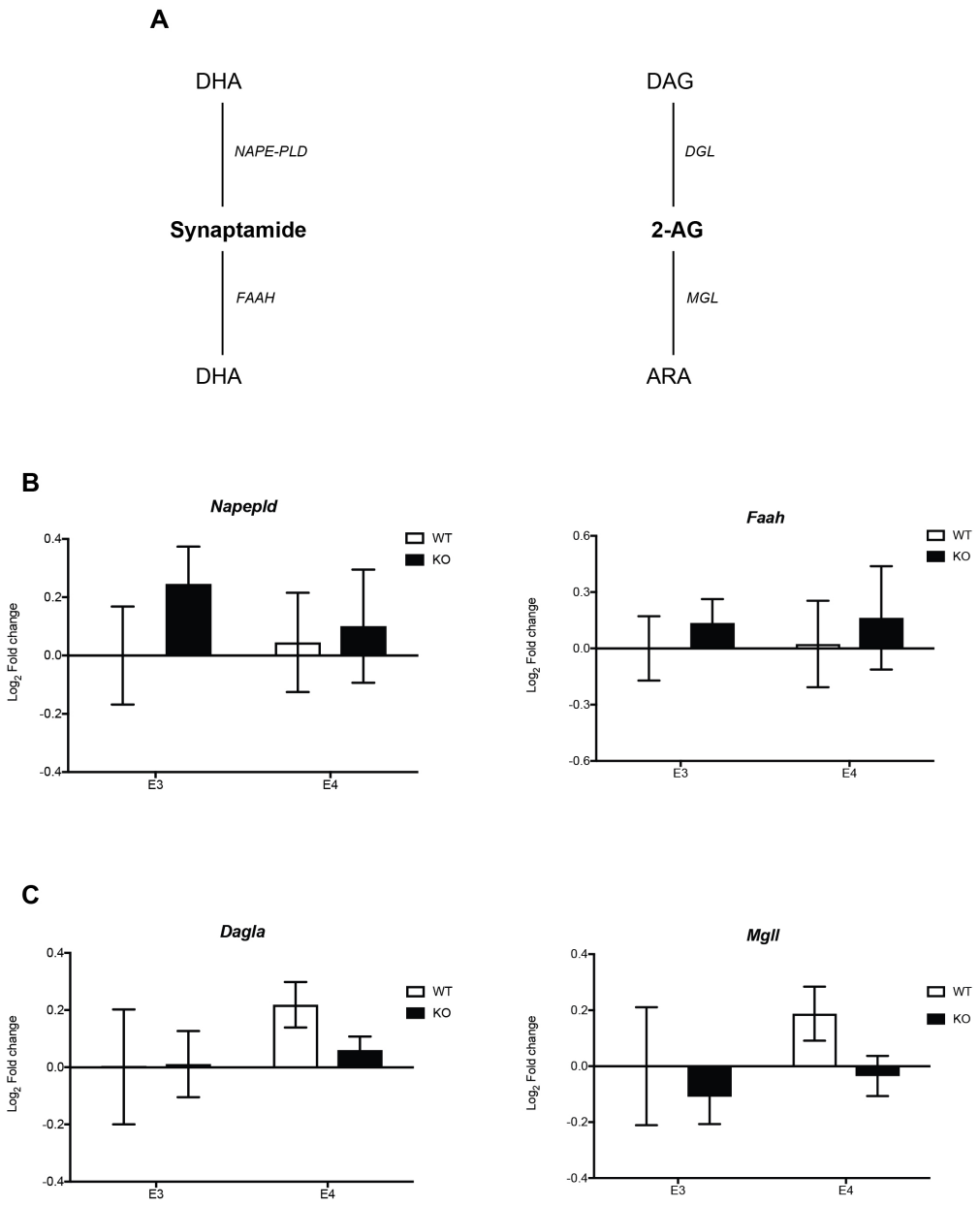

Figure 4.14: Sortilin and APOE isoforms do not affect mRNA levels of enzymes in neuronal eCB metabolism.

(**A**) Schematic representation of synaptamide and 2-AG metabolism. Synaptamide is produced from DHA by N-acyl phosphatidylethanolamine phospholipase D (NAPE-PLD) that in turn can be degraded fatty acid amide hydrolase (FAAH) to DHA. 2-AG is synthesized by diacylglycerol lipase

(DAGL) from diacylglycerol (DAG) and degraded by monoacylglycerol lipase (MAGL) to arachidonic acid. (**B**) Quantitative RT-PCR analysis of transcript levels of the indicated genes in brain cortices of (E3;WT), (E3;KO), (E4;WT), and (E4;KO) mice at 3 months of age. The values are given as mean ± SEM of log2 fold changes as compared to (E3;WT) mice set to 0 (n=6-9 mice per genotype).

Using quantitative RT-PCR analysis, I failed to document any genotype-dependent differences in transcript levels for *Napepld*, *Faah*, *Dagla,* and *Mgll* in brain cortices of my mouse strains (Figure 4.14B). These findings argued that changes in levels of 2-AG and synaptamide in (E3;KO) or in E4 animals as compared to (E3;WT) mice were likely not caused by alterations in neuronal enzyme activities.

4.6. The extracellular PUFA metabolism is not affected by sortilin or *APOE* genotypes

In the brain, APOE is secreted by astrocyte and microglia cells to deliver essential lipids to neurons in the form of APOE-containing lipoproteins (Holtzman and Herz 2012). Of note, the three APOE isoforms produced in humans form lipoproteins with different size and lipid composition. In detail, apoE4-containing particles have a smaller size and are less lipidated than those containing apoE3 or apoE2 (Cruchaga et al. 2012) (Grimm et al. 2017). Conceptually, alteration in eCB content seen in the mouse brain in this study may be explained by the differential association of their precursors DHA and ARA with lipoproteins containing E3 or E4. To test this hypothesis, I isolated APOE-containing lipoproteins from the cerebrospinal fluid of AD patients and healthy controls using heparin affinity chromatography (Figure 4.15A). When the lipid content in these lipoprotein preparations was measured, no impact of *APOE* genotype on the levels of DHA or ARA were detected in healthy individuals or in AD patients (Figure 4.15B).

In the CNS, APOE is produced predominantly by astrocytes. Alteration of APOE production may explain the changes in lipid homeostasis in the mouse brain. To understand if sortilin and/or *APOE* genotypes may influence APOE production in mice, primary astrocytes cultured from new-born mice of the various genotype groups were established.

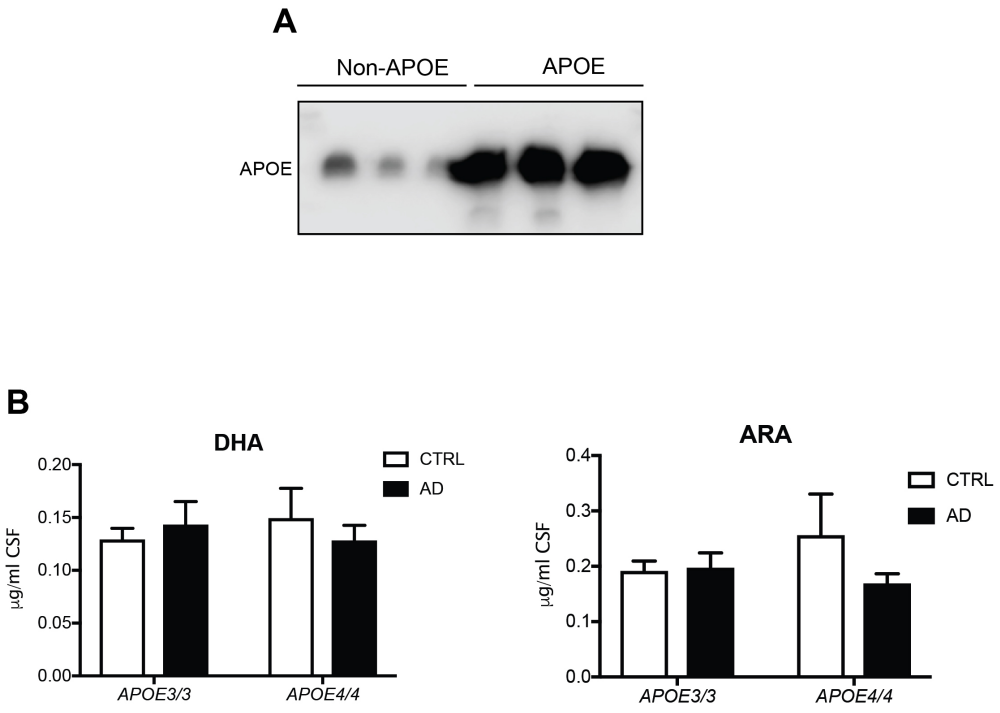

Figure 4.15: APOE-containing brain lipoproteins from healthy individuals or in AD patients have a similar PUFA profile.

(**A**) Human CSF lipoproteins were subjected to heparin affinity chromatography to separate APOE-containing from APOE-free lipoproteins. Western blot analysis documents the presence of APOE in the heparin-bound (APOE) but not in the column flow-through (non-APOE) fractions. (**B**) Levels of DHA and ARA in APOE-containing lipoproteins isolated from the CSF of healthy controls (CTRL) or Alzheimer patients (AD), homozygous for *APOE3* (*apoE3/3*) or *APOE4* (*apoE4/4*). The values are given as mean ± SEM (n=7-10 subjects per group).

Western blot analysis failed to show any obvious alteration in levels of APOE isoforms comparing mice with E3 or E4 genotypes, or/and deficient for sortilin (Figure 4.16A). Furthermore, levels of *APOE* mRNA was not changed in these primary mouse astrocyte culture (Figure 4.16B). Thus, astrocytes derived from the mouse models produce the same amount of APOE RNA and protein.

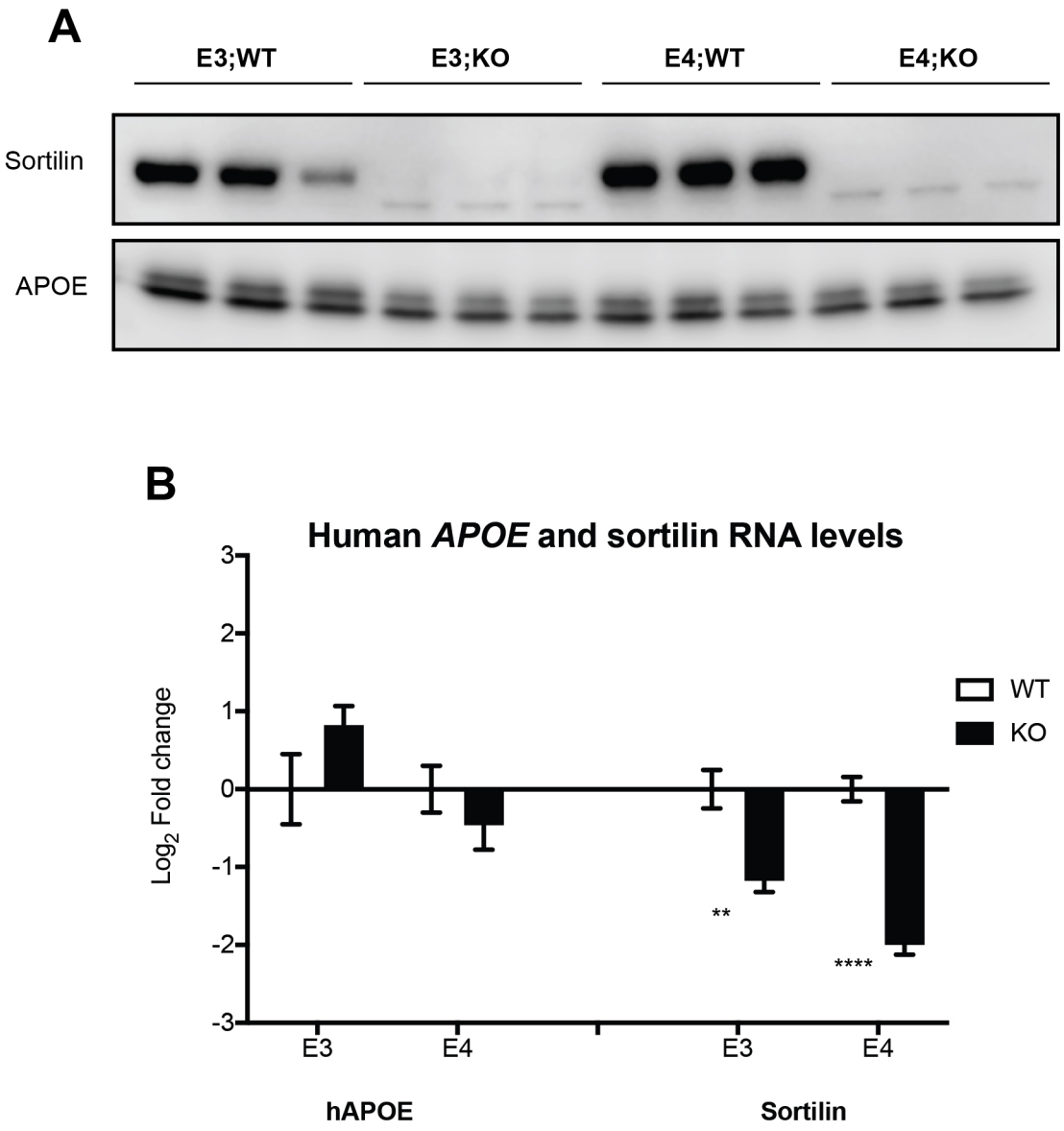

Figure 4.16: Primary astrocytes from the mouse models produce the same amount of APOE.

(**A**) Western blot analysis of APOE and sortilin expressed in primary astrocytes of the indicated genotype groups. (**B**) Quantitative RT-PCR analysis of *APOE* and sortilin transcript levels in primary astrocytes derived from (E3;WT), (E3;KO), (E4;WT), or (E4;KO) mouse brains. The values are given as mean ± SEM of log2 fold changes as compared to (E3;WT) set to 0. (n=5 cultures per genotype).

4.7. Sortilin affects FABP7 levels in neurons but not in glia cells in an APOE-dependent manner

So far, my analyses of the PUFA metabolism in human and mouse brains, in human CSF lipoproteins, and in primary mouse astrocytes failed to explain why

DHA and eCB levels were changed in the mouse brain in response to sortilin and APOE isoforms. These findings argued that transport and metabolism of these lipids into the extracellular space are not affected by sortilin and *APOE* genotypes. Moreover, the enzymes important for the synthesis and degradation of synaptamide and 2-AG were also not altered, suggesting that intracellular mechanisms other than enzyme activity may explain these lipid profiles. Sortilin is a sorting receptor that directs cargo proteins to various intracellular compartments in the biosynthetic and the endocytic pathways (Carlo et al. 2014). Thus, alteration of intracellular cargo sorting may explain the lipid imbalance seen in the brain of mic lacking this receptor. My hypothesis was supported by work from Dr. Anna Malik in Willnow's laboratory who used an unbiased proteomics approach to identify novel targets of sortilin in the neuronal proteome. She reasoned that the absence of sortilin may result in aberrant distribution of yet unknown receptor ligands between cell surface and intracellular compartments. To identify such targets, she biotinylated surface proteins in primary neurons from WT and sortilin KO animals. Subsequently, the biotinylated proteins were purified from cell extracts using streptavidin beads and subjected to quantitative label-free proteomics by LC-MS/MS. By this approach, she identified multiple proteins with altered abundance in the neuronal cell surface fraction upon loss of sortilin. Among these proteins was one hit with particular relevance for my work, namely fatty acid binding protein 7 (FABP7). FABP7 is a member of the fatty acid binding proteins, a family of intracellular lipid carriers expressed in various tissues, including the brain. These intracellular chaperons facilitate the complex intracellular trafficking of fatty acids, essential to control metabolism and action of these lipids. FABPs transport a variety of lipid ligands but have favors to bind long-chain over short-chain PUFAs (Furuhashi and Hotamisligil 2008). FABP7 is highly expressed in the brain and has a strong binding affinity for DHA (Balendiran et al. 2000).

To explore whether FABP7 activity may explain the lipid phenotypes seen in my mouse models, I first tested expression levels of the carrier in the brain of these mice.

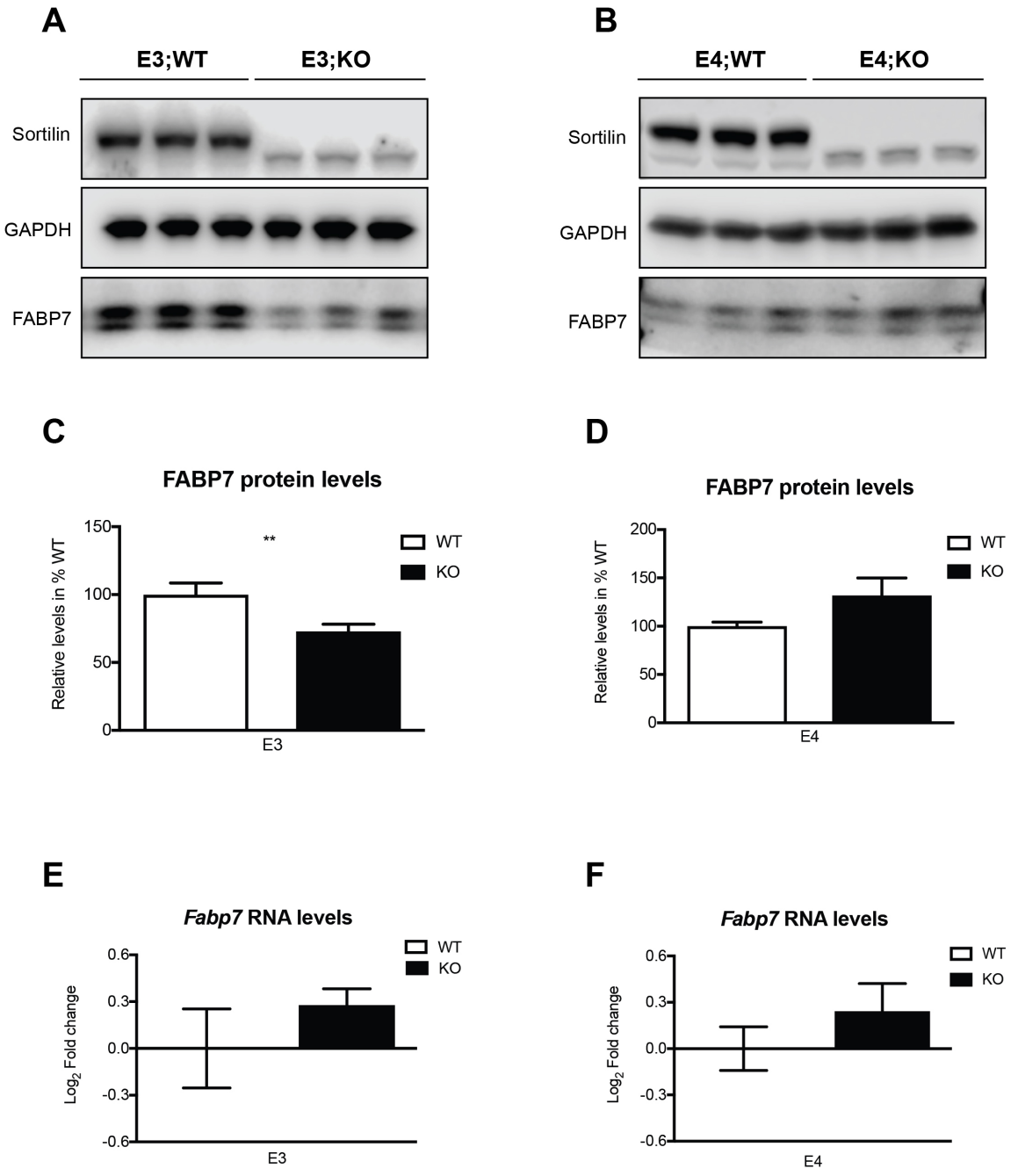

Figure 4.17: Sortilin affects FABP7 protein levels in E3 but not in E4 mice.

(**A**-**B**) Western blot analysis of sortilin, FABP7, and GAPDH (loading control) levels in brain cortex of the indicated genotype groups. (**C-D**) Densitometric quantification of FABP7 protein levels in (E3;WT), (E3;KO), (E4;WT) and (E4;KO) cortex at 3 months old mice using western blotting as exemplified in panels A and B (n=12-18 animals per genotype). Values are mean ± SEM given as percent of WT mice set to 100%. Student's *t*-test was used to test the significance of differences between genotypes (**p<0.01). (**E-F**) Quantitative RT-PCR analysis of *Fabp7* in (E3;WT), (E3;KO),

(E4;WT) and (E4;KO) cortex at 3 months old mice. The values are given as mean ± SEM of log2 fold changes as compared to the respective WT mice set to 0 (n=5-8 animals per genotype).

Intriguingly, cerebral cortex levels of FABP7 were decreased in (E3;KO) compared with (E3;WT) mice (Figure 4.17A-B). No alteration in FABP7 levels was observed comparing (E4;WT) with (E4;KO) animals (Figure 4.17C-D). This E3-dependent effect of sortilin on brain FABP7 levels was mediated by a post-transcriptional mechanism as brain levels of *Fabp7* RNA were not altered in (E3;KO) compared with (E3;WT) mice, or in (E4;WT) compared to (E4;KO) animals (Figure 4.17E-F).

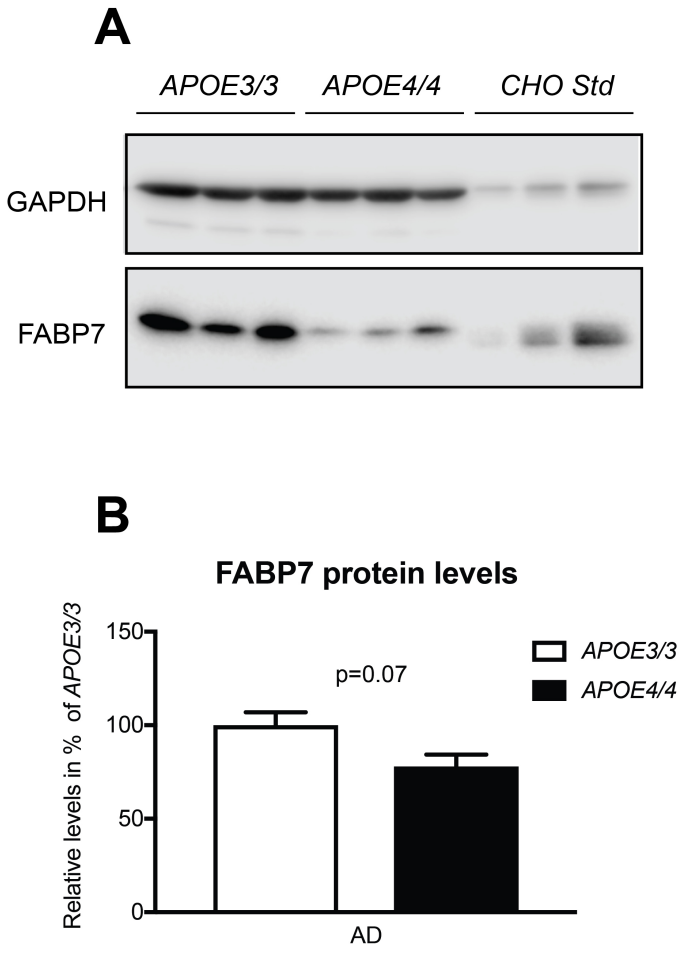

Figure 4.18: FABP7 protein levels in human brain.

(**A**) Western blot analysis of FABP7 levels in prefrontal cortex (PFC) specimens from AD patients of the indicated *APOE* genotypes. Detection of GAPDH was used as loading control. Also, known concentrations of recombinant FABP7 produced in CHO cells (CHO Std) were loaded as standard curve to enable comparative quantification of FABP7 levels across different western blot experiments. (**B**) Densitometric quantification of FABP7 protein expression in prefrontal cortex specimens of AD patients homozygous for *APOE3* or *APOE4*. (n=12-34 individuals per genotype).

Values are mean ± SEM given as percent of the *apoE3/3* samples set to 100%. Student's *t*-test was used to calculate the significance of differences between genotypes (p=0.07).

The impact of sortilin and *APOE* genotypes on proteins levels in human or mouse brains was specific to FABP7 and not seen for other lipid carriers, such as the related carrier FABP5, or FATP1, GPR40, or FACL4. Only the levels of the FA translocase, CD36 were decreased in (E4;KO) as compared with (E4;WT) mice (Table 4.2).

Lipid transporter	**Other name**	**Unpaired t-test**
FABP5	Fatty acid-binding protein 5	n.s.
CD36	Fatty acid translocase	** Decrease in (E4;KO) vs (E4;WT)
FATP1	Fatty acid transport protein 1	n.s.
GPR40	Free fatty acid receptor 1	n.s.
FACL4	Acyl-CoA synthetase long chain family member 4	n.s.

Table 4.2: Sortilin deficiency impacts levels of CD36 in E4 mice.

Western blot analysis and densitometric scanning of replicate blots were used to quantify the levels of FABP5, CD36, FATP1, GPR40, and FACL4 in the brain cortices of mice either (E3;WT), (E3;KO), (E4;WT) or (E4;KO) (primary data not shown). Student's *t*-test was used to calculate the significance of differences in protein levels comparing genotypes (**p<0.01).

FABP7 is mainly recognized as a protein highly expressed in astrocytes in the developing and mature brain (Matsumata et al. 2016). However, in mouse primary astrocyte cultures, FABP7 protein and mRNA levels were not altered comparing my four mouse genotype groups (Figure 4.19). This finding argued that the differences in FABP7 levels seen in human and mouse brains in my study groups likely reflected difference in neuronal expression of this carrier protein.

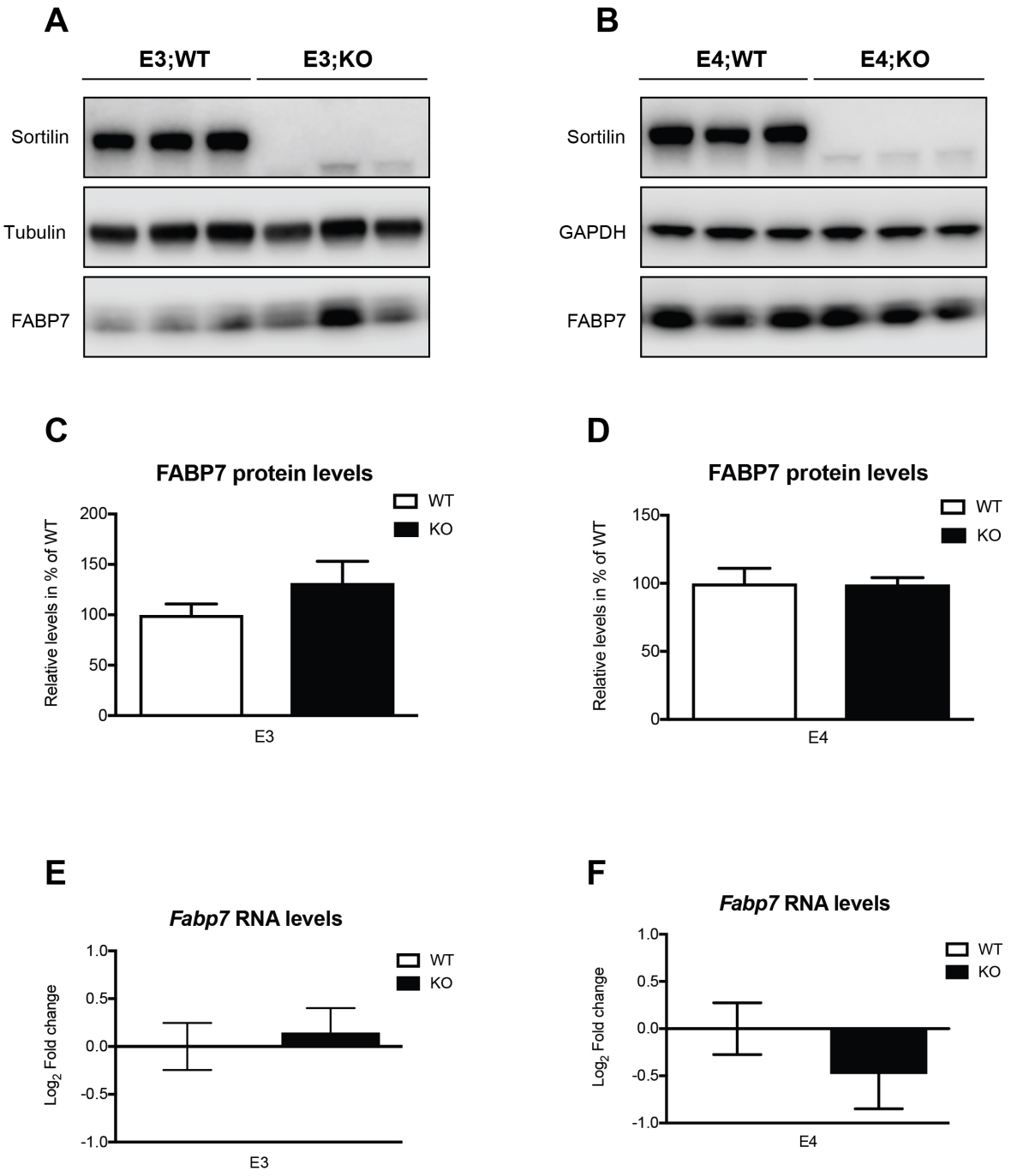

Figure 4.19: FABP7 levels are not altered in astrocytes derived from the mouse models.

(A-B) Western blot analysis of sortilin and FABP7 from primary astrocytes either (E3;WT), (E3;KO), (E4;WT) or (E4;KO). Detection of GAPDH and tubulin were used as loading control. (**C-D**) Densitometric quantification of FABP7 protein levels detected by western blotting in replicate cultures (n=5 individual cultures per genotype). Values are mean ± SEM given as percent of WT astrocyte culture set to 100%. (**E-F**) Quantitative RT-PCR analysis of *Fabp7* transcript levels in (E3;WT), (E3;KO), (E4;WT) and (E4;KO) primary astrocyte cultures. The values are given as mean

± SEM of log2 fold changes as compared to the respective WT culture set to 0 (n=5 individual cultures per genotype).

To test this idea, I prepared primary neuronal cultures from new born mice of the four genotype groups and quantified levels of FABP7 protein and transcript using western blotting or quantitative RT-PCR analyses, respectively. FABP7 protein levels were decreased in (E3;KO) as compared with (E3;WT) neuronal cultures (Figure 4.20A-B). As in the adult mouse brain, no alteration of FABP7 protein levels were observed comparing (E4;WT) with (E4;KO) primary neurons (Figure 4.20C-D). Moreover, *Fabp7* mRNA levels were not altered between the mouse genotypes (Figure 4.20C-F). These findings argued that changes in levels of FABP7 in the mouse brain are rather specific for neurons than for astrocytes. Moreover, a post-translation modification is likely responsible for the FABP7 decrease in (E3;KO) compared with (E3;WT).

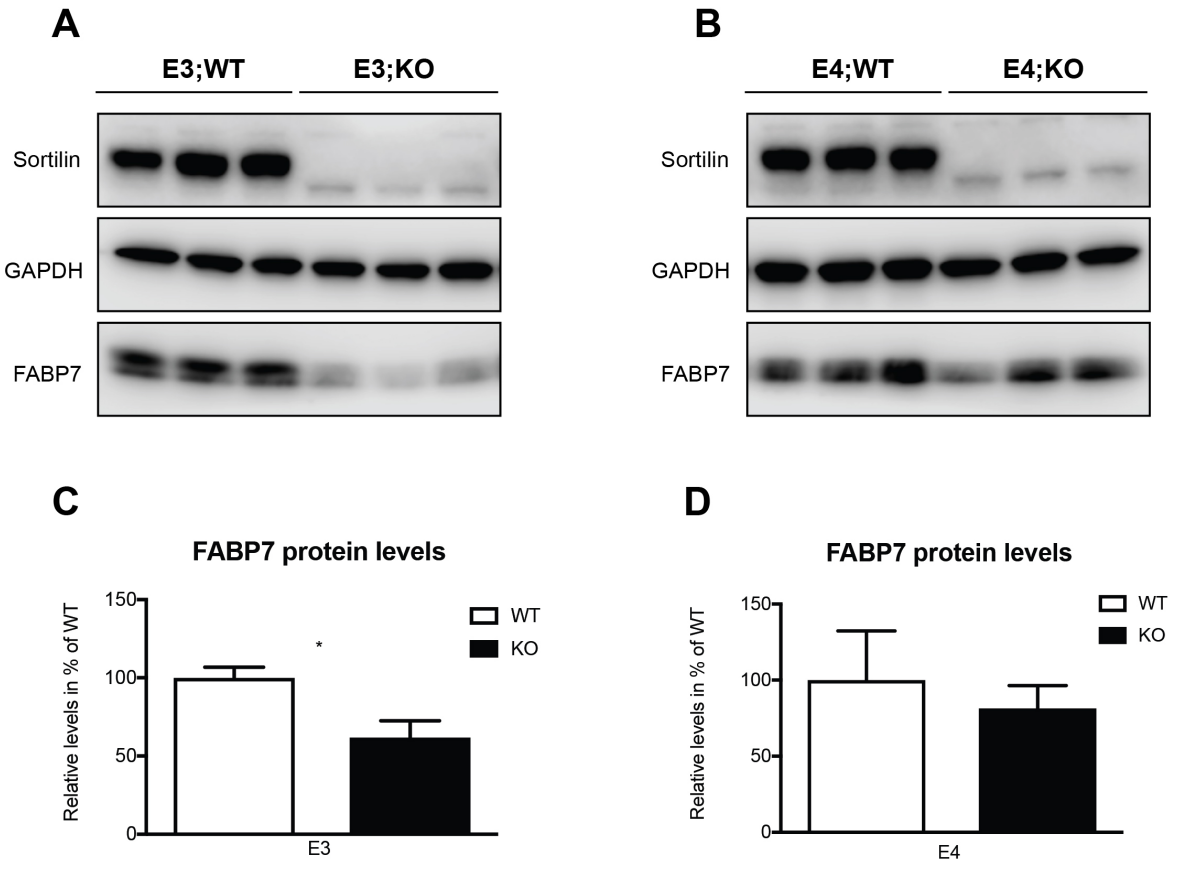

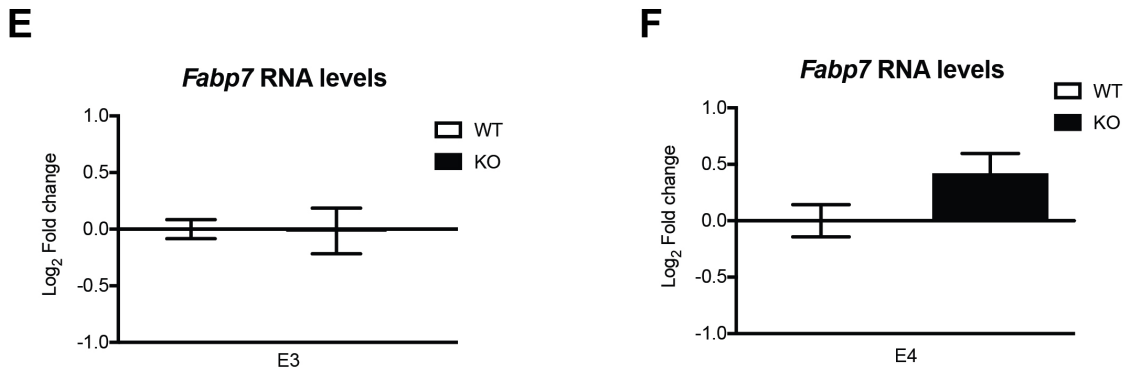

Figure 4.20: FABP7 protein levels are altered in sortilin-deficient neurons with E3 allele.

(**A-B**) Western blot analysis of sortilin and FABP7 in (E3;WT), (E3;KO), (E4;WT) and (E4;KO) primary neuronal cultures. Detection of GAPDH was used as loading control. (**C-D**) Densitometric quantification of replicate western blots for FABP7 protein levels (n=4-8 cultures per genotype). Values are mean ± SEM given as percent of the respective WT culture set to 100%. Student's *t*-test was used to calculate the significance of differences between genotypes (*p<0.05). (**E-F**) Quantitative RT-PCR analysis of *Fabp7* transcript levels in (E3;WT), (E3;KO), (E4;WT) and (E4;KO) primary neuronal cultures. The values are given as mean ± SEM of log2 fold changes as compared to the respective WT culture set to 0 (n=5-10 cultures per genotype).

4.8. Sortilin interacts with and stabilizes FABP7

So far, my studies suggested FABP7 as a likely candidate to explain the alterations in PUFA content as the decrease in FABP7 levels in neurons lacking sortilin reflected the decrease seen for PUFA and eCBs in the mouse brain. Still, the mechanism whereby sortilin and FABP7 interacted to control neuronal lipid homeostasis remained to be resolved. To do so, I used Chinese hamster ovary (CHO) cell lines recombinantly expressing sortilin and FABP7. When CHO cells were transiently transfected with a construct encoding for mouse FABP7, levels of this carrier were significantly higher in CHO cells stable overexpressing sortilin (CHO-S) as compared with parental CHO cells lacking this receptor (Figure 4.21). This result was in line with previous experiments in adult mouse brain and in primary neuronal culture suggesting the necessity of sortilin to promote FABP7 expression.

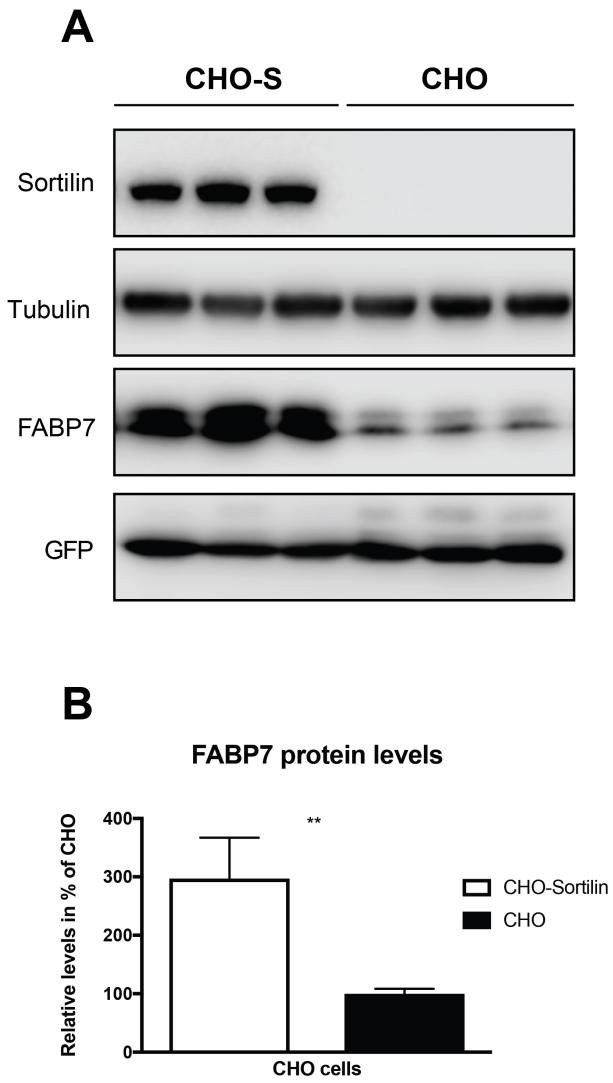

Figure 4.21: FABP7 levels are increased in CHO cells overexpressing sortilin.

(**A**) Western blot analysis of sortilin and FABP7 levels in parental Chinese hamster ovary (CHO) cells or CHO cells stably overexpressing sortilin (CHO-S) and transiently transfected with a construct encoding FABP7 and green fluorescence protein (GFP). Detection of tubulin was used as loading control. Detection of GFP was used as transfection control. (**B**) Densitometric quantification of FABP7 protein levels in CHO and CHO-S cells as exemplified in panel A (n= 9 replicate transfections from 3 independent experiments per cell line). Values are mean ± SEM given as percent of CHO set to 100%. Student's *t*-test was used to calculate the significant differences between genotypes (**, $p<0.01$).

Taken together, the sorting function of sortilin and the decrease of FABP7 levels in CHO cells, as well as in adult brain and primary neuronal culture lacking sortilin, suggested that sortilin may interact with FABP7 in the sorting of PUFA to various intracellular compartments. To test this hypothesis, immunoprecipitation (IP) was performed in CHO cells stably overexpressing murine sortilin and myc-tagged

FABP7 (CHO-S/F) to query a direct interaction of sortilin with this carrier protein (Figure 4.22).

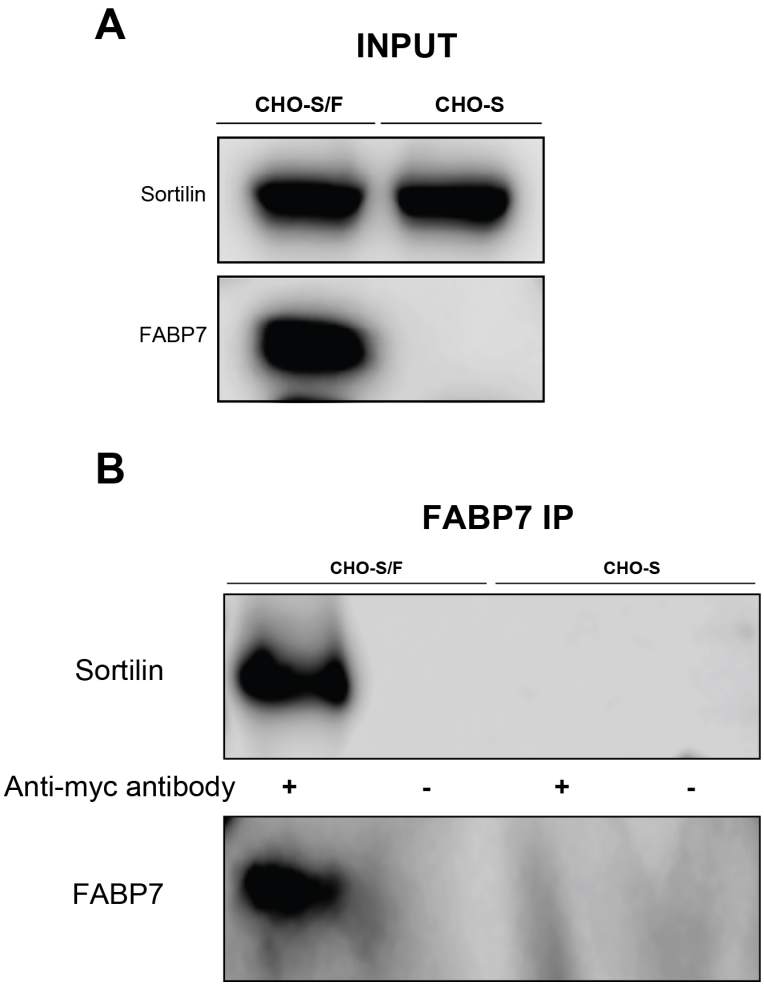

Figure 4.22: FABP7 interacts with sortilin in a co-immunoprecipitation (co-IP) assay.

(**A**) Western blot analysis of sortilin and FABP7 levels in total cell lysates of CHO cells expressing sortilin (CHO-S) or sortilin with myc-tagged mouse FABP7 (CHO-S/F) (INPUT). (**B**) Western blot analysis of sortilin and FABP7 in immunoprecipitations using anti-myc antibody couple to magnetic beads in the cell lysate from CHO-S and CHO-S/F cell lines (FABP7 IP). Co-immunoprecipitation of sortilin with FABP7 is seen in lysates from CHO-S/F cells (+) but not from CHO-S cells (+) using anti-myc antiserum. No immunoprecipitation of sortilin from CHO-S/F cells or CHO-S cells is detected in the absence of anti-myc antiserum (-).

To prove that sortilin also interacts with FABP7 in intact cells, I applied an alternative assay called proximity ligation assay (PLA) that allows the detection of the spatial proximity of two proteins in live cells. In detail, PLA employs oligonucleotide-conjugated antibodies directed against the target proteins (here FABP7-myc and sortilin). Binding of both antibody species in close proximity

allows for their hybridization by connector oligonucleotides, forming a circular DNA strand that can be amplified by PCR. Incorporation of fluorescence-labelled oligonucleotides in the PCR product enables localized detection of protein interaction. Using this technique I uncovered that sortilin and FABP7 were localized in close proximity based on a PLA signal inside the CHO cells (Figure 4.23). To understand whether the interaction between sortilin and FABP7 affects the half-life of the carrier protein, I next tested FABP7 stability in cells CHO cells. In detail, I treated CHO-S/F cells with cycloheximide (CHX), an inhibitor of protein translation and monitored the abundance of FABP7 at various time points by western blotting.

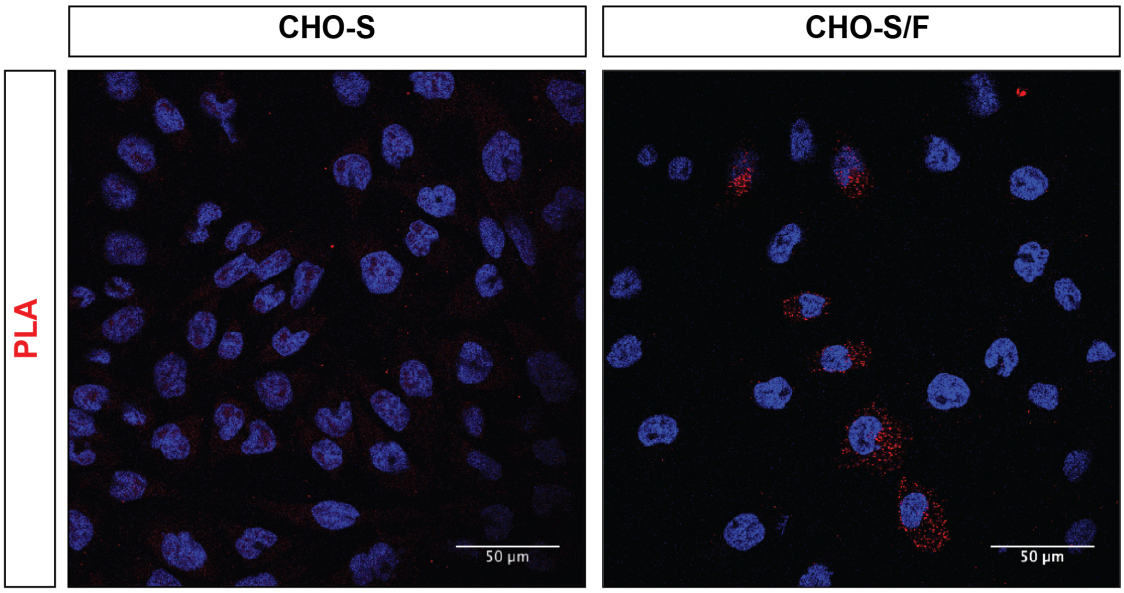

Figure 4.23: FABP7 interacts with sortilin in a proximity ligation assay (PLA).

CHO cells over expressing murine sortilin and FABP7-myc (CHO-S/F) were fixed and treated with primary antibodies directed against the two proteins. Subsequently, the cells were incubated with secondary PLA-probes, followed by ligation and PCR amplification as detailed in the method section. Sortilin and FABP7 interaction as deduced from a positive PLA signal (red) was detected by confocal microscopy. Cell nuclei were counterstained with DAPI (blue). As a negative control, no PLA signal was seen in cells expressing sortilin only (CHO-S). Scale bar: 50 µm.

In these experiments, FABP7 levels decreased significantly faster in parental CHO cells not expressing sortilin compared to CHO-S cells (Figure 4.24). These findings supported my assumption that elevated levels of FABP7 in CHO-S could be attributed to an increase in FABP7 protein half-life in presence of sortilin.

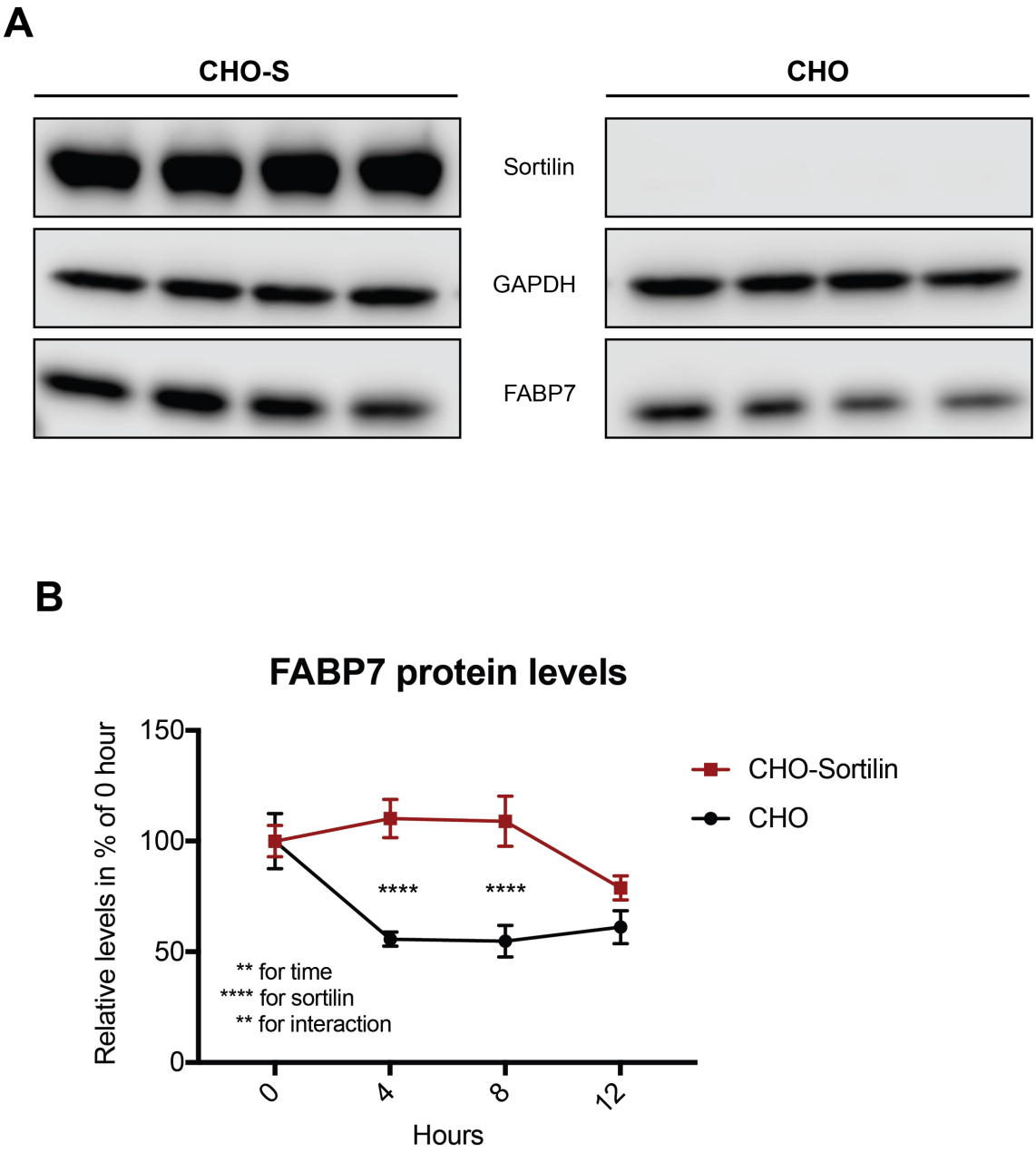

Figure 4.24: Sortilin stabilizes FABP7 protein in CHO cells.

CHO cells expressing (CHO-S) or lacking sortilin (CHO) were transiently transfected with an expression construct encoding FABP7-myc. Forty-eight hours post transfection, the cells were treated with 10 µg/ml of cycloheximide and replicate cultures collected at different time points post treatment (0, 4, 8, and 12 hours). The levels of sortilin and FABP7 were determined by western blot analysis (**A**). Detection of tubulin was used as loading control, (**B**) Densitometric quantification of FABP7 levels in CHO and CHO-S cells treated for various time points with cycloheximide. Values are mean ± SEM given as percent of FABP7 levels in CHO or CHO-S at 0 hour of treatment set to 100% (n= 12 replicate cultures per condition from 3 independent experiments). The significance of data was determined by Two-way ANOVA, followed by Bonferroni post-hoc analysis (**, $p<0.01$; ****, $p<0.0001$).

4.9. apoE4 alters cellular localization of FABP7 and sortilin

In earlier experiments, I showed that FABP7 levels were decreased in the E3 condition when sortilin was absent, an effect seen *in vivo* (Figure 4.17) and *ex vivo* (Figure 4.20). By contrast, absence of sortilin did not impact FABP7 cells with apoE4. To test whether E4 differentially impacts intracellular localization of sortilin and FABP7 as compared to E3, I treated CHO-S/F cells with exogenous E3 or E4.

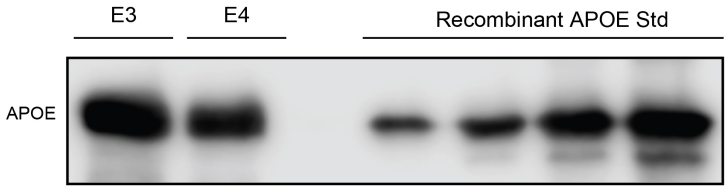

Figure 4.25: Production of E3 and E4 in HEK293 cells.

Western blot analysis of secreted APOE in the medium of HEK293 cells transiently transfected with constructs encoding human E3 or E4. The cell medium was conditioned for 48 hours in DMEM in the absence of fetal calf serum. Known amounts of commercially obtained recombinant APOE (human APOE, MBL) were loaded in parallel (recombinant APOE Std). Densitometric quantification of the immunosignals for HEK293-derived APOE as compared to the serial dilutions of recombinant human APOE were used to establish the respective concentrations of E3 and E4.

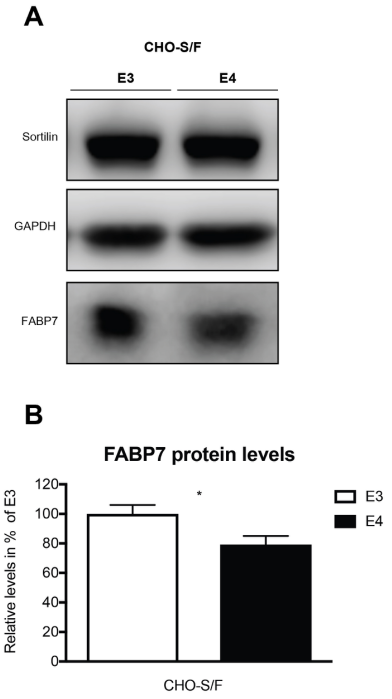

Figure 4.26: Levels of FABP7 protein is decreased in CHO-S/F treated with E4.

(**A**) Western blot analysis of sortilin and FABP7 in CHO cells stable overexpressing sortilin and FABP7 (CHO-S/F) and treated with E3 or E4 particles. Detection of GAPDH was used as loading control. (**B**) Densitometric quantification of FABP7 levels (n=10 replicate cultures from 4 independent experiments per cell line). Values are mean ± SEM given as percent of CHO-S/F treated with E3 set to 100%. Student's *t*-test was used to calculate the significant differences between genotypes (*, p<0.05).

Lipidated human E3 and E4 were produced by transiently transfecting HEK293 cells with the respective expression constructs and by collecting the conditioned media (Figure 4.25). To assure that the same amounts of E3 and E4 were applied to CHO cells, the levels of both APOE isoforms in the preparations were quantified by comparing their immune-signal intensities to those of known concentrations of recombinant APOE tested in the same western blots (Figure 4.25). When similar amounts of APOE were applied exogenously to CHO-S/F, levels of FABP7 decreased in the E4 compared with the E3 treatment condition (Figure 4.26).

I previous showed that sortilin, an endocytic protein, binds and stabilizes FABP7, thus E4 particles may interfere with the physiological sorting of sortilin and FABP7 and consequently E4 can decrease FABP7 protein levels.

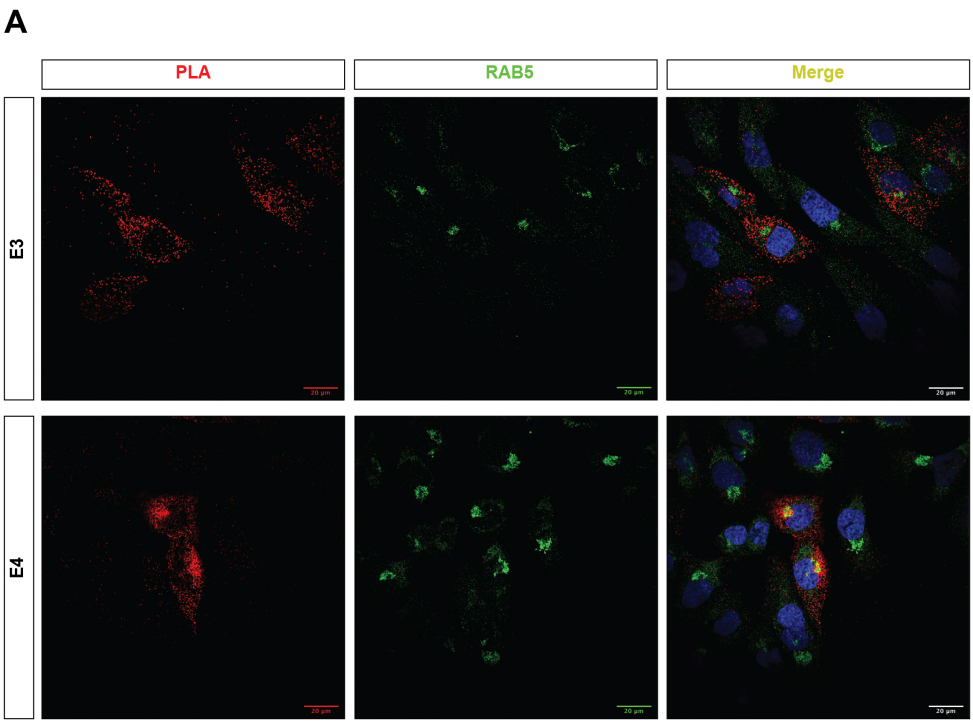

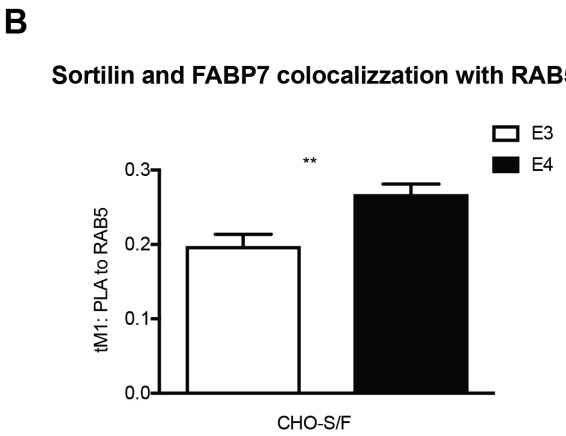

Figure 4.27: Sortilin and FABP7 more strongly co-localize with markers of the early endosomes in CHO-S/F cells treated with E4 compared with E3 particles.

(**A**) CHO cells stably overexpressing sortilin and murine FABP7 were treated with the same amount of E3 or E4 particles. PLA signals for sortilin and FABP7 interaction and immunodetection of RAB5, a marker of early endosome are showed in red and green, respectively. Scale bar: 20 µm. Cell nuclei were counterstained with DAPI (blue). (**B**) Quantitative co-localization analysis of RAB5 and PLA signals as determined by Manders' coefficient (tM1) calculating the fraction of sortilin and FABP7 that overlaps with RAB5 (n=33-35 cells per condition from 3 independent experiments). Values are mean ± SEM given as percent of CHO-S/F treated with E3 set to 100%. Student's *t*-test was used to calculate the significance of differences between treatment conditions (**, $p<0.01$).

Thus, to test whether E4 may impact sortilin and FABP7 localization, I compared the cellular distribution of sortilin-FABP7 complexes (PLA signal) with several subcellular markers in CHO-S/F cells treated with exogenous apoE3 or apoE4. PLA signals for sortilin and FABP7 showed colocalization with early (RAB5) (Figure 4.27) and recycling (RAB11) endosomes (Figure 4.28) in CHO-S/F treated with E4 compared with E3 particles.

In conclusion, my data showed that FABP7, the carrier for DHA and eCB in neurons, is controlled by sortilin. Sortilin binds and stabilizes FABP7 allowing the proper function of lipid metabolism and actions. However, the presence of the E4 destabilizes the functional interaction of FABP7 and sortilin by trapping this complex in the early endosomal and recycling compartments of the cells.

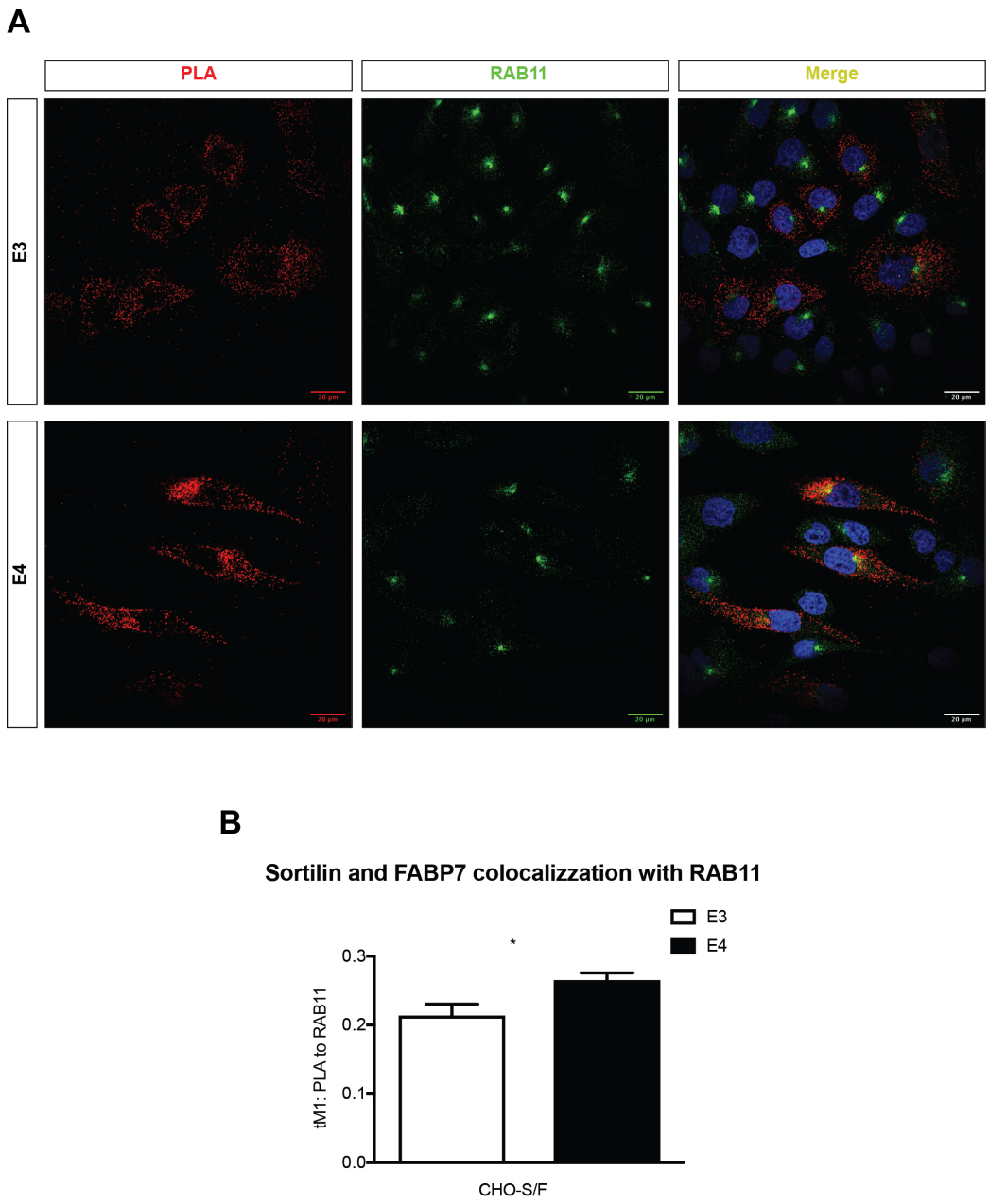

Figure 4.28: Sortilin and FABP7 more strongly co-localize with recycling endosomes in CHO-S/F treated with E4 compared with E3 particles.

(**A**) CHO cells stably overexpressing sotilin and murine FABP7 were treated with the same amount of E3 or E4 particles. The localization of PLA signals, indicating sortilin and FABP7 proximity, and RAB11, a marker of recycling endosome are showed in red and green, respectively. Scale bar: 20 µm. Cell nuclei were counterstained with DAPI (blue). (**B**) Quantitative co-localization analysis of RAB11 and PLA signals as determined by Manders' coefficient (tM1) calculating the fraction of sortilin and FABP7 that overlaps with RAB11 (n=38 cells per condition from 3 independent experiments). Values are mean ± SEM given as percent of CHO-S/F treated with E3 set to 100%. Student's *t*-test was used to calculate the significant differences between genotypes (*p<0.05).

5. DISCUSSION

5.1. APOE-dependent alteration in brain lipid homeostasis in mouse and human brains

The sporadic form of AD is a complex and multifactorial disease caused by a combination of genetic and environmental risk factors (Rao et al. 2014), with the apoE4 allele as the major underlying genetic risk factor (Corder et al. 1993). Lipid homeostasis is clearly altered in AD, as exemplified by aberrant lipid accumulation in ependymal cells in the neuronal stem cell niche in post-mortem AD brains and in mouse models of AD (Hamilton et al. 2015). Disturbances in genes related to lipid metabolism are a marker of aging that may also accelerate AD pathology (Podtelezhnikov et al. 2011).

Given the crucial role of the lipid transporter APOE in control of neuronal maturation and synaptogenesis *in vitro* (Mauch et al. 2001), it is not surprising that lipoprotein transport and lipid homeostasis are also considered crucial for normal brain function, including neuronal repair, membrane remodeling, and plasticity (Holtzman and Herz 2012). For example, altering lipid homeostasis in mice by knocking-out the liver X receptors (LXR), a transcription factor important for the regulation of cholesterol, fatty acid, and glucose homeostasis, causes severe brain abnormalities, including lipid accumulation, loss of neurons, and disorganization of myelin sheaths (Wang et al. 2002). Loss of APOE in mice increases the amount of sulfatide in the cortex and hippocampus as compared to wild-type mice (Han et al. 2003). Sulfatide levels in the cortex and hippocampus are also increased in apoE3 compared with apoE4 transgenic mice. The same effect of *APOE* is also seen in human CSF samples from apoE3 versus apoE4 carriers (Han et al. 2003).

Conceptually, the activity of APOE in brain lipid homeostasis should critically depend on the activity of neuronal APOE receptors, the major pathway to enable cellular uptake of lipids bound to this carrier. Not much is known about the link between APOE receptors and lipid metabolism. A cholesterol-enriched diet in LDLR KO mice leads to a significant decrease in cognitive functions because of impaired mitochondrial activity in the cerebral cortex (de Oliveira et al. 2011). LRP1 KO mice show a defect in brain lipid metabolism with decreased brain levels

of cholesterol, sulfatide, galactosylceramide, and triglyceride. These lipid alterations coincide with age-dependent dendritic spine degeneration, synapse loss, and neuroinflammation (Liu et al. 2010).

In addition to the LDLR and LRP1, there are other lipoprotein receptors with relevance to brain lipid metabolism, such as sortilin. In the periphery, the role of sortilin in controlling lipoprotein and lipid homeostasis is well described. Sortilin controls plasma cholesterol levels through regulating hepatic lipoprotein metabolism and PCSK9 action (Gustafsen et al. 2014) (Strong et al. 2012) (Musunuru et al. 2010) (Kjolby et al. 2010). However, sortilin is also highly expressed in the CNS where it binds and controls APOE levels as shown by accumulation of murine APOE in the brain of mice lacking this receptor (Carlo et al. 2013). A role for sortilin in APOE-dependent brain lipid homeostasis is supported by findings that sortilin-deficient mice show increased levels of sulfatides, a phenotype reported previously for *Apoe* knock-out animals (Carlo et al. 2013) (Han et al. 2003). In unpublished studies preceding my thesis work, Dr. Carlo-Spiewok in the Willnow group demonstrated that loss of sortilin also increased the brain levels of both human apoE3 and apoE4 in targeted replacement mice, arguing that sortilin is a neuronal receptor for murine and human APOE species alike.

In my thesis project, I set out to further elaborate on the role of sortilin in lipid homeostasis that may explain the isoform-specific actions of human apoE3 versus apoE4 in the risk of sporadic AD. To do this, I used targeted replacement mice expressing human apoE3 or apoE4 instead of the murine protein and combined them with mouse models genetically deficient for sortilin. APOE replacement mice have been commonly used in the field to study human specific aspects of brain lipid metabolism and AD progression. For example, mice expressing human apoE2 have higher spine density and dendritic complexity compared to the apoE3 and apoE4 mice (Dumanis et al. 2009). Mice expressing familial AD mutations and the apoE4 allele show an increase in oligomer Aβ as compared with apoE3 mice (Youmans et al. 2012). Importantly, my studies were performed in 12 weeks old adult mice without any trigger of amyloidogenesis such as overexpression of human APP or Tau transgenes. This approach allowed me to conduct my studies

without the interference of alterations in lipid homeostasis that may arise secondarily as a consequence of aberrant Aβ or Tau accumulation.

Using targeted lipidomics, I documented the impact of sortilin and *APOE* genotypes on lipid profiles. I found a decrease in the omega-3 lipid DHA and in synaptamide in mice with the apoE4 allele and in apoE3 mice lacking sortilin (Figure 4.4 and Figure 4.5). The alteration of the pool of total fatty acids reflected the decrease in DHA (Figure 4.1). Interestingly, levels of omega-6 lipids were not altered in the same manner (Figure 4.3). DHA is the main omega-3 lipid present in the brain and mice expressing the human apoE4 have decreased DHA levels in the cortex compared with apoE2 mice models (Vandal et al. 2014). Moreover, DHA intake protects the mouse brain from neurodegeneration (Calon et al. 2004). In line with the importance of DHA intake for normal brain function, AD patients show a decrease in brain DHA compared to controls (Soderberg et al. 1991) (Yuki et al. 2014). Although DHA has been linked to protective effects in the brain, the molecular basis of its action remains unknown. An equivalent role in protecting the brain from degeneration has been seen for synaptamide. This lipid is a DHA-derived potent neurogenic and synaptogenic factor with anti-inflammatory potential (Park et al. 2016) (Rashid et al. 2013). Since lower concentrations of synaptamide are needed to induce hippocampal neurite growth and synaptogenesis than of DHA, the neuroprotective effects seen with DHA may actually be mediated by synaptamide and not by DHA itself. Thus, DHA may represent the initial pool of lipids that can be converted into the active molecule synaptamide to perform its neuroprotective functions (Kim et al. 2011).

As well as for DHA and synaptamide, sortilin- and APOE-dependent changes in brain levels were also seen for two eCBs. The eCB system is a lipid-based signaling system highly active in the central and peripheral nervous system. It is mainly composed of two lipids, anandamide (AEA) and 2-arachidonoylglycerol (2-AG) (Muccioli 2010). Several research groups have found an increase in 2-AG levels but not anandamide in the brain of rodents in response to neurodegenerative processes (Van Der Stelt et al. 2006). Similarly, it was shown that 2-AG levels were increased in the plasma of AD patients, a mechanism thought to antagonize brain damage (Altamura et al. 2015). Consistently, I found an increase in 2-AG in the brain of mice with the apoE4 allele and lacking sortilin

compared with apoE3 (Figure 4.6). Moreover, I observed a sortilin-dependent effect on the levels of OEA and PEA in the brain independent of the *APOE* genotype (Figure 4.6). Taken together, my results strengthen the functional interaction of apoE3 and its receptor sortilin in regulating the handling of omega-3 lipids and eCBs in the brain.

Although differences in size and lipidation of lipoprotein-containing apoE3 or apoE4 have been reported (Heinsinger et al. 2016), I found no alteration DHA and arachidonic acids in CSF lipoproteins isolated from in healthy individuals or AD patients with apoE3 or apoE4 alleles (Figure 4.15). Furthermore, astrocytes, the main cell type in the brain responsible for the expression of APOE produces the same amount of APOE regardless of the *APOE* variant (Figure 4.16). Of clinical significance, I also observed the same effect of *APOE* genotype on 2-AG and synaptamide levels in the brain of AD patients compared with controls (Figure 4.7). These data, for the first time highlight APOE- and sortilin-dependent alteration of the DHA-derived/eCB-like lipid synaptamide in the mouse and human brain (Figure 4.5 and Figure 4.7).

5.2. The consequence of lipid alteration in the brain

PUFA and the endocannabinoid system have traditionally been viewed independently. However, there is a considerable overlap in their effects and it is conceivable that these lipids activate similar pathways. The endocannabinoid system has been shown to be of key importance in neurodegenerative processes due to its anti-inflammatory and neurogenic effects (Molina-Holgado and Molina-Holgado 2010).

Anandamide and 2-AG are endogenous signaling lipids that act by binding and activating G-protein-coupled-receptors termed CB1 and CB2 (Pertwee and Ross). Deletion of both CB receptors causes a decrease in hippocampal progenitor cell proliferation (Jin et al. 2004) (Palazuelos et al. 2006). However, despite the decrease in some eCBs in sortilin KO mice, adult neurogenesis in the subgranular layer of the hippocampal dentate gyrus (DG) and in the subventricular zone (SVZ) of the lateral ventricles were not altered in mice lacking sortilin as compared with wild-type controls (Figure 4.8 and Figure 4.9). Moreover, sortilin and *APOE* isoforms did not affect the dendritic complexity and arborization of pyramidal

neurons in cortical layers II/III in the mouse brain (Figure 4.10 and Figure 4.11). Jointly these results argue that this is not how apoE3 and sortilin work through eCBs.

An alternative mode of action of eCBs is through binding and activation of peroxisome proliferator-activated receptors (PPARs) (O'Sullivan 2016). Anandamide as well 2-AG bind and activate PPAR-γ-dependent transcriptional activities resulting in adipocyte differentiation and IL-2 suppression, respectively (Bouaboula et al. 2005) (Rockwell et al. 2006). With relevance to my findings, synaptamide does not bind to CBs and may thus also act mainly through PPARs. Finally, DHA is a natural ligand for PPAR-γ (Itoh et al. 2008) (Banga et al. 2009) (Niemoller and Bazan 2010).

PPARs are nuclear proteins that act as transcription factors once they are bound by lipid ligands. They regulate the expression of genes with a major role in inflammatory responses (Blumberg and Evans 1998). Increased inflammation in the brain has a central pathological role in AD. It is an important early component in AD that drives AD pathology independent of Aβ deposition (Heppner et al. 2015) (Tarkowski et al. 2003). For instance, it was shown that mice with age-associated chronic inflammation develop an AD-like pathology with activated microglia in the hippocampus prior to the accumulation of extracellular amyloid depositions (Krstic et al. 2012). In addition, aging, the strongest environmental risk factor for AD, is also characterized by an aberrant pro-inflammatory state (Sparkman and Johnson 2008). In line with a causal role for PPARs in containment of brain inflammation, the brain of AD patients is characterized by a pro-inflammatory state and by increased oxidative stress that induce compensatory protective responses in the brain by increasing PPAR-γ transcript levels (De La Monte and Wands 2006). Furthermore, non-steroidal anti-inflammatory drugs (NSAIDs) that act as agonists of PPAR-γ exert beneficial effects in AD mouse models and patients by attenuating learning deficits and memory loss, and by reducing glial activation and amyloid accumulation (Heneka et al. 2005) (Pedersen et al. 2006) (Escribano et al. 2010)(Watson et al. 2005).

In aged apoE3 mice, I found that the absence of sortilin coincides with increased levels of the pro-inflammatory markers GFAP and TNF-α compared with apoE3

mice expressing the receptor. By contrast, no changes in GFAP and TNF-α levels were seen in apoE4 expressing mice that expressed or lacked sortilin (Figure 4.13). Abnormal higher levels of the astrocyte activation marker GFAP were also reported in individuals with AD and in AD transgenic mice, suggesting that activation of glia are common pathological processes in neurodegenerative disorders in humans and animal models (Wyss-Coray 2006) (Liu et al. 2016) (Scuderi et al. 2014). Likewise, the pro-inflammatory cytokine TNF-α was also shown to have increased levels in the blood, CSF and brain of AD patients compared with healthy subjects (Brosseron et al. 2014) (Zhao et al. 2003) (Ofengeim et al. 2017). Interestingly, lipopolysaccharide (LPS) injections enhance the production of TNF-α in mice expressing apoE4 more than in apoE3 mice (Lynch et al. 2003). Synaptamide reduces TNF-α levels in microglia cultures, dampening LPS-induced inflammation (Park et al. 2016). These examples substantiate apoE4 as a risk of AD and underline the synaptamide-dependent neuroprotective role of apoE3 and sortilin.

Apart from an increase in pro-inflammatory markers GFAP and TNF-α, aged mouse models expressing apoE4 or mice expressing apoE3 without sortilin also showed transcriptional down-regulation of *VEGF* compared with (E3;WT) mice (Figure 4.13). VEGF is a neuroprotective factor that enhances neuronal survival and inhibits the expression of pro-inflammatory cytokines (Xu et al. 2017) (Sun et al. 2003). Increasing VEGF levels using encapsulated VEGF nanospheres implanted in the brain of mouse models of AD or transgenic mice overexpressing VEGF enhances neurogenesis and attenuates Aβ-induced AD symptoms (Religa et al. 2013) (Herran et al. 2015) (Spuch et al. 2010).

Jointly, these results argue that PUFA and eCBs can induce PPARs-mediated transcription of genes that produce an anti-inflammatory effect. Thus, factors such as sortilin and APOE isoforms that alter the metabolism of these lipids may shift the brain into a pro-inflammatory state, increasing the risk of neurodegenerative diseases.

5.3. The effect of sortilin and APOE isoforms on the intracellular lipid carrier FABP7

Lipid homeostasis in the brain of the mouse models can be perturbed in multiple ways, but how do sortilin and APOE isoforms alter lipid metabolism? Conceptually, sortilin and *APOE* genotypes may impact expression of the enzyme repertoire involved in metabolism of DHA and/or eCBs. However, I failed to observe any alteration in transcript levels of the genes encoding the enzymes *Napepld*, *Faah*, *Dagla,* and *Mgll* in the brain cortices of my mouse strains (Figure 4.14). Therefore, alterations in metabolic enzymes are likely not responsible for the alterations in levels of these lipids seen in brain tissues of mice and humans with apoE4 as compared with apoE3. Moreover, I showed before that sortilin and/or APOE isoforms did not impact the types of lipids bound to lipoproteins in plasma or CSF (Figure 4.15) (Figure 4.16), disproving altered extracellular lipid transport as the underlying cause of APOE-dependent lipid changes seen in the human or mouse brain.

Lipids require specific carriers to facilitate their transport not only in the extracellular space but also in the aqueous milieu of the cytoplasm. For the later, fatty acid binding proteins (FABPs) have evolved to deliver long-chain fatty acids to various compartments of the cell. For example, they transport lipids into lipid droplets for storage, to the mitochondria or peroxisome for oxidation, to the nucleus to control lipid-mediated transcriptional regulation, or to the extracellular space to signal in an autocrine or paracrine manner (Furuhashi and Hotamisligil 2008).

Members of the FABP family are expressed in many tissues. Several FABPs are expressed in the brain, including FABP3, FABP5 and FABP7. Of these, FABP7 is the only carrier affected by sortilin and APOE isoforms and these effects may explain the changes in PUFA and eCBs seen in the brains of my mouse models. Thus, I found that FABP7 is decreased in the brain of apoE3 mice lacking sortilin. This effect was not seen with apoE4 allele (Figure 4.17). The impact of apoE3 and sortilin genotypes on FABP7 levels was seen in primary neurons but not in astrocytes (Figure 4.19 and Figure 4.20). These findings argue for a functional

interaction of sortilin and FABP7 in neurons that depends on the presence of apoE3 (but not apoE4).

FABP7 is a cytoplasmic shuttle protein that binds DHA with high affinity. Deletion of FABP7 decreases DHA levels in the brain (Xu et al. 1996) (Owada et al. 2006). FABP7 facilitates cellular uptake, intracellular trafficking, and metabolism of eCBs (Kaczocha et al. 2009). Of interest to my studies, FABP7 transports DHA and also binds to PPAR-γ, thereby inducing expression of GFAP in astrocytes and decreasing the migration of malignant glioma cells (Adida and Spener 2006) (Mita et al. 2010) (Tripathi et al. 2017).

Previous studies showed FABP7 levels to be pathologically increased in patients with Down's syndrome or schizophrenia (Sánchez-Font et al. 2003) (Watanabe et al. 2007) (Furuhashi and Hotamisligil 2008). Now, I uncovered the relevance of this carrier for AD, as I showed a decrease in FABP7 levels in AD patients with apoE4 compared to apoE3 carriers (Figure 4.18).

How exactly may sortilin and *APOE* genotypes regulate the levels of FABP7 in neurons? In my studies, I was unable to detect significant changes in the levels of *Fabp7* transcript in the brain and in primary neuronal culture of the various mouse models. However, a significant decrease in expression at the protein level was observed, pointing to post-translation mechanisms being responsible for the change in FABP7 protein expression in apoE3 mice or primary cultures lacking sortilin as compared with the respective WT control (Figure 4.17; Figure 4.19 and Figure 4.20).

Interestingly, sortilin not only functions as an endocytic receptor at the cell membrane but also as an intracellular sorting receptor for the transport of a wide variety of intracellular proteins between the trans-Golgi network, endosomes, lysosome, and the plasma membrane (Schmidt and Willnow 2016). Thus, I hypothesize that sortilin may also be responsible for regulating intracellular sorting and stability of FABP7 in cells. I was able to substantiate my hypothesis by documenting that FABP7 directly interacts with sortilin (Figure 4.22 and Figure 4.23) and that lack of the receptor decreases the half-life of the carrier protein (Figure 4.24).

Sortilin facilitates uptake of apoE3 and apoE4 to the same extent *in vitro* (Carlo et al. 2013). Also, sortilin-deficient mice accumulate both isoforms in the brain with no apparent difference (Dr. Anne-Sophie Carlo-Spiewok, personal communication). Jointly, these findings argue that the effect of apoE4 on sortilin and FABP7 interaction and on lipid metabolism in neurons works intracellularly. This hypothesis is supported by the fact that sortilin mediates the intracellular sorting of apolipoprotein B (APOB), regulating nascent lipoprotein particles formation and secretion from liver cells (Strong et al. 2012) (Musunuru et al. 2010) (Kjolby et al. 2010).

Interestingly, several studies documented distinct intracellular trafficking pathways for apoE3 versus apoE4 that have profound consequences for the activities of APOE receptors. Thus, following endocytic uptake by APOE receptors, apoE3 recycles back to the cell surface for re-secretion. By contrast, apoE4 does not recycle but accumulates intracellularly to disrupt cellular functions. For example, in hepatoma cells, loss of apoE4 recycling interferes with intracellular cholesterol transport (Heeren et al. 2004). Likewise, apoE4 accelerates neuronal degeneration and synaptic plasticity or alters brain insulin signaling through the impairment of intracellular sorting of the APOE receptor-2 or the insulin receptor, respectively (Apoer2) (Zhao et al. 2017) (Chen et al. 2010).

Receptor-mediated endocytosis is a fundamental process that enables the selective uptake of macromolecules into cells. The endocytic pathway is necessary for many biological functions, including nutrient uptake, membrane remodeling, or control of cell surface receptor signaling. Endocytosis starts with the formation of early endosomes by engulfment of sections of the plasma membrane containing receptor/ligand complexes. Early endosomes mature to late endosomes that fuse with a lysosome (degradation pathway), or target the TGN (retrograde trafficking). Early endosomes may also directly move back to the cell surface via the recycling pathway (Huotari and Helenius 2011). Alterations in the endocytic machinery have been observed in patients and mouse models with AD. For example, upregulation of early endosomes marked by RAB5 were seen in the hippocampus of people with mild cognitive impairment (MCI) or AD as compared with health individuals (Ginsberg et al. 2010). Furthermore, the presence of apoE4 accentuates the enlargement of RAB5-positive early endosomes at preclinical

stages of AD and in aged mice expressing human apoE4 (Cataldo et al. 2000) (Zhao et al. 2017). Elevated levels of RAB4-marked recycling endosomes were also detected in early stage AD brains (Cataldo et al. 2000). In line with an important role of the endocytic machinery in neuronal health, I observed an alteration in the intracellular localization of sortilin-FABP7 complexes in CHO-S/F cells treated with exogenous apoE3 versus apoE4. PLA signals for sortilin and FABP7 showed increased colocalization of both proteins in early (RAB5) (Figure 4.27) and recycling (RAB11) endosomes (Figure 4.28) in CHO-S/F treated with apoE3 particles, confirming an impact of *APOE* genotypes on sortilin-dependent endosomal sorting of FABP7.

It is possible that different biophysical characteristics of APOE isoforms provide an explanation for the altered intracellular sorting of apoE4. The protein contains two distinct structural domains, a 22 kDa amino terminal domain that contains the LDLR binding site and a second 10 kDa carboxyl terminal domain that binds lipids. ApoE3 and apoE4 differ in only one amino acid (cysteine to arginine at position 112), however, this change has been suggested to underlie the functional differences between APOE isoforms. For example, the amino acid change in apoE4 in the amino terminal domain influences lipid binding to the other domain and, consequently, induces a preference of apoE4 for VLDL instead of HDL. This property is called “domain interaction”, whereby changes in one domain are known to influence the properties of the other domain (Weisgraber and Mahley 1996). In addition, at a lower pH, apoE4 has a greater propensity than apoE3 to form a molten globule, a stable folding intermediate that increases lipid binding and promotes self-aggregation (Morrow et al. 2002). It was proposed that altering endosomal pH by pharmacological or genetic inhibition of NHE6 activity (the primary proton leak channel in the early endosome) might be used to recycle apoE4 back to the surface of cells. The differences in conformational stability of these isoforms may explain why apoE4 is retained in the early and recycling compartments, and exerts its detrimental effect on APOE receptor recycling, as shown for sortilin herein.

Taken together, I proposed the following working model for the interaction of sortilin with APOE and FABP7 in control of brain lipid transport and metabolism.

Under physiological conditions, astrocytes in the brain produce APOE that it is secreted into the brain interstitial fluids to form HDL-like lipid transport particles.

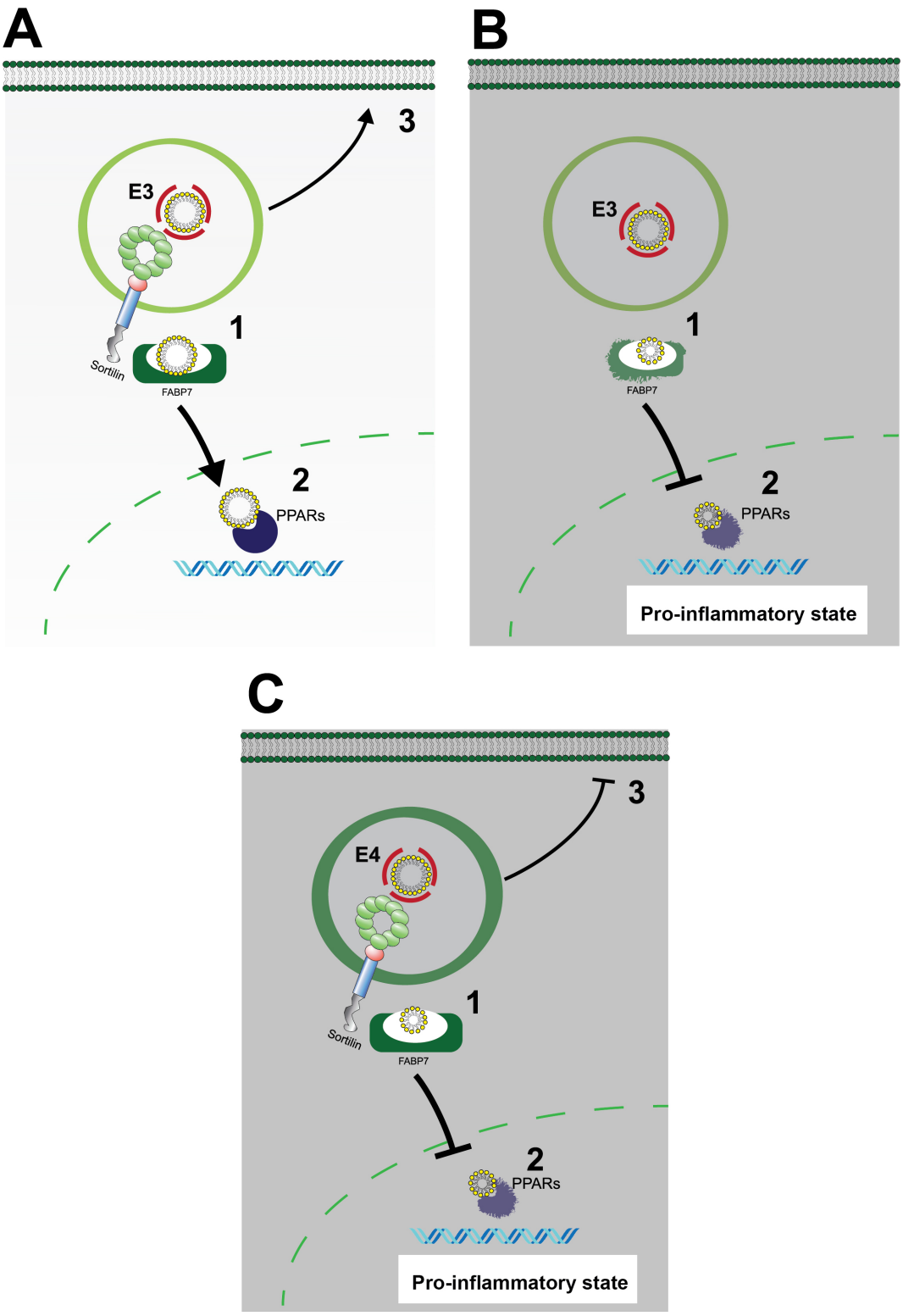

Figure 5.1: Proposed model of sortilin, FABP7 and APOE isoforms interaction in neurons.

(**A**) In the presence of apoE3-containing lipoprotein particles, interaction of sortilin with FABP7 (Step1) facilitates the neuronal lipid metabolism through PPARs activation in the nucleus (Step 2).

Then apoE3 is recycled back to the plasma membrane for re-secretion (Step 3). (**B**): Loss of sortilin in apoE3 mice impairs the trafficking and stability of FABP7 (Step 1) compromising lipid metabolism and PPARs function (Step 2), promoting pro-inflammatory effects. (**C**) Functional interaction and sorting of sortilin and FABP7 is disrupted by apoE4 (Step 1) as apoE4 traps sortilin inside the cell (Step 2) and it is not recycled back to the plasma membrane (Step 3). Ultimately, impairing the function of sortilin in FABP7 sorting has the same detrimental effects on neuronal lipid homeostasis as absence of the receptor in KO mice expressing apoE3 (Step 2).

These lipoprotein particles deliver essential lipids, including PUFA to neurons by binding to the APOE receptor, sortilin, which facilitates the endocytosis of APOE-containing lipoprotein particles. In the presence of apoE3, sortilin interacts with FABP7 to control proper intracellular sorting and biosynthesis of PUFAs to promote the beneficial actions of DHA, synaptamide, and eCBs. Among other modes of action, these lipids regulate PPARs-dependent gene expression, protecting the brain from inflammation (Figure 5.1A). Loss of sortilin alters trafficking and stability of FABP7 and disrupts its ability to support a proper PUFA metabolism, ultimately compromising the actions of lipid ligands on PPARs. Impaired activity of PPARs increases pro-inflammatory processes (Figure 5.1B). The interaction between sortilin and FABP7 in neuronal lipid homeostasis is lost in the presence of apoE4, the most known risk for AD. ApoE4 traps sortilin and FABP7 in intracellular endosomes and disrupts their physiological interaction to control PUFA and eCBs metabolism and action, ultimately impairing anti-inflammatory mechanisms mediated by the PPARs. (Figure 5.1 C).

5.4. Outlook

In summary, I found a novel cellular pathway, whereby sortilin, FABP7 and apoE3 interact to regulate lipid homeostasis and to protect the brain from inflammatory and neurodegenerative processes. This protective pathway is disrupted by apoE4, potentially contributing to the development of the sporadic forms of AD.

Certainly, my proposed model raises a number of important questions that requires further experimental exploration. Firstly, is DHA or synaptamide the final effector for the PPAR-mediated neuroprotection in apoE3? DHA and synaptamide are both altered in the same way in brain of my mouse models. Since synaptamide is still not well-studied, more experiments are required to understand the role of this lipid for brain function and neuroprotection. Luciferase reporter gene assays

using PPARs-responsive promoters could help in understanding whether synaptamide can bind and directly activate the PPARs target genes, and whether this function is influenced by sortilin, APOE, and /o FABP7.

Also, it remains to be substantiated that the interaction of sortilin and FABP7 with apoE3 supports a neuroprotective and anti-inflammatory state of the brain, and that the disturbances in the PUFA metabolism seen with apoE4 are pro-inflammatory. For example, using neuronal and glial cultures or brain organoids from the various *APOE* and sortilin genotype groups, it may be possible to perform inflammatory cytokines profiling to address this question. Moreover, the use CRISPR-Cas9 system to knock-out sortilin, FABP7, *APOE* isoforms or PPARs in brain organoids can be helpful to study their role in the regulation of inflammation in a more physiological environment.

Finally, we need to understand if and how inflammation affects the brain and causes neurodegeneration. I showed that aged mice expressing apoE4 or apoE3 animals lacking sortilin show a pro-inflammatory gene expression profile (Figure 4.13). To explore the pathophysiological relevance of these expression profiles, one may explore the inflammatory propensities of these genotype groups, for example by injecting lipopolysaccharide endotoxin (LPS) and by scoring accumulation of brain Aβ or neuronal loss induced by this inflammatory insult.

Although many obstacles still must be overcome before any of these investigations can be translated into the clinic to benefit patients at risk of AD, the challenges ahead are exciting and my studies demonstrate the potential of lipid biology for addressing the pathology of AD.

6. REFERENCES

Adibhatla RM, Hatcher JF. 2007. Role of lipids in brain injury and diseases. Future Lipidol. 2(4):403–422. doi:10.2217/17460875.2.4.403.

Adida A, Spener F. 2006. Adipocyte-type fatty acid-binding protein as inter-compartmental shuttle for peroxisome proliferator activated receptor γ agonists in cultured cell. Biochim Biophys Acta - Mol Cell Biol Lipids. 1761(2):172–181. doi:10.1016/j.bbalip.2006.02.006.

Altamura C, Ventriglia M, Martini MG, Montesano D, Errante Y, Piscitelli F, Scrascia F, Quattrocchi C, Palazzo P, Seccia S, et al. 2015. Elevation of plasma 2-arachidonoylglycerol levels in alzheimer's disease patients as a potential protective mechanism against neurodegenerative decline. J Alzheimer's Dis. 46(2):497–506. doi:10.3233/JAD-142349.

Andersen OM, Reiche J, Schmidt V, Gotthardt M, Spoelgen R, Behlke J, von Arnim CAF, Breiderhoff T, Jansen P, Wu X, et al. 2005. Neuronal sorting protein-related receptor sorLA/LR11 regulates processing of the amyloid precursor protein. Proc Natl Acad Sci. 102(38):13461–13466. doi:10.1073/pnas.0503689102.

Andersen OM, Schmidt V, Spoelgen R, Gliemann J, Behlke J, Galatis D, McKinstry WJ, Parker MW, Masters CL, Hyman BT, et al. 2006. Molecular dissection of the interaction between amyloid precursor protein and its neuronal trafficking receptor SorLA/LR11. Biochemistry. 45(8):2618–2628. doi:10.1021/bi052120v.

Baker M, Mackenzie IR, Pickering-Brown SM, Gass J, Rademakers R, Lindholm C, Snowden J, Adamson J, Sadovnick AD, Rollinson S, et al. 2006. Mutations in progranulin cause tau-negative frontotemporal dementia linked to chromosome 17. Nature. 442(7105):916–9. doi:10.1038/nature05016.

Balendiran GK, Schnütgen F, Scapin G, Börchers T, Xhong N, Lim K, Godbout R, Spener F, Sacchettini JC. 2000. Crystal structure and thermodynamic analysis of human brain fatty acid-binding protein. J Biol Chem. 275(35):27045–27054. doi:10.1074/jbc.M003001200.

Banga A, Unal R, Tripathi P, Pokrovskaya I, Owens RJ, Kern PA, Ranganathan G. 2009. Adiponectin translation is increased by the PPARgamma agonists pioglitazone and omega-3 fatty acids. Am J Physiol Endocrinol Metab. 296(3):E480-9. doi:10.1152/ajpendo.90892.2008.

Bartsch T, Wulff P. 2015. The hippocampus in aging and disease: From plasticity to vulnerability. Neuroscience. 309:1–16. doi:10.1016/j.neuroscience.2015.07.084.

Basavarajappa B. 2007. Critical Enzymes Involved in Endocannabinoid Metabolism. Protein Pept Lett. 14(3):237–246. doi:10.2174/092986607780090829.

Beher D, Hesse L, Masters CL, Multhaup G. 1996. Regulation of amyloid protein precursor (APP) binding to collagen and mapping of the binding sites on APP and collagen type I. J Biol Chem. 271(3):1613–1620. doi:10.1074/jbc.271.3.1613.

Benito C, Núñez E, Pazos MR, Tolón RM, Romero J. 2007. The endocannabinoid system and Alzheimer's disease. Mol Neurobiol. 36(1):75–81. doi:10.1007/s12035-007-8006-8.

Berchtold NC, Cotman CW. 1998. Evolution in the conceptualization of dementia and Alzheimer's disease: Greco-Roman period to the 1960s. Neurobiol Aging. 19(3):173–89.

Blennow K, Leon MJ De, Zetterberg H. 2001. Alzheimer's disease. 368:1–17.

Blumberg B, Evans RM. 1998. Orphan nuclear receptors - New ligands and new possibilities. Genes Dev. 12(20):3149–3155. doi:10.1101/gad.12.20.3149.

Bouaboula M, Hilairet S, Marchand J, Fajas L, Le Fur G, Casellas P. 2005. Anandamide induced PPARgamma transcriptional activation and 3T3-L1 preadipocyte differentiation. Eur J Pharmacol. 517(3):174–81. doi:10.1016/j.ejphar.2005.05.032.

Bright JJ, Kanakasabai S, Chearwae W, Chakraborty S. 2008. PPAR regulation of inflammatory signaling in CNS diseases. PPAR Res. 2008. doi:10.1155/2008/658520.

Brosseron F, Krauthausen M, Kummer M, Heneka MT. 2014. Body Fluid Cytokine Levels in Mild Cognitive Impairment and Alzheimer's Disease: a Comparative Overview. Mol Neurobiol. 50(2):534–544. doi:10.1007/s12035-014-8657-1.

Burgert T, Schmidt V, Caglayan S, Lin F, Fuchtbauer A, Fuchtbauer E-M, Nykjaer A, Carlo A-S, Willnow TE. 2013. SORLA-Dependent and -Independent Functions for PACS1 in Control of Amyloidogenic Processes. Mol Cell Biol. 33(21):4308–4320. doi:10.1128/mcb.00628-13.

Caglayan S, Takagi-Niidome S, Liao F, Carlo A-S, Schmidt V, Burgert T, Kitago Y, Füchtbauer E-M, Füchtbauer A, Holtzman DM, et al. 2014. Lysosomal sorting of amyloid-β by the SORLA receptor is impaired by a familial Alzheimer's disease mutation. Sci Transl Med. 6(223):223ra20. doi:10.1126/scitranslmed.3007747.

Cairns NJ, Bigio EH, Mackenzie IRA, Neumann M, Lee VM-Y, Hatanpaa KJ, White CL, Schneider JA, Grinberg LT, Halliday G, et al. 2007. Neuropathologic diagnostic and nosologic criteria for frontotemporal lobar degeneration: consensus of the Consortium for Frontotemporal Lobar Degeneration. Acta Neuropathol. 114(1):5–22. doi:10.1007/s00401-007-0237-2.

Calon F, Lim GP, Yang F, Morihara T, Teter B, Ubeda O, Rostaing P, Triller A, Salem N, Ashe KH, et al. 2004. Docosahexaenoic acid protects from dendritic pathology in an Alzheimer's disease mouse model. Neuron. 43(5):633–645. doi:10.1016/j.neuron.2004.08.013.

Campion D, Thomas-Anterion C, Belliard S, Dubois B, Charbonnier F, Martin C, Brice A, Dumanchin C, Raux G, Puel M, et al. 2002. Early-Onset Autosomal Dominant Alzheimer Disease: Prevalence, Genetic Heterogeneity, and Mutation Spectrum. Am J Hum Genet. 65(3):664–670. doi:10.1086/302553.

Cao D, Fukuchi K, Wan H, Kim H, Li L. 2006. Lack of LDL receptor aggravates learning deficits and amyloid deposits in Alzheimer transgenic mice. Neurobiol Aging. 27(11):1632–43. doi:10.1016/j.neurobiolaging.2005.09.011.

Carleton A, Petreanu LT, Lansford R, Alvarez-Buylla A, Lledo P. 2003. Becoming a new neuron in the adult olfactory bulb. Nat Neurosci. 6(5):507–18. doi:10.1038/nn1048.

Carlo A-S, Gustafsen C, Mastrobuoni G, Nielsen MS, Burgert T, Hartl D, Rohe M, Nykjaer A, Herz J, Heeren J, et al. 2013. The Pro-Neurotrophin Receptor Sortilin Is a Major Neuronal Apolipoprotein E Receptor for Catabolism of Amyloid- Peptide in the Brain. J Neurosci. 33(1):358–370. doi:10.1523/JNEUROSCI.2425-12.2013.

Carlo AS, Nykjaer A, Willnow TE. 2014. Sorting receptor sortilin - A culprit in cardiovascular and neurological diseases. J Mol Med. 92(9):905–911. doi:10.1007/s00109-014-1152-3.

Castellano JM, Kim J, Stewart FR, Jiang H, DeMattos RB, Patterson BW, Fagan AM, Morris JC, Mawuenyega KG, Cruchaga C, et al. 2011. Human apoE isoforms differentially regulate brain amyloid-β peptide clearance. Sci Transl Med. 3(89). doi:10.1126/scitranslmed.3002156.

Cataldo AM, Peterhoff CM, Troncoso JC, Gomez-Isla T, Hyman BT, Nixon RA. 2000. Endocytic pathway abnormalities precede amyloid β deposition in sporadic alzheimer's disease and down syndrome: Differential effects of APOE genotype and presenilin mutations. Am J Pathol. 157(1):277–286. doi:10.1016/S0002-9440(10)64538-5.

Chen Y, Durakoglugil MS, Xian X, Herz J. 2010. ApoE4 reduces glutamate receptor function and synaptic plasticity by selectively impairing ApoE receptor recycling. Proc Natl Acad Sci. 107(26):12011–12016. doi:10.1073/pnas.0914984107.

Chen Z-Y. 2005. Sortilin Controls Intracellular Sorting of Brain-Derived Neurotrophic Factor to the Regulated Secretory Pathway. J Neurosci. 25(26):6156–6166. doi:10.1523/JNEUROSCI.1017-05.2005.

Chitramuthu BP, Bennett HPJ, Bateman A. 2017. Progranulin: A new avenue towards the understanding and treatment of neurodegenerative disease. Brain. 140(12):3081–3104. doi:10.1093/brain/awx198.

Christoforou A, Mcghee KA, Morris SW, Thomson PA, Anderson S, Mclean A, Torrance HS, Hellard S Le, Pickard BS, Stclair D, et al. 2010. Convergence of linkage , association and GWAS findings for a candidate region for bipolar disorder and schizophrenia on chromosome 4p. Mol Psychiatry. 16(3):240–242. doi:10.1038/mp.2010.25.

Clee SM, Yandell BS, Schueler KM, Rabaglia ME, Richards OC, Raines SM, Kabara EA, Klass DM, Mui ET-K, Stapleton DS, et al. 2006. Positional cloning of Sorcs1, a type 2 diabetes quantitative trait locus. Nat Genet. 38(6):688–93. doi:10.1038/ng1796.

Corder EH, Saunders a M, Strittmatter WJ, Schmechel DE, Gaskell PC, Small GW, Roses a D, Haines JL, Pericak-Vance M a. 1993. Gene dose of apolipoprotein E type 4 allele and the risk of Alzheimer's disease in late onset families. Science. 261(5123):921–3. doi:10.1126/science.8346443.

Cruchaga C, Kauwe JSK, Nowotny P, Bales K, Pickering EH, Mayo K, Bertelsen S, Hinrichs A, Fagan AM, Holtzman DM, et al. 2012. Cerebrospinal fluid APOE levels: An endophenotype for genetic studies for Alzheimer's disease. Hum Mol Genet. 21(20):4558–4571. doi:10.1093/hmg/dds296.

Crystal H, Dickson D, Fuld P, Masur D, Scott R, Mehler M, Masdeu J, Kawas C, Aronson M, Wolfson L. 1988. Clinico-pathologic studies in dementia: nondemented subjects with pathologically confirmed Alzheimer's disease. Neurology. 38(11):1682–7. doi:10.1212/wnl.38.11.1682.

Cummings JL, Morstorf T, Zhong K. 2014. Alzheimer's disease drug-development pipeline: few candidates, frequent failures. Alzheimers Res Ther. 6(4):37. doi:10.1186/alzrt269.

Dodson SE, Andersen OM, Karmali V, Fritz JJ, Cheng D, Peng J, Levey AI, Willnow TE, Lah JJ. 2008. Loss of LR11/SORLA enhances early pathology in a mouse model of amyloidosis: evidence for a proximal role in Alzheimer's disease. J Neurosci. 28(48):12877–86. doi:10.1523/JNEUROSCI.4582-08.2008.

Dumanis SB, Burgert T, Caglayan S, Fuchtbauer A, Fuchtbauer E-M, Schmidt V, Willnow TE. 2015. Distinct Functions for Anterograde and Retrograde Sorting of SORLA in Amyloidogenic Processes in the Brain. J Neurosci. 35(37):12703–12713. doi:10.1523/JNEUROSCI.0427-15.2015.

Dumanis SB, Tesoriero JA, Babus LW, Nguyen MT, Trotter JH, Ladu MJ, Weeber EJ, Turner RS, Xu B, Rebeck GW, et al. 2009. ApoE4 Decreases Spine Density and Dendritic Complexity in Cortical Neurons In Vivo. J Neurosci. 29(48):15317–15322. doi:10.1523/JNEUROSCI.4026-09.2009.

Durakoglugil MS, Chen Y, White CL, Kavalali ET, Herz J. 2009. Reelin signaling antagonizes β-amyloid at the synapse. Proc Natl Acad Sci. 106(37):15938–15943. doi:10.1073/pnas.0908176106.

Echeverría F, Valenzuela R, Catalina Hernandez-Rodas M, Valenzuela A. 2017.

Docosahexaenoic acid (DHA), a fundamental fatty acid for the brain: New dietary sources. Prostaglandins Leukot Essent Fat Acids. 124(August):1–10. doi:10.1016/j.plefa.2017.08.001.

Ehehalt R, Keller P, Haass C, Thiele C, Simons K. 2003. Amyloidogenic processing of the Alzheimer β-amyloid precursor protein depends on lipid rafts. J Cell Biol. 160(1):113–123. doi:10.1083/jcb.200207113.

Escribano L, Simón A-M, Gimeno E, Cuadrado-Tejedor M, López de Maturana R, García-Osta A, Ricobaraza A, Pérez-Mediavilla A, Del Río J, Frechilla D. 2010. Rosiglitazone Rescues Memory Impairment in Alzheimer's Transgenic Mice: Mechanisms Involving a Reduced Amyloid and Tau Pathology. Neuropsychopharmacology. 35(7):1593–1604. doi:10.1038/npp.2010.32.

Fahnestock M, Michalski B, Xu B, Coughlin MD. 2001. The precursor pro-nerve growth factor is the predominant form of nerve growth factor in brain and is increased in Alzheimer's disease. Mol Cell Neurosci. 18(2):210–220. doi:10.1006/mcne.2001.1016.

Fahy E, Subramaniam S, Brown HA, Glass CK, Merrill AH, Murphy RC, Raetz CRH, Russell DW, Seyama Y, Shaw W, et al. 2005. A comprehensive classification system for lipids 1. 46. doi:10.1194/jlr.E400004-JLR200.

Farrer LA, Cupples LA, Haines JL, Hyman B, Kukull WA, Mayeux R, Myers RH, Pericak-Vance MA, Risch N, van Duijn CM. 1997. Effects of age, sex, and ethnicity on the association between apolipoprotein E genotype and Alzheimer disease. A meta-analysis. APOE and Alzheimer Disease Meta Analysis Consortium. Jama. 278(16):1349–56. doi:10.1001/jama.278.16.1349.

Finan GM, Okada H, Kim TW. 2011. BACE1 retrograde trafficking is uniquely regulated by the cytoplasmic domain of sortilin. J Biol Chem. 286(14):12602–12616. doi:10.1074/jbc.M110.170217.

Foley P. 2010. Biochimica et Biophysica Acta Lipids in Alzheimer ' s disease : A century-old story. BBA - Mol Cell Biol Lipids. 1801(8):750–753. doi:10.1016/j.bbalip.2010.05.004.

Furuhashi M, Hotamisligil GS. 2008. Fatty acid-binding proteins: Role in metabolic diseases and potential as drug targets. Nat Rev Drug Discov. 7(6):489–503.

doi:10.1038/nrd2589.

Gass J, Cannon A, Mackenzie IR, Boeve B, Baker M, Adamson J, Crook R, Melquist S, Kuntz K, Petersen R, et al. 2006. Mutations in progranulin are a major cause of ubiquitin-positive frontotemporal lobar degeneration. Hum Mol Genet. 15(20):2988–3001. doi:10.1093/hmg/ddl241.

Ginsberg SD, Mufson EJ, Counts SE, Wuu J, Alldred MJ. 2010. Regional Selectivity of rab5 and rab7 Protein Upregulation in Mild Cognitive Impairment and Alzheimer ' s Disease. 22:631–639. doi:10.3233/JAD-2010-101080.

Goncalves MB, Suetterlin P, Yip P, Molina-Holgado F, Walker DJ, Oudin MJ, Zentar MP, Pollard S, Yáñez-Muñoz RJ, Williams G, et al. 2008. A diacylglycerol lipase-CB2 cannabinoid pathway regulates adult subventricular zone neurogenesis in an age-dependent manner. Mol Cell Neurosci. 38(4):526–536. doi:10.1016/j.mcn.2008.05.001.

Granhall C, Park H-B, Fakhrai-Rad H, Luthman H. 2006. High-resolution quantitative trait locus analysis reveals multiple diabetes susceptibility loci mapped to intervals<800 kb in the species-conserved Niddm1i of the GK rat. Genetics. 174(3):1565–72. doi:10.1534/genetics.106.062208.

Grehan S, Tse E, Taylor JM. 2001. Two Distal Downstream Enhancers Direct Expression of the Human Apolipoprotein E Gene to Astrocytes in the Brain. 21(3):812–822.

Grimm MOW, Michaelson DM, Hartmann T. 2017. Omega-3 fatty acids, lipids, and apoE lipidation in Alzheimer's disease: a rationale for multi-nutrient dementia prevention. J Lipid Res. 58(11):2083–2101. doi:10.1194/jlr.R076331.

Guerreiro R, Ph D, Wojtas A, Bras J, Ph D, Carrasquillo M, Ph D, Rogaeva E, Ph D, Majounie E, et al. 2013. TREM2 Variants in Alzheimer's Disease Rita. N Engl J Med. 368(2):117–127. doi:10.1056/NEJMoa1211851.TREM2.

Gustafsen C, Glerup S, Pallesen LT, Olsen D, Andersen OM, Nykjaer A, Madsen P, Petersen CM. 2013. Sortilin and SorLA Display Distinct Roles in Processing and Trafficking of Amyloid Precursor Protein. J Neurosci. 33(1):64–71. doi:10.1523/jneurosci.2371-12.2013.

Gustafsen C, Kjolby M, Nyegaard M, Mattheisen M, Lundhede J, Buttenschøn H,

Mors O, Bentzon JF, Madsen P, Nykjaer A, et al. 2014. The hypercholesterolemia-risk gene SORT1 facilitates PCSK9 secretion. Cell Metab. 19(2):310–318. doi:10.1016/j.cmet.2013.12.006.

Haass C, Kaether C, Thinakaran G, Sisodia S. 2012. Trafficking and proteolytic processing of APP. Cold Spring Harb Perspect Med. 2(5):1–25. doi:10.1101/cshperspect.a006270.

Haass C, Selkoe DJ. 2007. Soluble protein oligomers in neurodegeneration: Lessons from the Alzheimer's amyloid β-peptide. Nat Rev Mol Cell Biol. 8(2):101–112. doi:10.1038/nrm2101.

Hamilton LK, Dufresne M, Joppé SE, Petryszyn S, Aumont A, Calon F, Barnabé-Heider F, Furtos A, Parent M, Chaurand P, et al. 2015. Aberrant Lipid Metabolism in the Forebrain Niche Suppresses Adult Neural Stem Cell Proliferation in an Animal Model of Alzheimer's Disease. Cell Stem Cell. 17(4):397–411. doi:10.1016/j.stem.2015.08.001.

Hampel H, Giegling I, Ph D, Andreassen O a, Jonsson T, Stefansson H, Steinberg S, Jonsdottir I, Jonsson P V, Snaedal J, et al. 2013. Variant of TREM2 associated with the risk of Alzheimer's disease. N Engl J Med. 368(2):107–116. doi:10.1056/NEJMoa1211103.Variant.

Han X, Cheng H, Fryer JD, Fagan AM, Holtzman DM. 2003. Novel Role for Apolipoprotein E in the Central Nervous System. J Biol Chem. 278(10):8043–8051. doi:10.1074/jbc.m212340200.

Hardy JA, Higgins GA. 1992. Alzheimer's disease: the amyloid cascade hypothesis. Science. 256(5054):184–5. doi:10.1126/science.1566067.

Harold D, Abraham R, Hollingworth P, Sims R, Gerrish A, Hamshere ML, Pahwa JS, Moskvina V, Dowzell K, Williams A, et al. 2009. Genome-wide association study identifies variants at CLU and PICALM associated with Alzheimer ' s disease. 41(10). doi:10.1038/ng.440.

He X, Huang Y, Li B, Gong C-X, Schuchman EH. 2013. Deregulation of sphingolipid metabolism in Alzheimer's disease. 185(2):974–981. doi:10.1038/mp.2011.182.doi.

Heeren J, Grewal T, Laatsch A, Becker N, Rinninger F, Rye KA, Beisiegel U.

2004. Impaired recycling of apolipoprotein E4 is associated with intracellular cholesterol accumulation. J Biol Chem. 279(53):55483–55492. doi:10.1074/jbc.M409324200.

Heinsinger NM, Gachechiladze MA, Rebeck GW. 2016. Apolipoprotein E Genotype Affects Size of ApoE Complexes in Cerebrospinal Fluid. 75(10):918–924. doi:10.1093/jnen/nlw067.

Heneka MT, Sastre M, Dumitrescu-Ozimek L, Hanke A, Dewachter I, Kuiperi C, O'Banion K, Klockgether T, Van Leuven F, Landreth GE. 2005. Acute treatment with the PPARγ agonist pioglitazone and ibuprofen reduces glial inflammation and Aβ1-42 levels in APPV717I transgenic mice. Brain. 128(6):1442–1453. doi:10.1093/brain/awh452.

Heppner FL, Ransohoff RM, Becher B. 2015. Immune attack : the role of inflammation in Alzheimer disease. Nat Publ Gr. 16(6):358–372. doi:10.1038/nrn3880.

Hermey G. 2009. The Vps10p-domain receptor family. Cell Mol Life Sci. 66(16):2677–89. doi:10.1007/s00018-009-0043-1.

Herran E, Perez-Gonzalez R, Igartua M, Pedraz JL, Carro E, Hernandez RM. 2015. Enhanced Hippocampal Neurogenesis in APP/Ps1 Mouse Model of Alzheimer's Disease After Implantation of VEGF-loaded PLGA Nanospheres. Curr Alzheimer Res. 12(10):932–40.

Holtzman D, Herz J. 2012. Apolipoprotein E and apolipoprotein receptors: normal biology and roles in Alzheimer's disease. Cold Spring Harb Perspect Med. 2(3):a006312. doi:10.1101/cshperspect.a006312.

Hu F, Padukkavidana T, Vægter CB, Brady OA, Zheng Y, Mackenzie IR, Feldman HH, Nykjaer A, Strittmatter SM. 2010. Sortilin-mediated endocytosis determines levels of the frontotemporal dementia protein, progranulin. Neuron. 68(4):654–667. doi:10.1016/j.neuron.2010.09.034.

Huotari J, Helenius A. 2011. Endosome maturation. EMBO J. 30(17):3481–500. doi:10.1038/emboj.2011.286.

Itoh T, Fairall L, Amin K, Inaba Y, Szanto A, Balint BL, Nagy L, Yamamoto K, Schwabe JWR. 2008. Structural basis for the activation of PPARgamma by

oxidized fatty acids. Nat Struct Mol Biol. 15(9):924–31.

Jacobsen L, Madsen P, Nielsen MS, Geraerts WPM, Gliemann J, Smit AB, Petersen CM. 2002. The sorLA cytoplasmic domain interacts with GGA1 and -2 and defines minimum requirements for GGA binding. FEBS Lett. 511(1–3):155–8. doi:10.1016/s0014-5793(01)03299-9.

Jansen P, Giehl K, Nyengaard JR, Teng K, Lioubinski O, Sjoegaard SS, Breiderhoff T, Gotthardt M, Lin F, Eilers A, et al. 2007. Roles for the pro-neurotrophin receptor sortilin in neuronal development, aging and brain injury. Nat Neurosci. 10(11):1449–1457. doi:10.1038/nn2000.

Jick H, Zornberg GL, Jick SS, Seshadri S, Drachman DA. 2000. Statins and the risk of dementia. Lancet (London, England). 356(9242):1627–31. doi:10.1016/s0140-6736(00)03155-x.

Jin K, Xie L, Kim SH, Parmentier-Batteur S, Sun Y, Mao XO, Childs J, Greenberg DA. 2004. Defective adult neurogenesis in CB1 cannabinoid receptor knockout mice. Mol Pharmacol. 66(2):204–8. doi:10.1124/mol.66.2.204.

Kaczocha M, Glaser ST, Deutsch DG. 2009. Identification of intracellular carriers for the endocannabinoid anandamide. Proc Natl Acad Sci U S A. 106(15):6375–80. doi:10.1073/pnas.0901515106.

Kamenetz, Kamenetz F, Tomita T, Hsieh H, Seabrook G, Borchelt D, Iwatsubo T, Sisodia S, Malinow R. 2003. APP Processing and Synaptic Function. Neuron. 37(6):925–937. doi:10.1016/S0896-6273(03)00124-7.

Kang HW, Kim HK, Moon BH, Lee Seo Jun, Lee Se Jung, Rhyu IJ. 2017. Comprehensive Review of Golgi Staining Methods for Nervous Tissue. Appl Microsc. 47(2):63–69. doi:10.9729/am.2017.47.2.63.

Kathiresan S, Melander O, Guiducci C, Surti A, Burtt NP, Rieder MJ, Cooper GM, Roos C, Voight BF, Havulinna AS, et al. 2008. Six new loci associated with blood low-density lipoprotein cholesterol, high-density lipoprotein cholesterol or triglycerides in humans. Nat Genet. 40(2):189–197. doi:10.1038/ng.75.

Kawakita E, Hashimoto M, Shido O. 2006. Docosahexaenoic acid promotes neurogenesis in vitro and in vivo. Neuroscience. 139(3):991–7. doi:10.1016/j.neuroscience.2006.01.021.

Kibbey MC, Juckert M, Weeks BS, Neve RL, Nostrandi WEVAN, Kleinman HK. 1993. Beta-amyloid precursor protein binds to the neurite-promoting IKVAV site of laminin CeH Biology : Proc Natl Acad Sci USA. 90(November):10150–10153.

Kim H-Y, Moon H-S, Cao D, Lee J, Kevala K, Jun SB, Lovinger DM, Akbar M, Huang BX. 2011. N -Docosahexaenoylethanolamide promotes development of hippocampal neurons . Biochem J. 435(2):327–336. doi:10.1042/bj20102118.

Kitago Y, Nagae M, Nakata Z, Yagi-Utsumi M, Takagi-Niidome S, Mihara E, Nogi T, Kato K, Takagi J. 2015. Structural basis for amyloidogenic peptide recognition by sorLA. Nat Struct Mol Biol. 22(3):199–206. doi:10.1038/nsmb.2954.

Kjolby M, Andersen OM, Breiderhoff T, Fjorback AW, Pedersen KM, Madsen P, Jansen P, Heeren J, Willnow TE, Nykjaer A. 2010. Sort1, encoded by the cardiovascular risk locus 1p13.3, is a regulator of hepatic lipoprotein export. Cell Metab. 12(3):213–223. doi:10.1016/j.cmet.2010.08.006.

Knouff C, Hinsdale ME, Mezdour H, Altenburg MK, Watanabe M, Quarfordt SH, Sullivan PM, Maeda N. 1999. Apo E structure determines VLDL clearance and atherosclerosis risk in mice. J Clin Invest. 103(11):1579–1586. doi:10.1172/JCI6172.

Kölsch H, Heun R, Kerksiek A, Bergmann K V., Maier W, Lütjohann D. 2004. Altered levels of plasma 24S- and 27-hydroxycholesterol in demented patients. Neurosci Lett. 368(3):303–308. doi:10.1016/j.neulet.2004.07.031.

Kracun I, Kalanj S, Talan-Hranilovic J, Cosovic C. 1992. Cortical distribution of gangliosides in Alzheimer's disease. Neurochem Int. 20(3):433–438. doi:10.1016/0197-0186(92)90058-Y.

Krstic D, Madhusudan A, Doehner J, Vogel P, Notter T, Imhof C, Manalastas A, Hilfiker M, Pfister S, Schwerdel C, et al. 2012. Systemic immune challenges trigger and drive Alzheimer-like neuropathology in mice. J Neuroinflammation. 9(1):699. doi:10.1186/1742-2094-9-151.

Kuda O. 2018. Bioactive metabolites of docosahexaenoic acid. (October). doi:10.1016/j.biochi.2017.01.002.

De La Monte SM, Wands JR. 2006. Molecular indices of oxidative stress and mitochondrial dysfunction occur early and often progress with severity of

Alzheimer's disease. J Alzheimer's Dis. 9(2):167–181. doi:10.3233/JAD-2006-9209.

LaDu MJ, Falduto MT, Manelli AM, Reardon CA, Getz GS, Frail DE. 1994. Isoform-specific binding of apolipoprotein E to β-amyloid. J Biol Chem. 269(38):23403–23406.

Lambert JC, Ibrahim-Verbaas CA, Harold D, Naj AC, Sims R, Bellenguez C, DeStafano AL, Bis JC, Beecham GW, Grenier-Boley B, et al. 2013. Meta-analysis of 74,046 individuals identifies 11 new susceptibility loci for Alzheimer's disease. Nat Genet. 45(12):1452–8. doi:10.1038/ng.2802.

Latifi S, Tamayol A, Habibey R, Sabzevari R, Kahn C, Geny D, Eftekharpour E, Annabi N, Blau A, Linder M, et al. 2016. Natural lecithin promotes neural network complexity and activity. Sci Rep. 6(April):1–9. doi:10.1038/srep25777.

Liang X, Slifer M, Martin ER, Schnetz-Boutaud N, Bartlett J, Anderson B, Züchner S, Gwirtsman H, Gilbert JR, Pericak-Vance MA, et al. 2009. Genomic convergence to identify candidate genes for Alzheimer disease on chromosome 10. Hum Mutat. 30(3):463–71. doi:10.1002/humu.20953.

Liu C-C, Zhao N, Yamaguchi Y, Cirrito JR, Kanekiyo T, Holtzman DM, Bu G. 2016. Neuronal heparan sulfates promote amyloid pathology by modulating brain amyloid-β clearance and aggregation in Alzheimer's disease. Sci Transl Med. 8(332):332ra44-332ra44. doi:10.1126/scitranslmed.aad3650.

Liu Chia-Chen, Liu Chia-Chan, Kanekiyo T, Xu H, Bu G. 2013. Apolipoprotein E and Alzheimer disease: risk, mechanisms and therapy. Nat Rev Neurol. 9(2):106–18. doi:10.1038/nrneurol.2012.263.

Liu Q, Trotter J, Zhang J, Peters MM, Cheng H, Bao J, Han X, Weeber EJ, Bu G. 2010. Neuronal LRP1 Knockout in Adult Mice Leads to Impaired Brain Lipid Metabolism and Progressive, Age-Dependent Synapse Loss and Neurodegeneration. J Neurosci. 30(50):17068–17078. doi:10.1523/jneurosci.4067-10.2010.

Liu Q, Zerbinatti C V., Zhang J, Hoe HS, Wang B, Cole SL, Herz J, Muglia L, Bu G. 2007. Amyloid Precursor Protein Regulates Brain Apolipoprotein E and Cholesterol Metabolism through Lipoprotein Receptor LRP1. Neuron. 56(1):66–78.

doi:10.1016/j.neuron.2007.08.008.

Luchsinger JA, Tang MX, Stern Y, Shea S, Mayeux R. 2001. Diabetes mellitus and risk of Alzheimer's disease and dementia with stroke in a multiethnic cohort. Am J Epidemiol. 154(7):635–641. doi:10.1093/aje/154.7.635.

Lynch JR, Tang W, Wang H, Vitek MP, Bennett ER, Sullivan PM, Warner DS, Laskowitz DT. 2003. APOE genotype and an ApoE-mimetic peptide modify the systemic and central nervous system inflammatory response. J Biol Chem. 278(49):48529–48533. doi:10.1074/jbc.M306923200.

Malik AR, Szydlowska K, Nizinska K, Asaro A, van Vliet EA, Popp O, Dittmar G, Fritsche-Guenther R, Kirwan JA, Nykjaer A, et al. 2019. SorCS2 Controls Functional Expression of Amino Acid Transporter EAAT3 and Protects Neurons from Oxidative Stress and Epilepsy-Induced Pathology. Cell Rep. 26(10):2792-2804.e6. doi:10.1016/j.celrep.2019.02.027.

MANDERS EMM, VERBEEK FJ, ATEN JA. 1993. Measurement of co-localization of objects in dual-colour confocal images. J Microsc. 169(3):375–382. doi:10.1111/j.1365-2818.1993.tb03313.x.

Marcusson EG, Horazdovsky BF, Cereghino JL, Gharakhanian E, Emr SD. 1994. The sorting receptor for yeast vacuolar carboxypeptidase Y is encoded by the VPS10 gene. Cell. 77(4):579–586. doi:10.1016/0092-8674(94)90219-4.

Marquer C, Devauges V, Cossec J-C, Liot G, Lécart S, Saudou F, Duyckaerts C, Lévêque-Fort S, Potier M-C. 2011. Local cholesterol increase triggers amyloid precursor protein-Bace1 clustering in lipid rafts and rapid endocytosis. FASEB J. 25(4):1295–1305. doi:10.1096/fj.10-168633.

Matsumata M, Inada H, Osumi N. 2016. Fatty acid binding proteins and the nervous system: Their impact on mental conditions. Neurosci Res. 102(January):47–55. doi:10.1016/j.neures.2014.08.012.

Mauch DH, Sapperstein SK, Christopherson KS, Barres BA, Ha BK, Zastrow M Von, Beattie MS, Malenka RC. 2001. CNS Synaptogenesis Promoted by Glia-Derived Cholesterol. Science (80-). 294(5545):1354–1357. doi:10.1126/science.294.5545.1354.

Mita R, Beaulieu MJ, Field C, Godbout R. 2010. Brain Fatty Acid-binding Protein

and ω-3/ω-6 Fatty Acids. J Biol Chem. 285(47):37005–37015. doi:10.1074/jbc.M110.170076.

Miyashita A, Koike A, Jun G, Wang L-S, Takahashi S, Matsubara E, Kawarabayashi T, Shoji M, Tomita N, Arai H, et al. 2013. SORL1 is genetically associated with late-onset Alzheimer's disease in Japanese, Koreans and Caucasians. PLoS One. 8(4):e58618. doi:10.1371/journal.pone.0058618.

Molina-Holgado E, Molina-Holgado F. 2010. Mending the broken brain: neuroimmune interactions in neurogenesis. J Neurochem. 114(5):1277–90. doi:10.1111/j.1471-4159.2010.06849.x.

Morrow JA, Hatters DM, Lu B, Hochtl P, Oberg KA, Rupp B, Weisgraber KH. 2002. Apolipoprotein E4 forms a molten globule. A potential basis for its association with disease. J Biol Chem. 277(52):50380–5. doi:10.1074/jbc.M204898200.

Muccioli GG. 2010. Endocannabinoid biosynthesis and inactivation, from simple to complex. Drug Discov Today. 15(11–12):474–483. doi:10.1016/j.drudis.2010.03.007.

Muendlein A, Geller-Rhomberg S, Saely CH, Winder T, Sonderegger G, Rein P, Beer S, Vonbank A, Drexel H. 2009. Significant impact of chromosomal locus 1p13.3 on serum LDL cholesterol and on angiographically characterized coronary atherosclerosis. Atherosclerosis. 206(2):494–9. doi:10.1016/j.atherosclerosis.2009.02.040.

Müller UC, Zheng H. 2012. Physiological functions of APP family proteins. Cold Spring Harb Perspect Med. 2(2):1–17. doi:10.1101/cshperspect.a006288.

Musunuru K, Strong A, Frank-Kamenetsky M, Lee NE, Ahfeldt T, Sachs K V., Li X, Li H, Kuperwasser N, Ruda VM, et al. 2010. From noncoding variant to phenotype via SORT1 at the 1p13 cholesterol locus. Nature. 466(7307):714–719. doi:10.1038/nature09266.

Nicolas G, Charbonnier C, Wallon D, Quenez O, Bellenguez C, Grenier-Boley B, Rousseau S, Richard A-C, Rovelet-Lecrux A, Le Guennec K, et al. 2016. SORL1 rare variants: a major risk factor for familial early-onset Alzheimer's disease. Mol Psychiatry. 21(6):831–6. doi:10.1038/mp.2015.121.

Nielsen MS, Gustafsen C, Madsen P, Nyengaard JR, Hermey G, Bakke O, Mari

M, Schu P, Pohlmann R, Dennes A, et al. 2007. Sorting by the Cytoplasmic Domain of the Amyloid Precursor Protein Binding Receptor SorLA. Mol Cell Biol. 27(19):6842–6851. doi:10.1128/MCB.00815-07.

Nielsen MS, Keat SJ, Hamati JW, Madsen P, Gutzmann JJ, Engelsberg A, Pedersen KM, Gustafsen C, Nykjaer A, Gliemann J, et al. 2008. Different motifs regulate trafficking of SorCS1 isoforms. Traffic. 9(6):980–94.

Niemoller TD, Bazan NG. 2010. Docosahexaenoic acid neurolipidomics. Prostaglandins Other Lipid Mediat. 91(3–4):85–89. doi:10.1016/j.prostaglandins.2009.09.005.

Nilsson SK, Christensen S, Raarup MK, Ryan RO, Nielsen MS, Olivecrona G. 2008. Endocytosis of apolipoprotein A-V by members of the low density lipoprotein receptor and the VPS10p domain receptor families. J Biol Chem. 283(38):25920–7. doi:10.1074/jbc.M802721200.

Nykjaer A, Lee R, Teng KK, Jansen P, Madsen P, Nielsen MS, Jacobsen C, Kliemannel M, Schwarz E, Willnow TE, et al. 2004. Sortilin is essential for proNGF-induced neuronal cell death. Nature. 427(6977):843–8. doi:10.1038/nature02319.

O'Sullivan SE. 2016. An update on PPAR activation by cannabinoids. Br J Pharmacol. 173(12):1899–1910. doi:10.1111/bph.13497.

Ofengeim D, Mazzitelli S, Ito Y, DeWitt JP, Mifflin L, Zou C, Das S, Adiconis X, Chen H, Zhu H, et al. 2017. RIPK1 mediates a disease-associated microglial response in Alzheimer's disease. Proc Natl Acad Sci U S A. 114(41):E8788–E8797. doi:10.1073/pnas.1714175114.

Offe K, Dodson SE, Shoemaker JT, Fritz JJ, Gearing M, Levey AI, Lah JJ. 2006. The lipoprotein receptor LR11 regulates amyloid beta production and amyloid precursor protein traffic in endosomal compartments. J Neurosci. 26(5):1596–603. doi:10.1523/JNEUROSCI.4946-05.2006.

de Oliveira J, Hort MA, Moreira ELG, Glaser V, Ribeiro-do-Valle RM, Prediger RD, Farina M, Latini A, de Bem AF. 2011. Positive correlation between elevated plasma cholesterol levels and cognitive impairments in LDL receptor knockout mice: relevance of cortico-cerebral mitochondrial dysfunction and oxidative stress.

Neuroscience. 197:99–106. doi:10.1016/j.neuroscience.2011.09.009.

Owada Y, Abdelwahab SA, Kitanaka N, Sakagami H, Takano H, Sugitani Y, Sugawara M, Kawashima H, Kiso Y, Mobarakeh JI, et al. 2006. Altered emotional behavioral responses in mice lacking brain-type fatty acid-binding protein gene. Eur J Neurosci. 24(1):175–187. doi:10.1111/j.1460-9568.2006.04855.x.

Palazuelos J, Aguado T, Egia A, Mechoulam R, Guzmán M, Galve-Roperh I. 2006. Non-psychoactive CB2 cannabinoid agonists stimulate neural progenitor proliferation. FASEB J. 20(13):2405–7. doi:10.1096/fj.06-6164fje.

Park T, Chen H, Kevala K, Lee JW, Kim HY. 2016. N-Docosahexaenoylethanolamine ameliorates LPS-induced neuroinflammation via cAMP/PKA-dependent signaling. J Neuroinflammation. 13(1):1–15. doi:10.1186/s12974-016-0751-z.

Parks BW, Nam E, Org E, Kostem E, Norheim F, Hui ST, Pan C, Civelek M, Rau CD, Bennett BJ, et al. 2013. Genetic control of obesity and gut microbiota composition in response to high-fat, high-sucrose diet in mice. Cell Metab. 17(1):141–52. doi:10.1016/j.cmet.2012.12.007.

Pearson HA, Peers C. 2006. Physiological roles for amyloid β peptides. J Physiol. 575(1):5–10. doi:10.1113/jphysiol.2006.111203.

Pedersen WA, McMillan PJ, Kulstad JJ, Leverenz JB, Craft S, Haynatzki GR. 2006. Rosiglitazone attenuates learning and memory deficits in Tg2576 Alzheimer mice. Exp Neurol. 199(2):265–273. doi:10.1016/j.expneurol.2006.01.018.

Perez RG, Zheng H, Van der Ploeg LHT, Koo EH. 1997. The β-Amyloid Precursor Protein of Alzheimer's Disease Enhances Neuron Viability and Modulates Neuronal Polarity. J Neurosci. 17(24):9407–9414. doi:10.1523/jneurosci.17-24-09407.1997.

Pertwee RG, Ross RA. Cannabinoid receptors and their ligands. Prostaglandins Leukot Essent Fatty Acids. 66(2–3):101–21. doi:10.1054/plef.2001.0341.

Petersen CM, Nielsen MS, Nykjaer A, Jacobsen L, Tommerup N, Rasmussen HH, Roigaard H, Gliemann J, Madsen P, Moestrup SK. 1997. Molecular identification of a novel candidate sorting receptor purified from human brain by receptor-associated protein affinity chromatography. J Biol Chem. 272(6):3599–605.

doi:10.1074/jbc.272.6.3599.

Pfrieger FW. 2003. Cholesterol homeostasis and function in neurons of the central nervous system. Cell Mol Life Sci. 60(6):1158–1171. doi:10.1007/s00018-003-3018-7.

Pfrieger FW, Ungerer N. 2011. Cholesterol metabolism in neurons and astrocytes. Prog Lipid Res. 50(4):357–71. doi:10.1016/j.plipres.2011.06.002.

Pitas RE, Boyles JK, Lee SH, Foss D, Mahley RW. 1987. Astrocytes synthesize apolipoprotein E and metabolize apolipoprotein E-containing lipoproteins. Biochim Biophys Acta. 917(1):148–61. doi:10.1016/0005-2760(87)90295-5.

Podtelezhnikov AA, Tanis KQ, Nebozhyn M, Ray WJ, Stone DJ, Loboda AP. 2011. Molecular insights into the pathogenesis of Alzheimer's disease and its relationship to normal aging. PLoS One. 6(12):e29610. doi:10.1371/journal.pone.0029610.

Pottier C, Hannequin D, Coutant S, Rovelet-Lecrux A, Wallon D, Rousseau S, Legallic S, Paquet C, Bombois S, Pariente J, et al. 2012. High frequency of potentially pathogenic SORL1 mutations in autosomal dominant early-onset Alzheimer disease. Mol Psychiatry. 17(9):875–9. doi:10.1038/mp.2012.15.

Profenno LA, Porsteinsson AP, Faraone S V. 2010. Meta-Analysis of Alzheimer's Disease Risk with Obesity, Diabetes, and Related Disorders. Biol Psychiatry. 67(6):505–512. doi:10.1016/j.biopsych.2009.02.013.

Putcha D, Brickhouse M, O'Keefe K, Sullivan C, Rentz D, Marshall G, Dickerson B, Sperling R. 2011. Hippocampal Hyperactivation Associated with Cortical Thinning in Alzheimer's Disease Signature Regions in Non-Demented Elderly Adults. J Neurosci. 31(48):17680–17688. doi:10.1523/jneurosci.4740-11.2011.

Quistgaard EM, Madsen P, Grøftehauge MK, Nissen P, Petersen CM, Thirup SS. 2009. Ligands bind to Sortilin in the tunnel of a ten-bladed β-propeller domain. Nat Struct Mol Biol. 16(1):96–98. doi:10.1038/nsmb.1543.

Rao AT, Degnan AJ, Levy LM. 2014. Genetics of Alzheimer disease. Am J Neuroradiol. 35(3):457–458. doi:10.3174/ajnr.A3545.

Rapp A, Gmeiner B, Hüttinger M. 2006. Implication of apoE isoforms in cholesterol

metabolism by primary rat hippocampal neurons and astrocytes. Biochimie. 88(5):473–83. doi:10.1016/j.biochi.2005.10.007.

Rashid MA, Katakura M, Kharebava G, Kevala K, Kim HY. 2013. N-docosahexaenoylethanolamine is a potent neurogenic factor for neural stem cell differentiation. J Neurochem. 125(6):869–884. doi:10.1111/jnc.12255.

Reitz C, Brayne C, Mayeux R. 2011. Epidemiology of Alzheimer disease. Nat Rev Neurol. 7(3):137–152. doi:10.1038/nrneurol.2011.2.

Reitz C, Tokuhiro S, Clark LN, Conrad C, Vonsattel J-P, Hazrati L-N, Palotás A, Lantigua R, Medrano M, Z Jiménez-Velázquez I, et al. 2011. SORCS1 alters amyloid precursor protein processing and variants may increase Alzheimer's disease risk. Ann Neurol. 69(1):47–64. doi:10.1002/ana.22308.

Reitz C, Tosto G, Vardarajan B, Rogaeva E, Ghani M, Rogers RS, Conrad C, Haines JL, Pericak-vance MA. 2013. Independent and epistatic effects of variants in VPS10-d receptors on Alzheimer disease risk and processing of the amyloid precursor protein (APP). 3(5):e256-12. doi:10.1038/tp.2013.13.

Religa P, Cao R, Religa D, Xue Y, Bogdanovic N, Westaway D, Marti HH, Winblad B, Cao Y. 2013. VEGF significantly restores impaired memory behavior in Alzheimer's mice by improvement of vascular survival. Sci Rep. 3. doi:10.1038/srep02053.

Rockwell CE, Snider NT, Thompson JT, Vanden Heuvel JP, Kaminski NE. 2006. Interleukin-2 suppression by 2-arachidonyl glycerol is mediated through peroxisome proliferator-activated receptor gamma independently of cannabinoid receptors 1 and 2. Mol Pharmacol. 70(1):101–11. doi:10.1124/mol.105.019117.

Rogaeva E, Meng Y, Lee JH, Gu Y, Kawarai T, Zou F, Katayama T, Baldwin CT, Cheng R, Hasegawa H, et al. 2007. The neuronal sortilin-related receptor SORL1 is genetically associated with Alzheimer disease. Nat Genet. 39(2):168–77. doi:10.1038/ng1943.

Rohe M, Carlo A-S, Breyhan H, Sporbert A, Militz D, Schmidt V, Wozny C, Harmeier A, Erdmann B, Bales KR, et al. 2008. Sortilin-related receptor with A-type repeats (SORLA) affects the amyloid precursor protein-dependent stimulation of ERK signaling and adult neurogenesis. J Biol Chem. 283(21):14826–34.

doi:10.1074/jbc.M710574200.

Sánchez-Font MF, Bosch-Comas A, Gonzàlez-Duarte R, Marfany G. 2003. Overexpression of FABP7 in Down syndrome fetal brains is associated with PKNOX1 gene-dosage imbalance. Nucleic Acids Res. 31(11):2769–2777. doi:10.1093/nar/gkg396.

Scarmeas N, Stern Y, Tang M, Luchsinger JA. 2011. Mediterranean Diet and Risk for Alzheimer's Disease Nikolaos. Ann Neurol. 59(6):912–921. doi:10.1002/ana.20854.Mediterranean.

Scherzer C, Offe K, Lah JJ. 2004. Loss of Apolipoprotein E Receptor LR11 in Alzheimer Disease. Arch Neurol. 61:1200–5.

Scheuner D, Eckman C, Jensen M, Song X, Citron M, Suzuki N, Bird TD, Hardy J, Hutton M, Kukull W, et al. 1996. Secreted amyloid beta-protein similar to that in the senile plaques of Alzheimer's disease is increased in vivo by the presenilin 1 and 2 and APP mutations linked to familial Alzheimer's disease. Nat Med. 2(8):864–70.

Schmidt V, Sporbert A, Rohe M, Reimer T, Rehm A, Andersen OM, Willnow TE. 2007. SorLA/LR11 regulates processing of amyloid precursor protein via interaction with adaptors GGA and PACS-1. J Biol Chem. 282(45):32956–32964. doi:10.1074/jbc.M705073200.

Schmidt V, Willnow TE. 2016. Protein sorting gone wrong--VPS10P domain receptors in cardiovascular and metabolic diseases. Atherosclerosis. 245(December 2015):194–9. doi:10.1016/j.atherosclerosis.2015.11.027.

Scuderi C, Stecca C, Valenza M, Ratano P, Bronzuoli MR, Bartoli S, Steardo L, Pompili E, Fumagalli L, Campolongo P, et al. 2014. Palmitoylethanolamide controls reactive gliosis and exerts neuroprotective functions in a rat model of Alzheimer's disease. Cell Death Dis. 5(9):e1419-12. doi:10.1038/cddis.2014.376.

Selkoe DJ. 1991. The Molecular of Alzheimer's. 6:487–498. doi:10.1016/0896-6273(91)90052-2.

Selkoe DJ. 2008. Soluble oligomers of the amyloid beta-protein impair synaptic plasticity and behavior. Behav Brain Res. 192(1):106–13. doi:10.1016/j.bbr.2008.02.016.

Sloane JA, Pietropaolo MF, Rosene DL, Moss MB, Peters A, Kemper T, Abraham CR. 1997. Lack of correlation between plaque burden and cognition in the aged monkey. Acta Neuropathol. 94(5):471–8.

Smith EN, Chen W, Kähönen M, Kettunen J, Lehtimäki T, Peltonen L, Raitakari OT, Salem RM, Schork NJ, Shaw M, et al. 2010. Longitudinal genome-wide association of cardiovascular disease risk factors in the Bogalusa heart study. PLoS Genet. 6(9):e1001094. doi:10.1371/journal.pgen.1001094.

Soderberg M, Edlund C, Kristensson K, Dallner G. 1991. Fatty Acid Composition of Brain Phospholipids in Aging and in Alzheimer ' s Disease. 26(6):421–425.

Sparkman NL, Johnson RW. 2008. Neuroinflammation Associated with Aging Sensitizes the Brain to the Effects of Infection or Stress Nathan. 15:323–330. doi:10.1159/000156474.Neuroinflammation.

Spuch C, Antequera D, Portero A, Orive G, Hernández RM, Molina JA, Bermejo-Pareja F, Pedraz JL, Carro E. 2010. The effect of encapsulated VEGF-secreting cells on brain amyloid load and behavioral impairment in a mouse model of Alzheimer's disease. Biomaterials. 31(21):5608–18. doi:10.1016/j.biomaterials.2010.03.042.

Van Der Stelt M, Mazzola C, Esposito G, Matias I, Petrosino S, De Filippis D, Micale V, Steardo L, Drago F, Iuvone T, et al. 2006. Endocannabinoids and β-amyloid-induced neurotoxicity in vivo: Effect of pharmacological elevation of endocannabinoid levels. Cell Mol Life Sci. 63(12):1410–1424. doi:10.1007/s00018-006-6037-3.

Strong A, Ding Q, Edmondson AC, Millar JS, Sachs K V, Li X, Kumaravel A, Wang MY, Ai D, Guo L, et al. 2012. Hepatic sortilin regulates both apolipoprotein B secretion and LDL catabolism. J Clin Invest. 122(8):2807–16. doi:10.1172/JCI63563.

Sun Y, Jin K, Xie L, Childs J, Mao XO, Logvinova A, Greenberg D a. 2003. VEGF-induced neuroprotection, neurogenesis, and angiogenesis after focal cerebral ischemia. J Clin Invest. 111(12):1843–1851. doi:10.1172/JCI17977.

Svennerholm L, Gottfries C -G. 1994. Membrane Lipids, Selectively Diminished in Alzheimer Brains, Suggest Synapse Loss as a Primary Event in Early-Onset Form

(Type I) and Demyelination in Late-Onset Form (Type II). J Neurochem. 62(3):1039–1047. doi:10.1046/j.1471-4159.1994.62031039.x.

Tarabal O, Casanovas A, Ciutat D, Casas C, Caldero J, Esquerda JE. 2007. Glutamate mediated receptor excitotoxicity seems to be an important mechanism in the pathogenesis of many neurologic disorders, including motoneuron (MN). J Neurosci Res. 2740(July):2726–2740. doi:10.1002/jnr.

Tarkowski E, Andreasen N, Tarkowski A, Blennow K. 2003. Intrathecal inflammation precedes development of Alzheimer's disease. J Neurol Neurosurg Psychiatry. 74(9):1200–1205. doi:10.1136/jnnp.74.9.1200.

Tosto G, Reitz C. 2013. Genome-wide association studies in Alzheimer's disease: A review topical collection on dementia. Curr Neurol Neurosci Rep. 13(10). doi:10.1007/s11910-013-0381-0.

Tripathi S, Kushwaha R, Mishra J, Gupta MK, Kumar H, Sanyal Somali, Singh D, Sanyal Sabyasachi, Sahasrabuddhe AA, Kamthan M, et al. 2017. Docosahexaenoic acid up-regulates both PI3K/AKT-dependent FABP7–PPARγ interaction and MKP3 that enhance GFAP in developing rat brain astrocytes. J Neurochem. 140(1):96–113. doi:10.1111/jnc.13879.

Van Uden E, Mallory M, Veinbergs I, Alford M, Rockenstein E, Masliah E. 2002. Increased extracellular amyloid deposition and neurodegeneration in human amyloid precursor protein transgenic mice deficient in receptor-associated protein. J Neurosci. 22(21):9298–304. doi:10.1523/jneurosci.22-21-09298.2002.

Vaegter CB, Jansen P, Fjorback AW, Glerup S, Skeldal S, Kjolby M, Richner M, Erdmann B, Nyengaard JR, Tessarollo L, et al. 2011. Sortilin associates with Trk receptors to enhance anterograde transport and neurotrophin signaling. Nat Neurosci. 14(1):54–63. doi:10.1038/nn.2689.

Vandal M, Alata W, Tremblay C, Rioux-Perreault C, Salem N, Calon F, Plourde M. 2014. Reduction in DHA transport to the brain of mice expressing human APOE4 compared to APOE2. J Neurochem. 129(3):516–526. doi:10.1111/jnc.12640.

Verheijen J, Van den Bossche T, van der Zee J, Engelborghs S, Sanchez-Valle R, Lladó A, Graff C, Thonberg H, Pastor P, Ortega-Cubero S, et al. 2016. A comprehensive study of the genetic impact of rare variants in SORL1 in European

early-onset Alzheimer's disease. Acta Neuropathol. 132(2):213–24. doi:10.1007/s00401-016-1566-9.

Wang L, Schuster GU, Hultenby K, Zhang Q, Andersson S, Gustafsson J-A. 2002. Liver X receptors in the central nervous system: From lipid homeostasis to neuronal degeneration. Proc Natl Acad Sci. 99(21):13878–13883. doi:10.1073/pnas.172510899.

Watanabe A, Toyota T, Owada Y, Hayashi T, Iwayama Y, Matsumata M, Ishitsuka Y, Nakaya A, Maekawa M, Ohnishi T, et al. 2007. Fabp7 maps to a quantitative trait locus for a schizophrenia endophenotype. PLoS Biol. 5(11):2469–2483. doi:10.1371/journal.pbio.0050297.

Watson GS, Cholerton BA, Reger MA, Baker LD, Plymate SR, Asthana S, Fishel MA, Kulstad JJ, Green PS, Cook DG, et al. 2005. Preserved Cognition in Patients With Early Alzheimer Disease and Amnestic Mild Cognitive Impairment During Treatment With Rosiglitazone. Am J Geriatr Psychiatry. 13(11):950–958. doi:10.1097/00019442-200511000-00005.

Weisgraber KH, Mahley RW. 1996. Human apolipoprotein E: the Alzheimer's disease connection. FASEB J. 10(13):1485–1494. doi:10.1096/fasebj.10.13.8940294.

Westergaard UB, Kirkegaard K, Sørensen ES, Jacobsen C, Nielsen MS, Petersen CM, Madsen P. 2005. SorCS3 does not require propeptide cleavage to bind nerve growth factor. FEBS Lett. 579(5):1172–1176. doi:10.1016/j.febslet.2004.12.088.

Willer CJ, Sanna S, Jackson AU, Scuteri A, Bonnycastle LL, Clarke R, Heath SC, Timpson NJ, Najjar SS, Stringham HM, et al. 2008. Newly identified loci that influence lipid concentrations and risk of coronary artery disease. Nat Genet. 40(2):161–169. doi:10.1038/ng.76.

William Rebeck G, Reiter JS, Strickland DK, Hyman BT. 1993. Apolipoprotein E in sporadic Alzheimer's disease: Allelic variation and receptor interactions. Neuron. 11(4):575–580. doi:10.1016/0896-6273(93)90070-8.

Willnow TE, Petersen CM, Nykjaer A. 2008. VPS10P-domain receptors - Regulators of neuronal viability and function. Nat Rev Neurosci. 9(12):899–909. doi:10.1038/nrn2516.

Winblad B, Amouyel P, Andrieu S, Ballard C, Brayne C, Brodaty H, Cedazo-Minguez A, Dubois B, Edvardsson D, Feldman H, et al. 2016. Defeating Alzheimer's disease and other dementias: a priority for European science and society. Lancet Neurol. 15(5):455–532. doi:10.1016/s1474-4422(16)00062-4.

Wolozin B, Wang SW, Li N-C, Lee A, Lee TA, Kazis LE. 2007. Simvastatin is associated with a reduced incidence of dementia and Parkinson's disease. BMC Med. 5(9242):20. doi:10.1186/1741-7015-5-20.

Wood PL. 2012. Lipidomics of Alzheimer ' s disease : current status. Alzheimers Res Ther. 4(5):1–10. doi:10.1186/alzrt103.

Wyss-Coray T. 2006. Inflammation in Alzheimer disease: driving force, bystander or beneficial response? Nat Med. 12(9):1005–15. doi:10.1038/nm1484.

Xu LZ, Sánchez R, Sali A, Heintz N. 1996. Ligand specificity of brain lipid-binding protein. J Biol Chem. 271(40):24711–24719. doi:10.1074/jbc.271.40.24711.

Xu Q, Bernardo A, Walker D, Kanegawa T, Mahley RW, Huang Y. 2006. Profile and regulation of apolipoprotein E (ApoE) expression in the CNS in mice with targeting of green fluorescent protein gene to the ApoE locus. J Neurosci. 26(19):4985–94. doi:10.1523/JNEUROSCI.5476-05.2006.

Xu Z, Han K, Chen J, Wang C, Dong Y, Yu M, Bai R, Huang C, Hou L. 2017. Vascular endothelial growth factor is neuroprotective against ischemic brain injury by inhibiting scavenger receptor A expression on microglia. J Neurochem. 142(5):700–709. doi:10.1111/jnc.14108.

Youmans KL, Tai LM, Nwabuisi-Heath E, Jungbauer L, Kanekiyo T, Gan M, Kim J, Eimer WA, Estus S, Rebeck GW, et al. 2012. APOE4-specific changes in Aβ accumulation in a new transgenic mouse model of Alzheimer disease. J Biol Chem. 287(50):41774–86. doi:10.1074/jbc.M112.407957.

Yuki D, Sugiura Y, Zaima N, Akatsu H, Takei S, Yao I, Maesako M, Kinoshita A, Yamamoto T, Kon R, et al. 2014. DHA-PC and PSD-95 decrease after loss of synaptophysin and before neuronal loss in patients with Alzheimer's disease. Sci Rep. 4. doi:10.1038/srep07130.

Zhao M, Cribbs DH, Anderson AJ, Cummings BJ, Su JH, Wasserman AJ, Cotman CW. 2003. The induction of the TNFalpha death domain signaling pathway in

Alzheimer’s disease brain. Neurochem Res. 28(2):307–18.

Zhao N, Liu CC, Van Ingelgom AJ, Martens YA, Linares C, Knight JA, Painter MM, Sullivan PM, Bu G. 2017. Apolipoprotein E4 Impairs Neuronal Insulin Signaling by Trapping Insulin Receptor in the Endosomes. Neuron. 96(1):115-129.e5. doi:10.1016/j.neuron.2017.09.003.

Zheng H, Jiang M, Trumbauer ME, Sirinathsinghji DJS, Hopkins R, Smith DW, Heavens RP, Dawson GR, Boyce S, Conner MW, et al. 1995. B-Amyloid Precursor Protein-Deficient Mice Show Reactive Gliosis and Decreased Locomotor Activity. Cell. 81(4):525–531. doi:10.1016/0092-8674(95)90073-X.

7.1. Acknowledgments

To all the people who have contributed directly or indirectly to the achievement of this PhD thesis project...Many Thanks…

First of all, a special thanks to Prof. Dr. Thomas Willnow for giving me the opportunity to work in his group. To him goes my gratitude for the support and help during these years in Berlin. If I have acquired and developed a scientist mind, it is to be attributed to him.

I'm very grateful to all the collaborators, including Dr. Carola Schipke for providing the human materials, Dr. Michael Rothe for the lipids analysis and the microscopy facility at MDC for the training and the troubleshooting during the confocal images acquisition. I sincerely thank Sandra Ehret and Prof. Dr. Jörg Heeren for teaching and helping me to isolate APOE-containing lipoproteins.

I would like to thank all the past and present members of the lab. A very immense gratitude goes to Verona Kuhle, our super secretary. Tatjana Pasternack, Maria Kahlow, Kristin Kampf, Maria Kamprath, Christine Kruse and Andra Eisenmann for their impeccable every day technical support. I extend my gratitude to Dr. Vanessa Schmidt especially for her help during the writing of my thesis and to Dr. Anna Malik with whom I shared and discussed this project. Also I want to thank Dr. Annabel Christ and Lena Bunatyan for providing their support with histological techniques. Finally, Rishabhdev Sinha, Maike Marczenke and Alexis Zi Le Shih are my adventure friends. With them I discussed ideas and suggestions that greatly benefited my work.

I'm really grateful to Dr. Anne-Sophie Carlo who started this project many years ago. I'm thankful to her for the enthusiasm and encouragement since my first day in the lab and for believing in the success of this research.

The last but not the least, this last paragraph goes to Hazel Quinn. I'm indebted to her for proofreading my thesis and mostly for the support and confidence during my most difficult times. Words are not enough to express what I feel…

7.2. Selbstständigkeitserklärung

Hiermit erkläre ich, dass ich die vorliegende Arbeit mit dem Titel “The effect of apolipoprotein E isoforms and sortilin in brain lipid homeostasis and Alzheimer’s disease” selbstständig und ohne Hilfe Dritter angefertigt habe. Sämtliche Hilfsmittel, Hilfen sowie Literaturquellen sind als solche kenntlich gemacht. Außerdem erkläre ich hiermit, dass ich mich nicht anderweitig um einen entsprechenden Doktorgrad beworben habe. Die Promotionsordnung des Fachbereichs Biologie, Chemie und Pharmazie der Freien Universität Berlin habe ich gelesen und akzeptiert.

Berlin, July 2019

Antonino Asaro

For reasons of data protection, the curriculum vitae is not published in the electronic version

For reasons of data protection, the curriculum vitae is not published in the electronic version